

# **Ozonesonde Launches in San Antonio and El Paso**

## **Final Report**

**PGA Number: 582-20-10914-009**

Prepared for the Texas Commission on Environmental Quality (TCEQ)

### ***Principal Investigators***

James Flynn, University of Houston

Paul Walter, St. Edward's University

Marilyn Wooten, Trinity University

Rosa Fitzgerald, University of Texas at El Paso

### ***Co-Investigators***

Mark Estes, St. Edward's University

Gary Morris, St. Edward's University

Kristina Trevino, Trinity University

Yuxuan Wang, University of Houston

### ***Contributors***

Zoe Lacey, Trinity University

Wei Li, University of Houston

**Project Time Period:** November 7, 2019 – June 30, 2021

## Executive Summary

During the period 15 July – 15 October 2020, a team of researchers from the University of Houston, St. Edward's University, Trinity University, and the University of Texas at El Paso carried out a total of 81 ozonesonde launches in El Paso and San Antonio, Texas (41 launches from El Paso and 40 from San Antonio). This effort had the primary purpose to sample, characterize, and explain ozone and meteorological features in the boundary layer, the lower free troposphere (LFT), and the upper troposphere/lower stratosphere (UTLS) in these regions. Launches were targeted at days when ozone was expected to exceed the level of the Federal standard to inform and improve our understanding of conditions under which such exceedances could occur. While both San Antonio and El Paso have encountered air pollution challenges over several decades, either approaching or, in a few instances, exceeding Federal standards, neither has hosted extensive *in situ* vertical sampling of the atmosphere up to the stratosphere. Data from this project support analyses of conditions associated with high ozone events in these two regions.

During the sampling period, there were ten days where the max daily 8-hour average (MDA) ozone concentration for the El Paso region exceeded the 2015 National Ambient Air Quality Standard (NAAQS) of MDA8 [O<sub>3</sub>] ≤ 70 ppbv. The profiles of the dawn flights showed that background ozone leftover in the residual layer from the previous day significantly contributed to the higher ozone days in El Paso. On 21 August 2020, in which the C49 Socorro Hueco station measured the highest maximum daily eight-hour average ozone (102 ppbv) of any continuous air monitoring station in Texas in 2020, was likely to have been affected in some way by smoke from the then-ongoing wildfires in California.

For the 2020 San Antonio campaign, two days in August and four days in October exceeded the NAAQS ozone standard. The days exceeding the ozone standard were during post-frontal conditions. The monitor recording the highest ozone was on the northwest side of San Antonio for all but one of those days, and some such days showed flow reversals with winds out of the NW in the morning shifting to out the S or SE in the afternoon. For days that did not exceed the ozone standard, consistent southerly flow regularly brought relatively clean marine air and strong winds to San Antonio.

In this report, we review each exceedance day and provide results from the ozonesondes flights during the campaign, first for El Paso, then for San Antonio. For context, this report also provides an overview of past results from San Antonio and El Paso. Then, clustering analysis was applied to group the days with similar features and found four distinct O<sub>3</sub> vertical distribution patterns in San Antonio and El Paso. Finally, we provide an overview of the preparations and procedures for ozonesonde flights as well as the standard analysis done for each flight.

|  |           |
|--|-----------|
| <b>1. Introduction</b>   | <b>5</b>  |
| <b>1.1 Identifying Long-range Transport</b>                        | <b>6</b>  |
| 1.1.1 Potential Influences due to Biomass Burning                  | 8         |
| 1.1.2 Stratosphere-Troposphere Exchange                            | 9         |
| <b>1.2 Identifying Contributions from the Residual Layer</b>       | <b>9</b>  |
| <b>2. El Paso</b>  | <b>11</b> |
| <b>2.1 2020 Ozonesonde Campaign from El Paso</b>                   | <b>12</b> |
| 2.1.1 Listing of All 2020 El Paso Flights                          | 12        |
| 2.1.2 Exceedance Days in El Paso Region During 2020 Campaign       | 14        |
| 2.1.2.1 25 July 2020   | 15        |
| 2.1.2.2 1 August 2020  | 16        |
| 2.1.2.3 4 August 2020  | 16        |
| 2.1.2.4 8 August 2020  | 18        |
| 2.1.2.5 14 August 2020   | 18        |
| 2.1.2.6 19 August 2020   | 19        |
| 2.1.2.7 21 August 2020   | 20        |
| 2.1.2.8 22 August 2020   | 24        |
| 2.1.2.9 27 August 2020   | 25        |
| 2.1.2.10 29 August 2020  | 26        |
| 2.1.3 Profiles of 2020 El Paso Dawn and Afternoon Paired Flights   | 27        |
| <b>2.2 2019 Ozonesonde Campaign from El Paso</b>                   | <b>30</b> |
| 2.2.1 Exceedance Days in El Paso Region During 2019 Campaign       | 30        |
| 2.2.1.1 5 August 2019  | 30        |
| 2.2.1.2 7 August 2019  | 32        |
| 2.2.1.3 8 August 2019  | 33        |
| 2.2.1.4 10 August 2019   | 34        |
| 2.2.1.5 15 August 2019   | 35        |
| 2.2.2 Flight on 29 August 2019: Landed in Juarez                   | 36        |
| 2.2.3 Possible Influence of Border-crossing Traffic to El Paso     | 37        |
| <b>2.3 2017 Ozonesonde Campaign from El Paso</b>                   | <b>38</b> |
| 2.3.1 15 – 18 May 2017 (Indications of long-range transport)       | 40        |
| 2.3.2 Simultaneous flights on 19 July 2017                         | 42        |
| <b>2.4 Residual layer Influences on Afternoon Ozone in El Paso</b> | <b>43</b> |
| <b>2.5 Average Afternoon Profiles by Wind Direction</b>            | <b>45</b> |
| <b>3. San Antonio</b>  | <b>47</b> |
| <b>3.1 2020 Ozonesonde Campaign from San Antonio</b>               | <b>47</b> |
| 3.1.1 Listing of All 2020 San Antonio Flights                      | 47        |
| 3.1.2 Exceedance Days in San Antonio During 2020 Campaign          | 50        |
| 3.1.2.1 19 August 2020   | 50        |
| 3.1.2.2 20 August 2020   | 51        |
| 3.1.2.3 1 October 2020   | 52        |
| 3.1.2.4 6 October 2020   | 53        |
| 3.1.2.5 7 October 2020   | 55        |
| 3.1.2.6 13 October 2020  | 56        |
| 3.1.3 Profiles of 2020 Dawn and Afternoon Paired Flights           | 58        |

|            |   |           |
|------------|---|-----------|
| <b>3.2</b> | <b>2019 Ozonesonde Campaign From San Antonio</b> .....                            | <b>60</b> |
| 3.2.1      | Exceedance Day in San Antonio During 2019 Campaign .....                          | 61        |
| <b>3.3</b> | <b>2017 Ozonesonde Campaign from San Antonio</b> .....                            | <b>64</b> |
| <b>3.4</b> | <b>Residual Layer Influence on Afternoon Ozone in San Antonio</b> .....           | <b>69</b> |
| <b>3.5</b> | <b>Average Afternoon Profiles by Wind Direction</b> .....                         | <b>70</b> |
| <b>4.</b>  | <b><i>Clustering Analysis of Ozonesondes in San Antonio and El Paso</i></b> ..... | <b>71</b> |
| 4.1        | Clustering in San Antonio .....   | 71        |
| 4.2        | Clustering in El Paso .....   | 74        |
| <b>5.</b>  | <b><i>Conclusions and Recommendations for Future Work</i></b> .....               | <b>78</b> |
| 5.1        | El Paso.....  | 78        |
| 5.2        | San Antonio .....   | 78        |
| 5.3        | Recommendations for Future Work.....  | 79        |
| <b>6.</b>  | <b><i>References</i></b> .....  | <b>83</b> |
| <b>7.</b>  | <b><i>Appendix: Overview of Ozonesondes and Flight Data</i></b> .....             | <b>86</b> |
| 7.1        | Flight Data .....   | 86        |
| 7.2        | Standard HYSPLIT Back Trajectories for Each Flight .....                          | 88        |

## 1. INTRODUCTION

The Tropospheric Ozone Pollution Project (TOPP) has engaged in weather balloon launches across the state of Texas since 2004, with ~1,000 flights of payloads designed to measure ozone, temperature, humidity, pressure, wind speed, and wind direction. Two components of the payload make measurements: the ozonesonde, which measures ozone, and the radiosonde, which measures pressure, temperature, humidity, latitude, longitude, altitude, wind speed, and wind direction (with the last five in the list coming from an integrated GPS instrument). Connected to the ozonesonde, the radiosonde transmits a packet of data every second in the reserved FM radio band for meteorological instruments to researchers at the surface using an antenna and a receiver, who collect the data with an antenna attached to a receiver and a computer with software to decode the signal. As a result, researchers do not need recover the ozonesonde after the flight to obtain the data. Hereafter, we will refer to the entire payload as an ozonesonde.

Ozonesondes rise at ~5 m/s and make it to altitudes of ~24 km or ~30 km depending on the size of the balloon we use. A key advantage of ozonesondes is that they augment two-dimensional surface observations by providing a vertical component, a profile of ozone and meteorology, resulting in a three-dimensional snapshot of the ozone concentration throughout the troposphere and into the stratosphere. The surface monitoring network can provide an estimate of background transported ozone but is not able to measure ozone aloft that may mix down into the boundary layer, influencing daily ozone maxima. Furthermore, information from ozonesondes allow researchers to determine the boundary layer height, a key element that influences surface pollution concentrations in both the real and modeled atmosphere.

In Section 1.1 we will examine how ozonesonde data can be used to identify the long-range transport of ozone that contributes to the observed ozone concentrations in the boundary layer. In so doing, we will discuss how to identify potential contributions from biomass burning influences and to identify potential stratospheric air that has made its way into the troposphere.

In Section 1.2 we demonstrate how ozonesonde flights at dawn provide information about ozone concentrations in both the nocturnal boundary layer (at the surface) as well as the residual layer (aloft, but at an altitude that can be entrained in the growing morning boundary layer). Both layers can influence ozone concentrations near the surface and in the afternoon boundary layer.

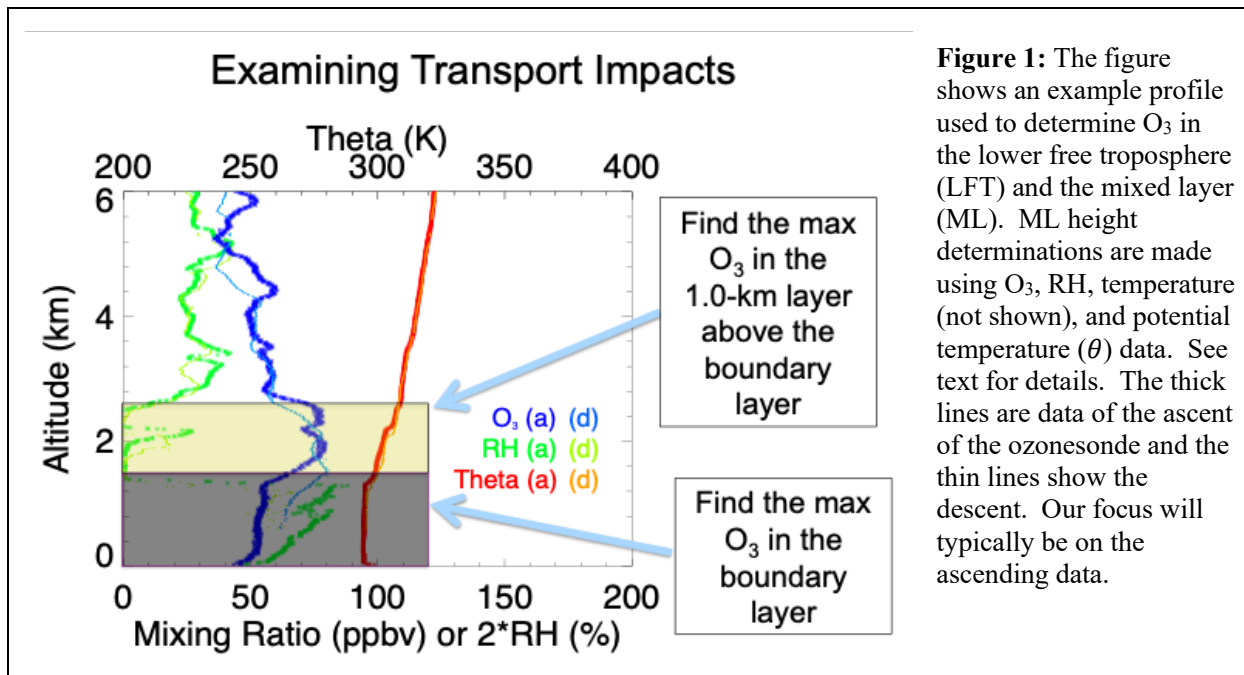
In Sections 2 and 3 we will review the field campaigns in El Paso and San Antonio, respectively. In Section 4 we show the results of clustering analysis applied to ozonesonde profiles. In Section 5 we provide conclusions and suggestions for future work. In the Appendix we provide an overview of prepping ozonesondes, ozonesonde flight data, and the standard HYSPLIT analyses we do for each flight.

In 2020, a total of 81 ozonesondes were launched from San Antonio and El Paso (41 from El Paso and 40 from San Antonio). The processed data from those flights that include vertical profiles can be found at <http://ir.stedwards.edu/natural-sciences/ozone>. All flight times in this report are in Coordinated Universal Time (UTC or Z). Note that 21Z is the same as 21:00 UTC. UTC is 6 hours ahead of Central Standard Time (local San Antonio time), and 7 hours ahead of Mountain Standard Time (local El Paso time).

## 1.1 IDENTIFYING LONG-RANGE TRANSPORT

Signs of long-range transport of ozone that can contribute to the boundary layer can be identified through analysis of ozonesonde profiles. Such cases of long-range transport are often the result of either stratosphere-troposphere exchange (STE) or influences of biomass burning.

In an effort to better understand the factors controlling vertical O<sub>3</sub> distribution, we examine the difference in O<sub>3</sub> between the 1-km layer in the lower free troposphere (LFT) immediately above the mixed layer (ML) and the O<sub>3</sub> in the ML. Figure 1 shows an example profile identifying these two layers from a flight that occurred from Houston. The mixed layer height is determined by examining gradients in relative humidity (RH), O<sub>3</sub>, temperature, and potential temperature ( $\theta$ ) and is identified as the height at which most (if not all of) these variables show a sharp vertical gradient. Furthermore, we define three cases based on the RH and O<sub>3</sub> found in the 1-km layer in the LFT: Case 1 finds a maximum O<sub>3</sub> < 70 ppb with a minimum RH < 10%; Case 2 finds a maximum O<sub>3</sub> > 70 ppb with a minimum RH > 40%; and Case 3 finds a maximum O<sub>3</sub> > 70 ppb and a minimum RH < 10%. Case 1 potentially suggests UT/LS air has been transported to the LFT which may be high in O<sub>3</sub>, but not high enough on its own to trigger a violation of the EPA 8-hour O<sub>3</sub> standard. Case 2 is potentially indicative of high O<sub>3</sub> air that likely has an anthropogenic or biomass burning source. The high RH values associated with the high O<sub>3</sub> suggest sources near the surface or in the lower troposphere. The O<sub>3</sub> concentrations exceed the EPA 8-hour O<sub>3</sub> standard. On these occasions, local violations may occur with contributions from transported O<sub>3</sub>. Finally, Case 3 is potentially indicative of high O<sub>3</sub> air descending from the UT/LS to the LFT, low enough where it may interact with the ML or residual layer (RL) air masses. Since the O<sub>3</sub> concentration in this LFT layer exceeds the EPA 8-hour O<sub>3</sub> standard, these are cases in which violations may occur with contributions from naturally produced and transported stratospheric O<sub>3</sub>. For each of the cases, support for the interpretations of the observed vertical ozone distributions can be strengthened by performing HYSPLIT back trajectories to determine where the air parcels were transported from, comparing to other available chemical measurements, and other nearby soundings of radiosondes, if available.



The image on the left in Figure 2 shows the profile from the first flight of the 2017 campaign from El Paso. The top of the boundary layer is specified by the black horizontal line. Higher ozone above the boundary layer suggests ozone has been transported into the area. Much more common is the situation we see in the image on the right in Figure 2 where the ozone gradient is negative (the ozone concentration decreases) just above the boundary layer. This pattern suggests the highest ozone has formed locally in the boundary layer instead of being transported into the area. Once an ozone enhancement associated long-range transport is identified, as with the afternoon flight on 15 May 2017, further investigations are needed to identify potential upwind sources.

In most cases, the top of the boundary layer is straightforward to identify for afternoon profiles. The afternoon boundary layer is well mixed and thus the ozone concentration is relatively uniform throughout (somewhat lower concentrations near the surface due to deposition and/or titration of ozone by fresh NO emissions). At the top of the afternoon boundary layer, there are simultaneously sharp gradients (i.e., kinks) in the relative humidity, ozone concentration, and potential temperature.

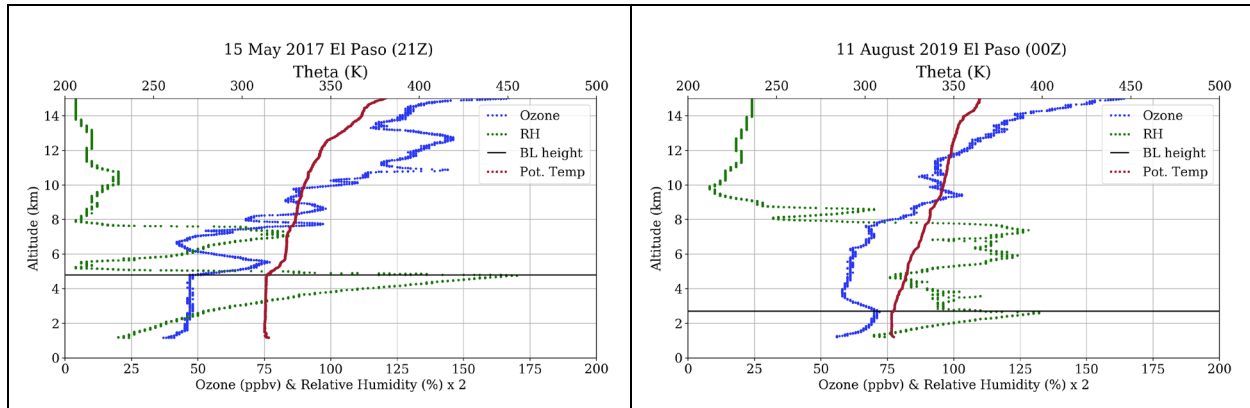


**Figure 2:** Left: Just above the boundary layer there is a positive gradient in the ozone concentration (it increases), which is a sign of long-range transport. Right: Just above the boundary layer there is a negative gradient in the ozone concentration (it decreases), which is more common, meaning long-range transport is less likely and that the ozone in the boundary layer is more likely the result of local photochemical production, local transport, and contributions from the nocturnal boundary layer of the previous night.

### 1.1.1 Potential Influences due to Biomass Burning

Ozone enhancements, like the one just above the boundary layer on the left image in Figure 2, can potentially be the result influences due to biomass burning. We use NOAA HYSPLIT back trajectories (<https://ready.arl.noaa.gov/hypub-bin/trajtype.pl?runtype=archive>) overlaid on top of recent hot spots using MODIS or NOAA Hazard Mapping System Fire and Smoke Product (<https://www.ospo.noaa.gov/Products/land/hms.html>) to ascertain whether smoke and biomass burning influences are contributing to particular ozone enhancements observed in the profiles.

Figure 3 shows the back trajectories of air parcels with starting altitudes at the height of the ozone enhancement just above the boundary layer on the afternoon flight of 15 May 2017 from El Paso. The back trajectories show likely paths that the air parcels above El Paso at that time followed over the prior 96 hours. The back trajectories are overlaid on top of recent MODIS hot spots where the red dots show sites of possible biomass burning from the previous 24 hours and the yellow dots show the sites of possible biomass burning from the previous seven days. The ozone enhancement we see on 15 May 2017 may have had contributions resulting from long-range transport resulting from the influences of biomass burning emissions. A series of soundings during 15-18 May 2017 is discussed in Section 2.3.1. The Appendix contains more information about the standard HYSPLIT trajectories that we calculate and guidelines about their range of applicability. The ozonesonde data and analysis suggest that this event could make a good case study for modeling to ascribe relative contributions of biomass burning and local production to the boundary layer ozone concentrations.

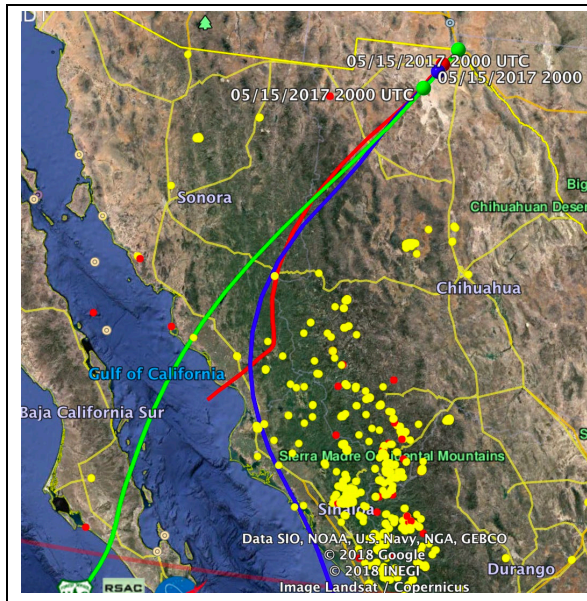


**Figure 3:** The profile of the sounding on 15 May 2017 (Figure 2) has an ozone enhancement in the LFT with a peak at 5500 m AMSL. The enhancement may have resulted from the long-range transport of biomass burning emissions. Left: HYSPLIT back trajectories at 3000 m (red), 4250 m (blue), and 5500 m (green) AMSL overlaid on recent MODIS hot spots (red and yellow dots).

### 1.1.2 Stratosphere-Troposphere Exchange

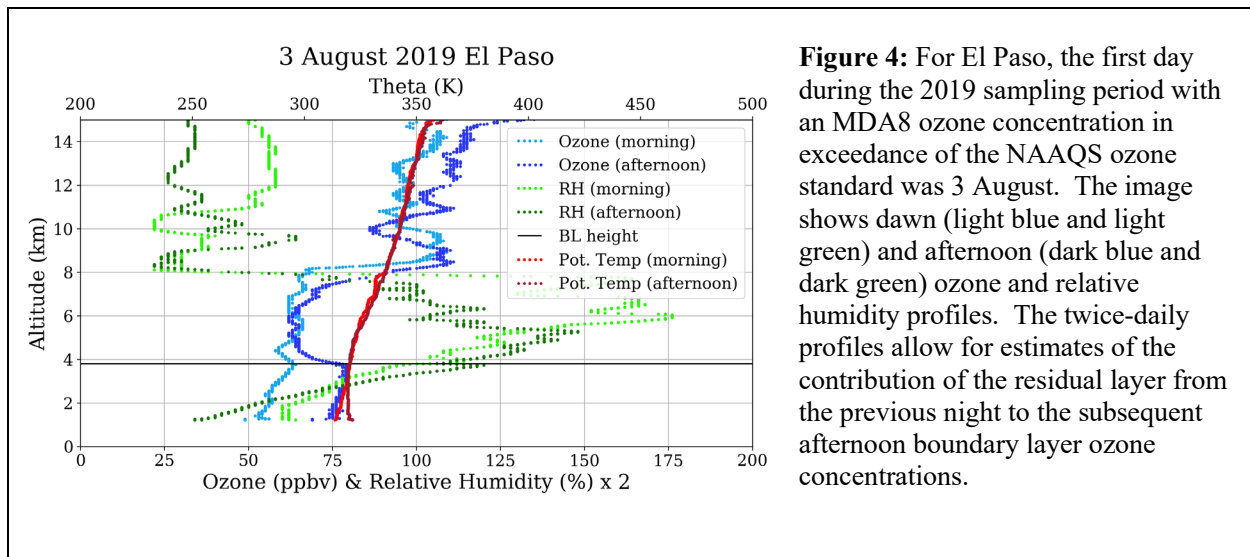
The stratospheric ozone layer has ozone concentrations that are a couple of orders of magnitude greater than what is observed at the surface. After a cold front, a tropopause fold may in stratospheric air (high in ozone) mixing down into the troposphere a process known as stratosphere-troposphere exchange (STE) (Reiter 1975; Shapiro 1980). Post-frontal conditions often consist of clear skies, dry air, and weak or stagnant winds, conditions conducive to local ozone formation (Ngan et al. 2012). Such conditions, typically found one to three days after a frontal passage, often correlate with high ozone days.

Stratospheric air is very dry, and thus a sign of potential STE is when there is an ozone enhancement that simultaneously has very dry air with relative humidity (RH) < 5% (Appenzeller and Davies 1992). HYSPLIT back trajectories typically show some descent for the air contributing to such a feature (Langford et al. 2018). Further, for cases where the back trajectories pass over the Rocky Mountains, the mountain range may facilitate downward transport (Langford et al. 2009).

## 1.2 IDENTIFYING CONTRIBUTIONS FROM THE RESIDUAL LAYER

During most flight days in the 2019 campaign there were twice-daily launches with one at dawn to capture the nocturnal boundary layer and residual layer, and the other in the afternoon near the time of peak surface ozone. Figure 4 shows the profiles of two ozonesonde flights on 3 August 2019 from El Paso. The altitude on the vertical axis is km above mean sea level (AMSL). Profiles of the ozone are shown in light blue for the morning flight and dark blue for the afternoon flight. Profiles of relative humidity (RH) are shown in green for the morning flight

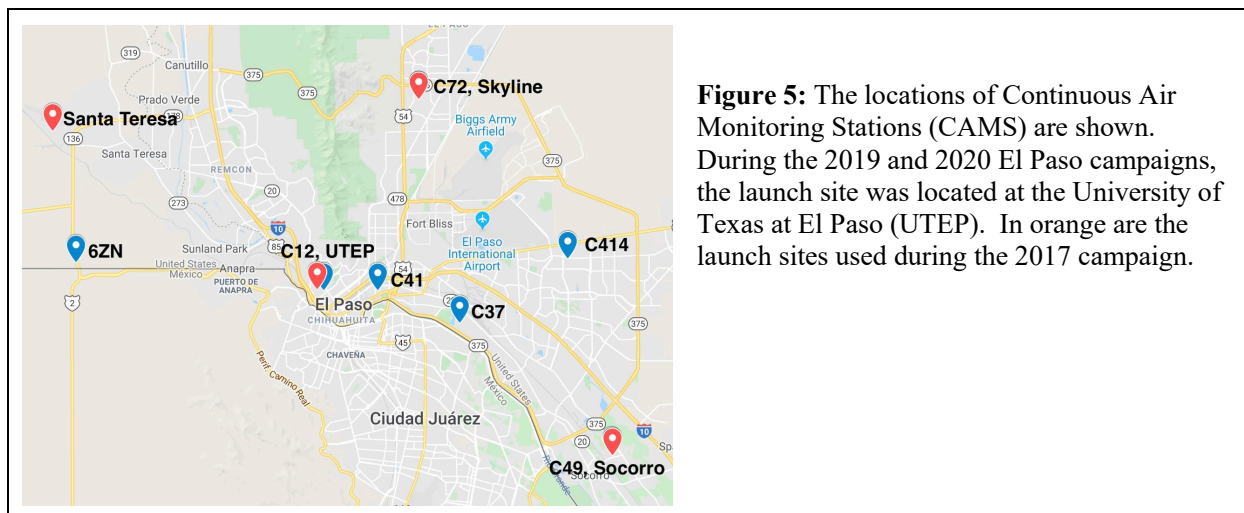
and dark green for the afternoon flight. Potential temperature ( $\theta$ ) profiles are shown in red for the morning flight and dark red for the afternoon flight. The potential temperature is the temperature (in Kelvin) that a parcel of air would have if adiabatically transported to a standard pressure (i.e., 1000 hPa or surface pressure). The stability of the air can be determined by the vertical gradient (as a function of height  $z$ ) of the potential temperature. The top of the afternoon boundary layer (BL) is marked by the black horizontal line. Just above the surface for the afternoon potential temperature profile,  $\partial\theta/\partial z < 0$ , which indicates the air is unstable (due to surface heating). After the initial negative gradient near the surface, the potential temperature is approximately constant ( $\partial\theta/\partial z = 0$  to the top of the boundary layer near 3.9 km AMSL on this day. A near zero gradient in potential temperature is common. Above the boundary layer, the atmosphere is stable as indicated by the potential temperature gradient is positive ( $\partial\theta/\partial z > 0$ ). The larger a positive potential temperature gradient is, the stronger the stability of the atmosphere at that altitude.



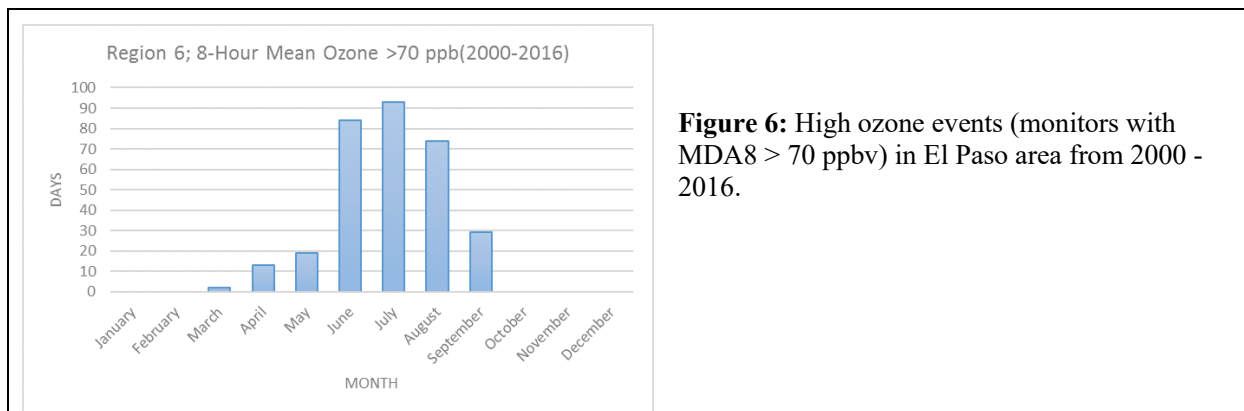
Air in the morning residual layer will become entrained in the growing morning boundary layer, mixing into what becomes the afternoon boundary layer. Measurements of the morning residual layer ozone concentrations can provide an estimate of the starting point for production of the boundary layer ozone concentrations seen in the afternoon. Section 2.1.3 shows all of the profiles on days where there were twice-daily flights from El Paso and Section 3.1.3 shows the same from San Antonio.

## 2. EL PASO

During May-October 2017, there were 58 ozonesonde launches from the four launch sites in and near the El Paso area. Figure 5 shows the locations of the Continuous Air Monitoring Stations (CAMS) in the El Paso area and the launch locations of the 2017, 2019, and 2020 campaigns. During 31 July – 6 September 2019, there were a total of 27 ozonesonde launches from the University of Texas at El Paso (UTEP; 31.7709°N, 106.5013°W) campus. During 15 July – 3 September 2020, there were a total 41 ozonesonde launches from the UTEP campus. This report includes some preliminary analysis of the weather balloon data and its implications for air quality in El Paso.



The ozone season in El Paso has a single summer peak. Figure 6 shows the distribution of days with MDA8 ozone concentrations > 70 ppbv for Region 6 (El Paso area) from 2000 – 2016. There were 10 days during the 2020 sampling period, 5 days during the 2019 sampling period, and 12 days during the longer 2017 sampling period for which at least one monitor in the El Paso area exceeded of the 8-hour ozone standard.



## 2.1 2020 OZONESONDE CAMPAIGN FROM EL PASO

### 2.1.1 Listing of All 2020 El Paso Flights

Table 1 shows all days during the sampling period. Some days we are unable to fly due to unfavorable balloon trajectory forecasts. For the 2020 campaign, these conditions occurred for approximately 25% of planned flights (see Table 1 below). For safety reasons and in accordance with flight protocols developed in conjunction with the FAA, we avoid flying on days when the pre-flight balloon trajectory forecasts indicates that the payloads are likely to land in a metropolitan area. For El Paso flights, this metropolitan area includes both El Paso and Juarez.

**Table 1:** Maximum daily 8-hour average (MDA8) ozone concentrations (ppb) at six surface monitors in the El Paso area, July 15 – October 15, 2020, with ozonesonde flights noted.

| Flight(s) | Date      | Morning flight number | Afternoon flight number | Final TCEQ Daily Air Quality Forecast | C12 EI Paso UTEP | C37 Ascarate Park | C41 Chamizal | C49 Socorro Hueco | C72 Skyline Park | C414 Ivanhoe |
|-----------|-----------|-----------------------|-------------------------|---------------------------------------|------------------|-------------------|--------------|-------------------|------------------|--------------|
| 1, 2      | 7/15/2020 | EP044 <sup>t</sup>    | EP045 <sup>t</sup>      |                                       | NA               | 61                | 61           | 65                | 59               | 62           |
|           | 7/16/2020 |                       |                         |                                       | NA               | 46                | 47           | NV                | 53               | 48           |
| 3, 4      | 7/17/2020 | EP046                 | EP047                   | *                                     | NV               | 59                | 57           | 69                | 59               | NV           |
|           | 7/18/2020 |                       |                         | *                                     | 56               | 50                | 55           | 60                | 53               | 54           |
|           | 7/19/2020 |                       |                         |                                       | 66               | 52                | 58           | 55                | 56               | 53           |
|           | 7/20/2020 |                       |                         |                                       | 61               | 57                | 58           | 57                | 60               | 53           |
| 5, 6      | 7/21/2020 | EP048                 | EP049                   | *                                     | 62               | 57                | 60           | 64                | 57               | 56           |
|           | 7/22/2020 |                       |                         |                                       | 47               | 39                | 39           | 43                | 46               | 41           |
|           | 7/23/2020 |                       |                         |                                       | 61               | 50                | 52           | 53                | 51               | 52           |
|           | 7/24/2020 |                       |                         |                                       | 60               | 45                | 50           | 54                | 57               | 53           |
|           | 7/25/2020 |                       |                         |                                       | 83               | 58                | 71           | 56                | 62               | 59           |
|           | 7/26/2020 |                       |                         |                                       | 47               | 37                | 42           | 41                | 43               | 41           |
| 7, 8      | 7/27/2020 | EP050                 | EP051                   |                                       | 50               | 40                | 42           | 45                | 47               | 43           |
| 9, 10     | 7/28/2020 | EP052                 | EP053                   | *                                     | 58               | 44                | 49           | 44                | 50               | 47           |
| 11, 12    | 7/29/2020 | EP054                 | EP055                   |                                       | 55               | 47                | 49           | 50                | 50               | 49           |
|           | 7/30/2020 |                       |                         |                                       | 64               | 57                | 61           | 60                | 50               | 54           |
|           | 7/31/2020 |                       |                         |                                       | 59               | 49                | NV           | 54                | 53               | 54           |
|           | 8/1/2020  |                       |                         |                                       | 81               | 69                | 73           | 74                | 69               | 67           |
| 13, 14    | 8/2/2020  | EP056                 | EP057                   | *                                     | 60               | 56                | 58           | 63                | 58               | 58           |
| 15, 16    | 8/3/2020  | EP058                 | EP059                   | *                                     | 68               | 60                | 64           | 65                | 59               | 58           |
| 17, 18    | 8/4/2020  | EP060                 | EP061                   | *                                     | 60               | 59                | 57           | 74                | 74               | 71           |
|           | 8/5/2020  |                       |                         | *                                     | 54               | 54                | 51           | 59                | 54               | 64           |
|           | 8/6/2020  |                       |                         |                                       | 62               | 56                | 55           | 58                | 62               | 59           |

Ozonesonde Launches for San Antonio and El Paso – Final Report  
 PGA 582-20-10914-009

|        |           |       |       |   |    |    |    |     |    |    |
|--------|-----------|-------|-------|---|----|----|----|-----|----|----|
|        | 8/7/2020  | ***   | ***   | * | 56 | 50 | 51 | 67  | 54 | 54 |
|        | 8/8/2020  | ***   | ***   |   | 85 | 63 | 73 | 55  | 73 | 61 |
|        | 8/9/2020  | ***   | ***   |   | 59 | 54 | 56 | 56  | 57 | 57 |
|        | 8/10/2020 | ***   | ***   | * | NV | 60 | 56 | 69  | 62 | 64 |
| 19     | 8/11/2020 | ***   | EP062 | * | 62 | 52 | NV | 58  | 53 | 53 |
| 20, 21 | 8/12/2020 | EP063 | EP064 | * | 58 | 51 | 57 | 52  | 64 | 55 |
| 22, 23 | 8/13/2020 | EP065 | EP066 | * | 62 | NV | 57 | 48  | 65 | 54 |
| 24, 25 | 8/14/2020 | EP067 | EP068 | * | 59 | 71 | 65 | 74  | 60 | 68 |
| 26, 27 | 8/15/2020 | EP069 | EP070 |   | 55 | 44 | 49 | 43  | 52 | 45 |
|        | 8/16/2020 |       |       |   | 45 | 41 | 42 | 44  | 43 | 42 |
|        | 8/17/2020 |       |       |   | 47 | 41 | 40 | 45  | 46 | 42 |
| 28, 29 | 8/18/2020 | EP071 | EP072 |   | 64 | 61 | 61 | 71  | 61 | 58 |
| 30, 31 | 8/19/2020 | EP073 | EP074 | * | 72 | 65 | NV | 67  | 71 | 73 |
| 32, 33 | 8/20/2020 | EP075 | EP076 | * | 53 | 53 | 52 | 60  | 58 | 60 |
|        | 8/21/2020 |       |       | * | 64 | 77 | 68 | 102 | 79 | 82 |
| 34, 35 | 8/22/2020 | EP077 | EP078 | * | 72 | 69 | 68 | 73  | 66 | 67 |
|        | 8/23/2020 |       |       |   | 67 | 59 | 60 | 61  | 62 | 62 |
|        | 8/24/2020 |       |       |   | 61 | 53 | 51 | 57  | 59 | 56 |
|        | 8/25/2020 |       |       |   | 55 | 47 | 46 | 52  | 54 | 51 |
| 36, 37 | 8/26/2020 | EP079 | EP080 |   | 64 | 57 | 55 | 57  | 59 | 56 |
| 38, 39 | 8/27/2020 | EP081 | EP082 | * | 71 | 56 | 56 | 54  | 63 | 55 |
|        | 8/28/2020 | ***   | ***   | * | 67 | 64 | 58 | 63  | 67 | 68 |
|        | 8/29/2020 | ***   | ***   | * | 72 | 67 | 69 | 68  | 58 | 61 |
|        | 8/30/2020 | ***   | ***   |   | 47 | 41 | 45 | 47  | 49 | 45 |
|        | 8/31/2020 |       |       |   | 45 | 35 | 41 | 44  | 46 | 43 |
|        | 9/1/2020  |       |       |   | 51 | 43 | 47 | 48  | 50 | 49 |
|        | 9/2/2020  |       |       |   | NV | 57 | 55 | 60  | NV | 57 |
| 40, 41 | 9/3/2020  | EP083 | EP084 |   | 67 | 63 | 59 | 68  | 60 | 68 |
|        | 9/4/2020  |       |       |   | 54 | 52 | 45 | 52  | 52 | 54 |
|        | 9/5/2020  |       |       |   | 48 | 43 | 42 | 45  | 45 | 44 |
|        | 9/6/2020  |       |       |   | 47 | 36 | 40 | 38  | 43 | 39 |
|        | 9/7/2020  |       |       |   | 43 | 38 | 39 | 43  | 45 | 46 |
|        | 9/8/2020  |       |       |   | 43 | 35 | 41 | 44  | 43 | 43 |
|        | 9/9/2020  |       |       |   | 22 | 20 | 18 | 22  | 23 | 22 |
|        | 9/10/2020 |       |       |   | 26 | 24 | 23 | 25  | 25 | 25 |
|        | 9/11/2020 |       |       |   | 39 | 35 | 36 | 37  | 37 | 37 |
|        | 9/12/2020 |       |       |   | 47 | 37 | 39 | 40  | 41 | 40 |
|        | 9/13/2020 |       |       |   | 55 | 51 | 50 | 53  | 51 | 52 |
|        | 9/14/2020 |       |       |   | 42 | 38 | 33 | 42  | 43 | 41 |
|        | 9/15/2020 |       |       |   | 58 | 50 | 51 | 49  | 51 | 51 |
|        | 9/16/2020 |       |       |   | 58 | 50 | 49 | 55  | 53 | 52 |
|        | 9/17/2020 |       |       |   | 55 | 52 | 50 | 54  | 54 | 51 |

Ozonesonde Launches for San Antonio and El Paso – Final Report  
 PGA 582-20-10914-009

|  |            |  |  |  |    |    |    |    |    |    |
|--|------------|--|--|--|----|----|----|----|----|----|
|  | 9/18/2020  |  |  |  | 59 | 55 | 48 | 57 | 57 | 55 |
|  | 9/19/2020  |  |  |  | 60 | 55 | 53 | 57 | 56 | 53 |
|  | 9/20/2020  |  |  |  | 55 | 47 | 48 | 51 | 52 | 49 |
|  | 9/21/2020  |  |  |  | 58 | 51 | 48 | 56 | 61 | 54 |
|  | 9/22/2020  |  |  |  | 59 | 57 | 47 | 65 | 58 | 60 |
|  | 9/23/2020  |  |  |  | 52 | 48 | 53 | 53 | 53 | 52 |
|  | 9/24/2020  |  |  |  | 55 | 54 | 48 | 60 | 58 | 56 |
|  | 9/25/2020  |  |  |  | 50 | 45 | 49 | 56 | 52 | 52 |
|  | 9/26/2020  |  |  |  | 50 | 45 | 45 | 50 | 53 | 51 |
|  | 9/27/2020  |  |  |  | 48 | 46 | 46 | 49 | 49 | 49 |
|  | 9/28/2020  |  |  |  | 42 | 40 | 46 | 41 | 41 | 40 |
|  | 9/29/2020  |  |  |  | 53 | 46 | 33 | 49 | 52 | 49 |
|  | 9/30/2020  |  |  |  | 54 | 48 | 42 | 61 | 54 | 53 |
|  | 10/1/2020  |  |  |  | 50 | 48 | 40 | 49 | 49 | 48 |
|  | 10/2/2020  |  |  |  | 50 | 43 | 40 | 43 | 51 | 46 |
|  | 10/3/2020  |  |  |  | 47 | 42 | 41 | 47 | 45 | 45 |
|  | 10/4/2020  |  |  |  | 57 | 48 | 47 | 50 | 52 | 48 |
|  | 10/5/2020  |  |  |  | 45 | 40 | 41 | 49 | 49 | 51 |
|  | 10/6/2020  |  |  |  | 52 | 48 | 44 | 49 | 55 | 56 |
|  | 10/7/2020  |  |  |  | 57 | 47 | 45 | 53 | 59 | 53 |
|  | 10/8/2020  |  |  |  | 54 | 49 | 43 | 58 | 52 | 57 |
|  | 10/9/2020  |  |  |  | 45 | 35 | 42 | 46 | 49 | 47 |
|  | 10/10/2020 |  |  |  | 41 | 36 | 40 | 42 | 44 | 43 |
|  | 10/11/2020 |  |  |  | 39 | 35 | 37 | 40 | 38 | 39 |
|  | 10/12/2020 |  |  |  | 44 | 41 | 32 | 43 | 43 | 42 |
|  | 10/13/2020 |  |  |  | 45 | 43 | 41 | 48 | 52 | 51 |
|  | 10/14/2020 |  |  |  | 40 | 34 | 37 | 41 | 44 | NV |
|  | 10/15/2020 |  |  |  | 42 | 38 | 35 | 43 | 41 | 43 |

Notes: The El Paso 2020 campaign sampling period was from 15 July - 15 October 2020, with training flights (“t”) on 15 July 2020. The final projection from the TCEQ Daily Air Quality Forecast that was available for a potential flight at dawn is shown, where \* denotes that it was an Ozone Action Day. Launch days with \*\*\* denotes that forecast balloon trajectories were unsuitable for a launch. Cell shading corresponds to the AQI category for that ozone concentration (“Good”, “Moderate”, etc.) for concentrations greater than 54 ppb.

### 2.1.2 Exceedance Days in El Paso Region During 2020 Campaign

There were ten days during the 2020 ozonesonde campaign where at least one monitor in the El Paso region exceeded the 8-hour ozone standard.

### 2.1.2.1 25 July 2020

Plots of wind runs were constructed using hourly wind surface monitor (Li et al. 2020; Allwine and Whiteman 1994). Wind runs are indicative of the length and direction of transport possible within the boundary layer, but cannot be treated as trajectories, since all of the data for each wind run is from a single location. Figure 7, which is a reproduction of Figure 2 from Li et al. 2020, shows an example of wind runs for cases with high recirculation and low recirculation. Each hourly wind vector calculated during the day for a single monitoring site is added together for make a daily wind run.

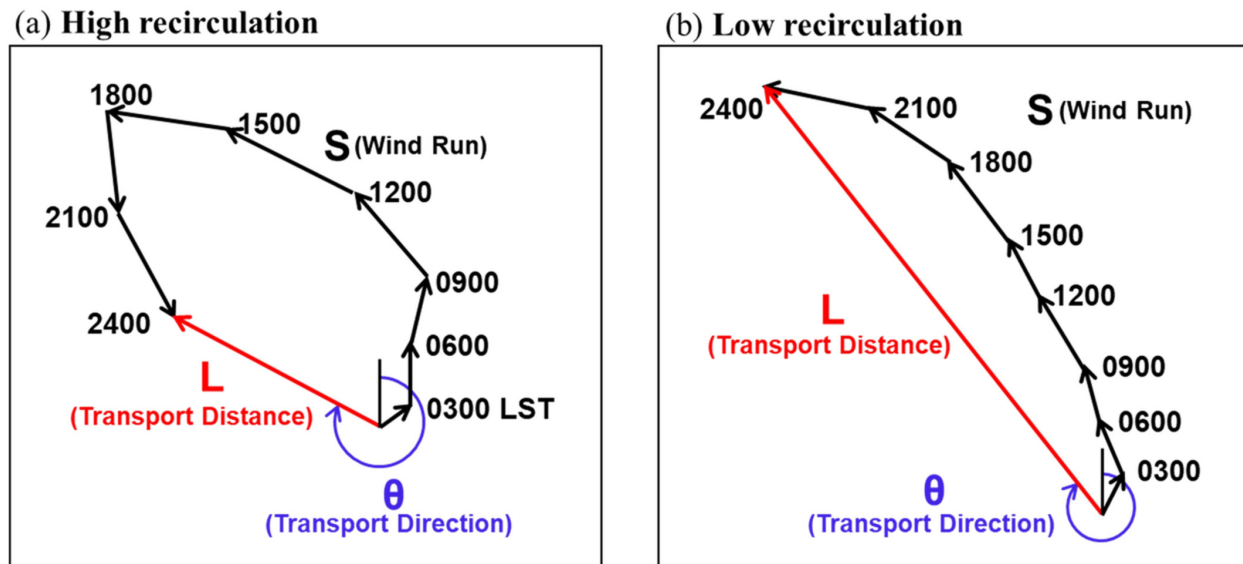


**Figure 7:** Reproduction of Figure 2 in Li et al. 2020 showing (a) high and (b) low recirculation scenarios. The black arrows show the wind vectors for three-hour periods. The transport distance  $L$  is the magnitude to of the vector sum of a 24-hour period (red arrow). The wind run  $S$  is the sum of the magnitudes of the three-hour periods in a 24-hour period. The transport direction is shown by the angle in blue.

For this report, the wind run starts from the 00 MST hour, located at  $(0, 0)$  on the graph, and concludes on the 23 MST hour. The figures show wind vectors for each hour. The red arrow represents the vector sum and its length is the transport distance  $L$ . The total distance of all of the hourly wind vectors (i.e., the sum of the magnitudes of the wind vectors) we denote  $S$ . The parameter related to the amount of potential recirculation is given by the ratio of  $1 - L/S$ , which ranges from 0 (no recirculation) to 1 (much recirculation) (Levy, Dayan, and Mahrer 2008). Wind runs from different locations can show how much the wind pattern for a given day varies through the urban area. Quite often, ozone exceedance days exhibit distinctive wind run patterns (e.g., Li et al., 2020). One major difference in El Paso, however, is that different wind monitors will show very different wind run patterns on the same day due to the complex local terrain.

The wind runs in Figure 8 show what may be a typical pattern for an exceedance day at the C12 UTEP monitor where the units on each axis are miles. The winds are slow, very light in the later

afternoon, and out of the ESE. Twenty-one of the 28 days in 2017, 2019, and 2020 where the C12 UTEP monitor exceeded the ozone standard fit this general surface wind flow pattern in the late morning and early afternoon and the other 7 days showed stagnation and/or recirculation.

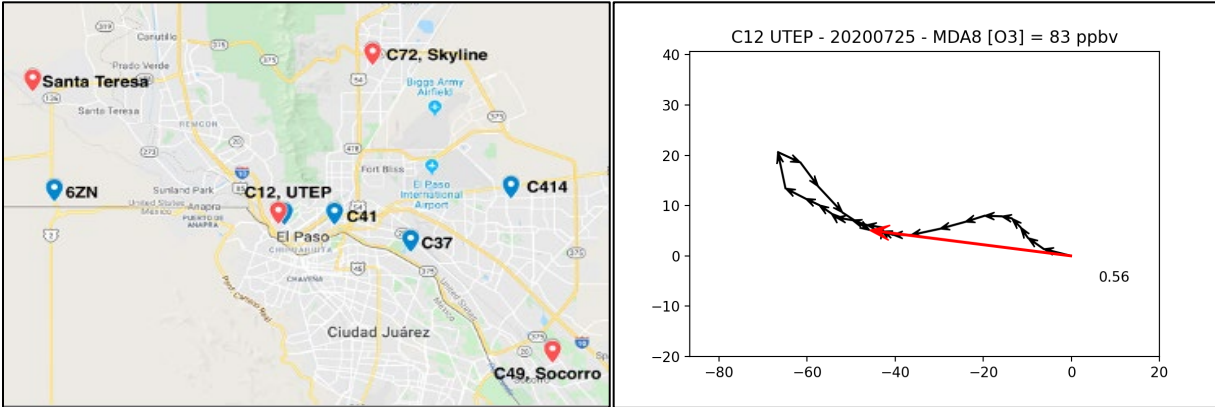


**Figure 8:** The left image shows the El Paso area and the locations of air monitoring stations along with the launch site at UTEP. Wind runs from 25 July 2020 are shown for C12 UTEP (right) for which the units on each axis are miles.

### 2.1.2.2 1 August 2020

In what was an exceedance day at multiple monitors in the El Paso area, the wind runs show stagnant air in the mid to late afternoon. At the C12 UTEP monitor, the winds were out of the E-ENE in the morning but were out of the ESE (when not almost entirely stagnant) in the afternoon.

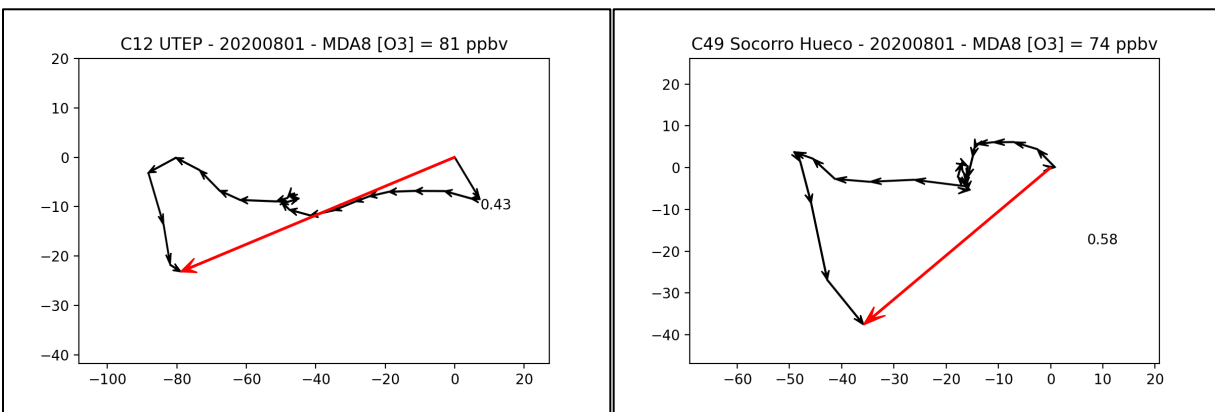


**Figure 9:** Wind runs from 1 August 2020 are shown for C12 UTEP (left) and C49 Socorro Hueco (right).

### 2.1.2.3 4 August 2020

The high monitors for ozone were C49 Socorro Hueco (MDA8 [O<sub>3</sub>] of 74 ppbv, located on the southeast of El Paso) and C72 Skyline Park (MDA8 [O<sub>3</sub>] of 74 ppbv, located on the north side of El Paso), and for C414 Ivanhoe (MDA8 [O<sub>3</sub>] was 71 ppbv, located on the east side of El Paso).

Ozonesonde Launches for San Antonio and El Paso – Final Report  
 PGA 582-20-10914-009

The surface wind speeds at C49 Socorro Hueco were typically 1-2 m/s throughout the day and the wind direction was highly variable. The surface wind speeds at C72 Skyline Park were out of the south in throughout the morning before switching to being more out the east at slow speeds 1-2 m/s in the early to mid-afternoon and stronger westerly winds in the evening hours.

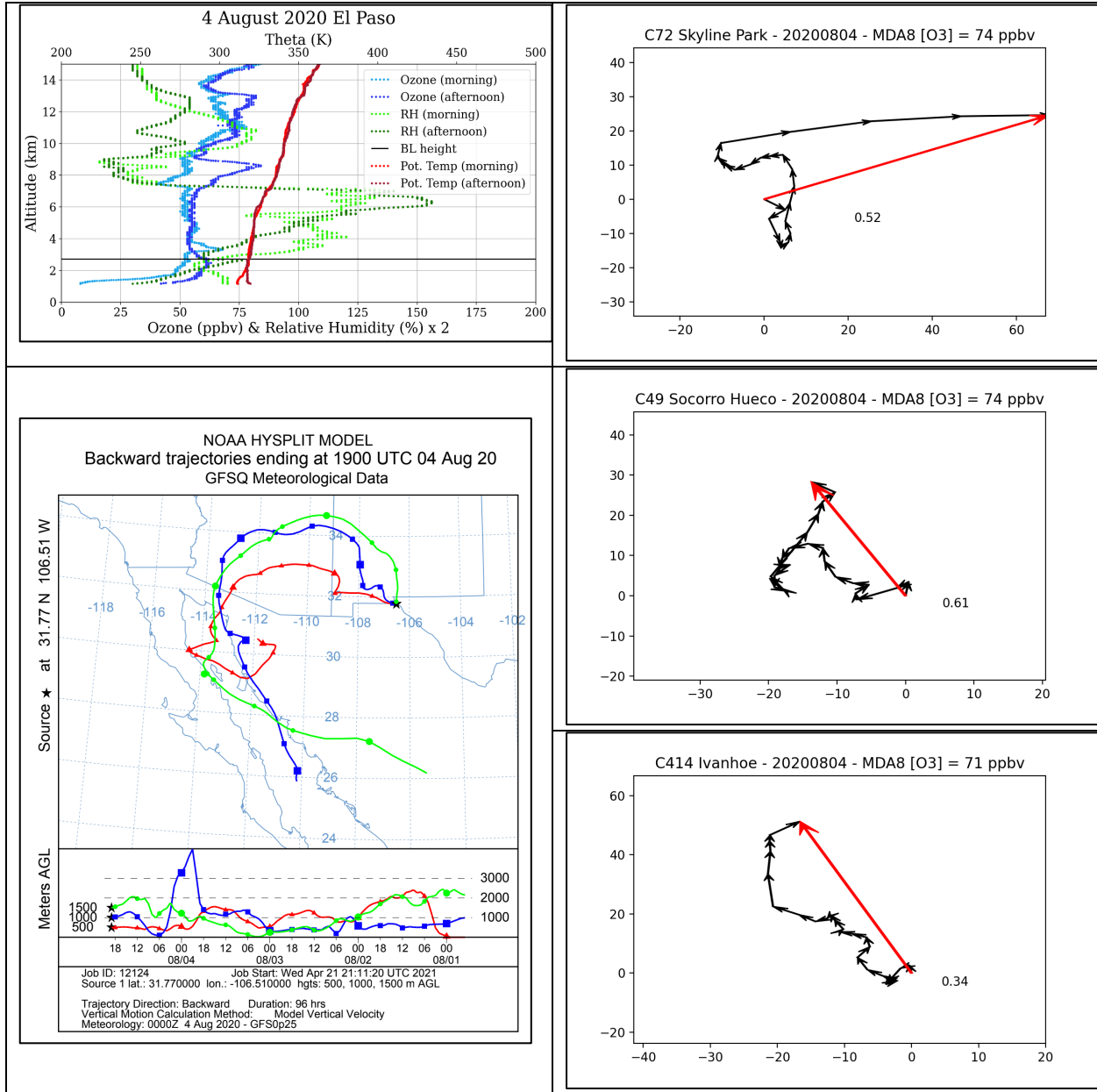


**Figure 10:** The five images shown are for 4 August 2020. Top left: Tropospheric profiles for a pair of flights (one at dawn and the other in the early afternoon) from the UTEP campus in El Paso. The black line shows the afternoon boundary layer height, the light blue and light green are the morning ozone and RH data, while the dark blue and dark green are the afternoon ozone and RH data respectively. Bottom left: HYSPLIT back trajectories for the boundary layer air measured during the afternoon flight. The three panels on the right are wind runs shown for C72 Skyline Park (top right), C49 Socorro Hueco (middle right), and C414 Ivanhoe (bottom right).

#### 2.1.2.4 8 August 2020

This day was an exceedance day at multiple monitors in the El Paso area, including C12 UTEP (MDA8 ozone concentration of 85 ppbv), C41 Chamizal and C72 Skyline Park (each 73 ppbv). At the C12 UTEP monitor, the winds were out of the ESE throughout the afternoon, which is common when the C12 monitor has MDA8 ozone concentrations that are more than 10 ppbv higher than what is measured at other monitors in the El Paso region. Winds in this direction place the C12 monitor downwind of many of the urban emissions in the El Paso – Juarez area.

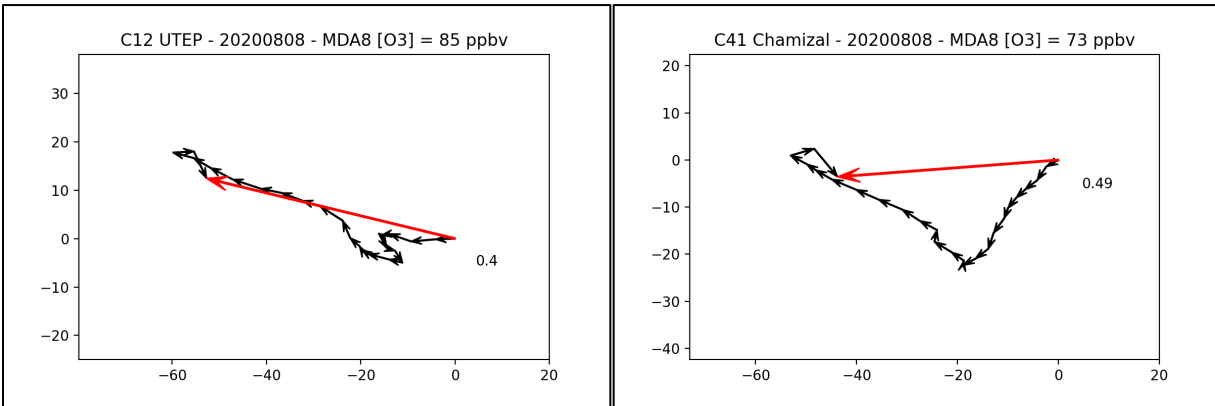


**Figure 11:** Wind runs from 8 August 2020 are shown for C12 UTEP (left) and C41 Chamizal (right).

#### 2.1.2.5 14 August 2020

The high monitors for ozone were C49 Socorro Hueco (MDA8 [O<sub>3</sub>] of 74 ppbv) and for C37 Ascarate Park SE (MDA8 [O<sub>3</sub>] of 71 ppbv). At both locations, the winds speeds were slow to stagnant in the afternoon. The ozone concentrations in the morning boundary layer were near 0, indicating significant ozone titration overnight. Such profiles suggest significant production potential after sunrise as available NO<sub>x</sub>, which contributed to the overnight titration, now contributes to morning production. The morning profile also shows residual layer ozone concentrations of 50 – 55 ppbv (near 3 km asl, light blue data). The subsequent afternoon profile (dark blue) shows enhancements of boundary layer ozone to around 60 ppbv.

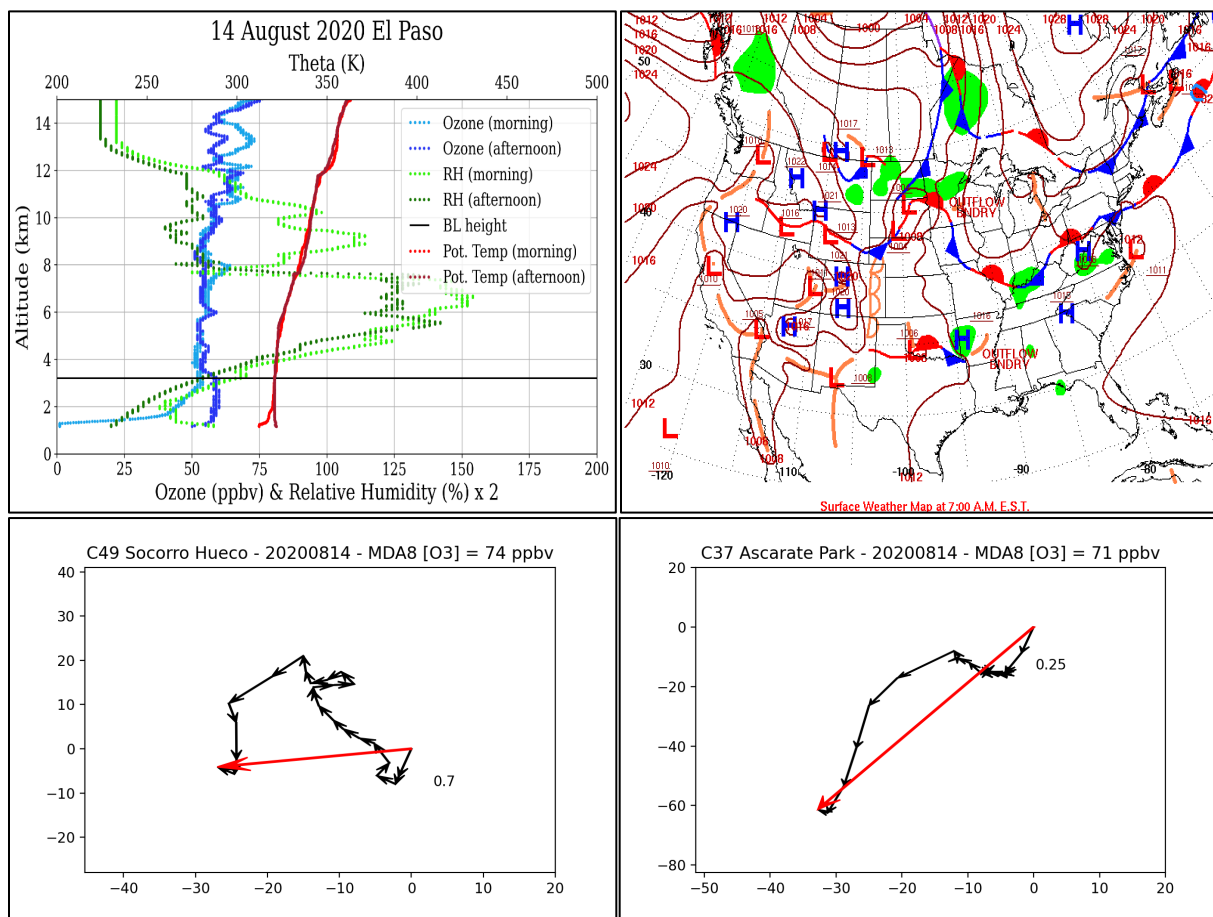


**Figure 12:** The four images shown are for 14 August 2020. Top left: Tropospheric profiles for a pair of flights (one at dawn and the other in the early afternoon) from the UTEP campus in El Paso. The black horizontal line shows the afternoon boundary layer height. Top right: Weather map. Bottom left: Wind run from the C49 Socorro Hueco monitor. Bottom right: Wind run from the C37 Ascarate Park SE monitor.

### 2.1.2.6 19 August 2020

The MDA8 [O<sub>3</sub>] for C414 Ivanhoe was 73 ppbv, C12 UTEP was 72 ppbv, and C72 Skyline Park was 71 ppbv. The HYSPLIT back trajectories show anti-cyclonic flow around high pressure centered in Colorado. At C414 Ivanhoe, the wind speeds were slow and showed signs of recirculation. At C12 UTEP, the winds were slow and out of the ESE. Throughout the day, the wind speeds at C72 Skyline Park were slow and out of the south. The ozone concentrations in the morning boundary layer were near 0, indicating significant ozone titration overnight. Such profiles suggest significant production potential after sunrise as available NO<sub>x</sub>, which contributed to the overnight titration, now contributes to morning production. The morning profile also shows residual layer ozone concentrations > 60 ppbv (near 2 km, light blue data), providing an elevated starting point for morning ozone production as well. We note the lower altitude of the morning residual layer on this date as compared with the altitude of the morning residual layer on 14 August. The subsequent afternoon profile (dark blue) shows enhancements of boundary layer ozone > 80 ppbv, with surface concentrations > 75 ppbv).

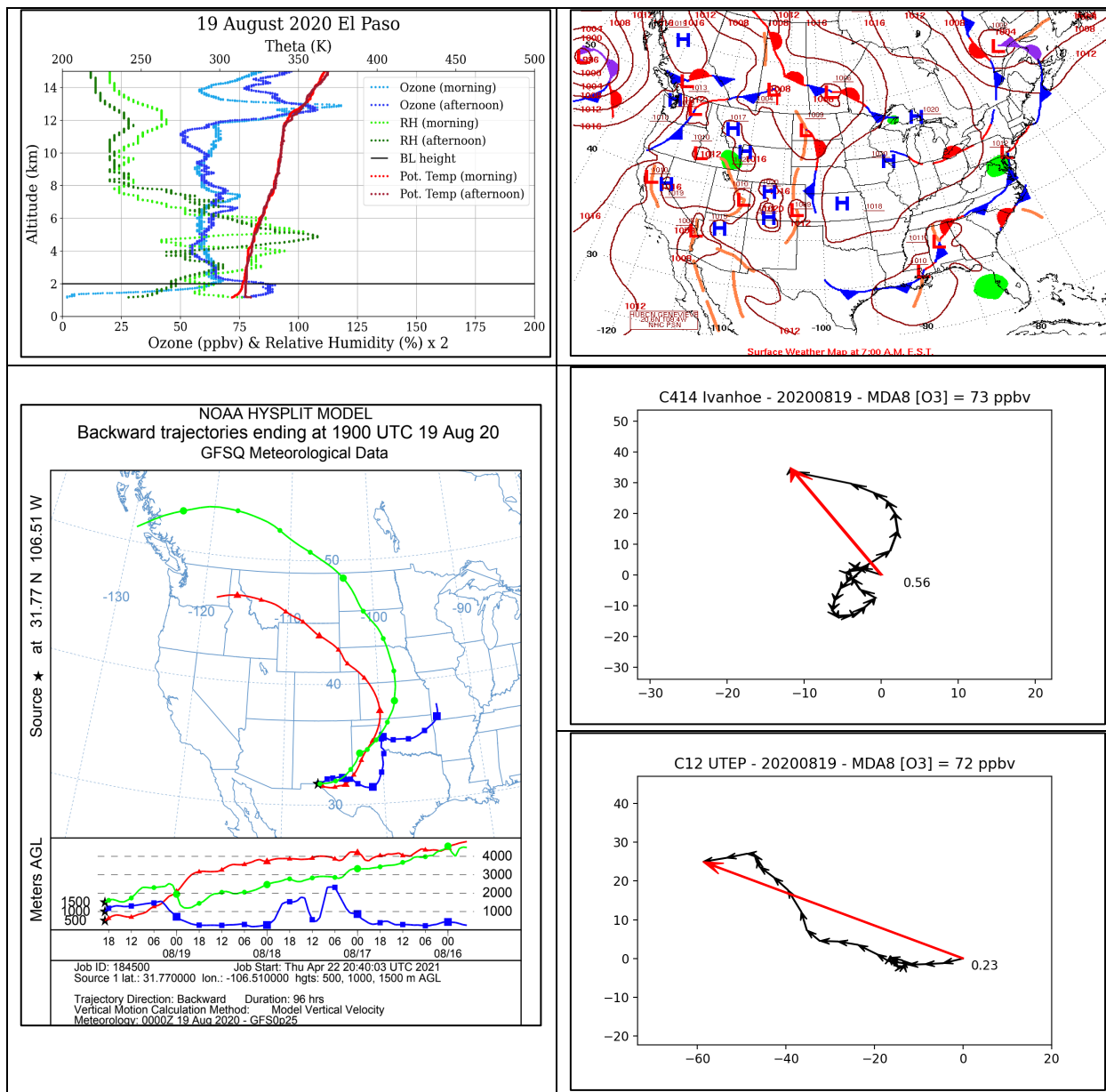
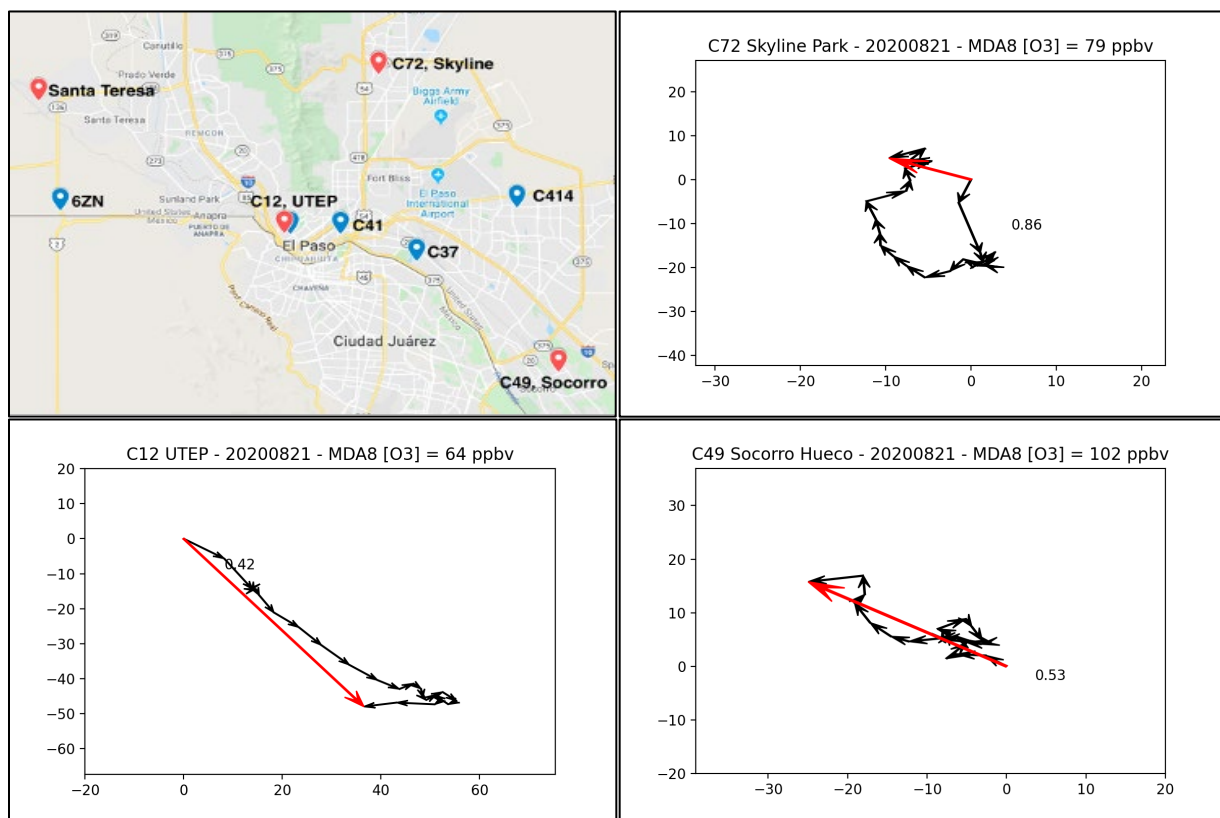


**Figure 13:** The five images shown are for 19 August 2020. Top left: Tropospheric profiles for a pair of flights (one at dawn and the other in the early afternoon) from the UTEP campus in El Paso. The black line shows the afternoon boundary layer height. Top right: Weather map. Bottom left: HYSPLIT back trajectories for the boundary layer of the afternoon flight. Wind runs are shown for C14 Ivanhoe (middle right) and C12 UTEP (bottom right).

### 2.1.2.7 21 August 2020

On this day, the C49 Socorro monitor recorded the highest MDA8 ozone concentration (102 ppbv) in the state of Texas during 2020. The wind runs starting at the monitors C12, C49, and C72 shown in Figure 14 all differ considerably. At the C12 UTEP monitor, the winds were out of the WNW (in the direction of less densely populated areas) in the morning and became stagnant later in the day. The background air that contributed to the readings at the C12 monitor

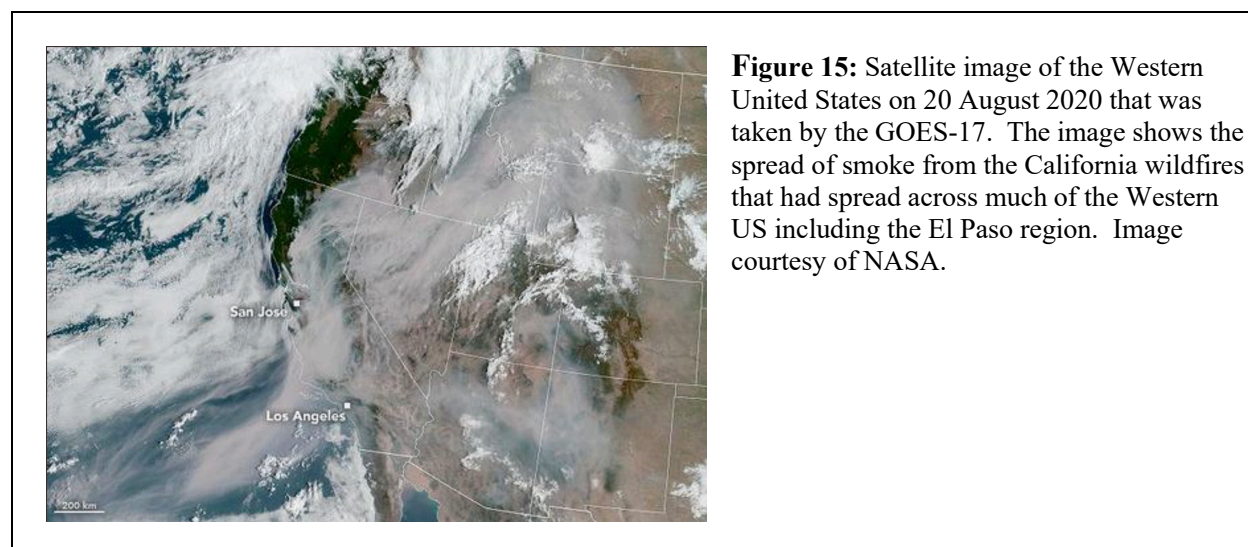
(MDA8 ozone concentration of 64 ppbv) may have been rather different than the background that contributed to what was observed at the C49 and C72 monitors. At C72 Skyline Park, located located north of El Paso and east of the Franklin mountains, the winds were fairly stagnant in the morning and then there were slow winds out of the south throughout the afternoon. The visibility at the C37 Ascarate Park monitor was lower (reaching a low of 6.57 miles during the 9 pm MST hour) and the PM<sub>2.5</sub> levels were elevated compared with the three days preceding and after 21 August. At the C12 UTEP, C41 Chamizal, the C49 Socorro Hueco monitors, the PM<sub>2.5</sub> levels were also elevated on 21 August compared the three days preceding and after. Also, the peak in PM<sub>2.5</sub> levels on 21 August were in the late evening (i.e., the 8 pm or 9 pm MST hour) with a peak of 40.2  $\mu\text{g}/\text{m}^3$  at the C49 Socorro Hueco monitor; the next highest peak was at the C37 Ascarate Park monitor of 35.2  $\mu\text{g}/\text{m}^3$  with C12 UTEP and C41 Chamizal reaching  $> 30 \mu\text{g}/\text{m}^3$  at the same time.



**Figure 14:** The top-left image shows the El Paso area and the locations of C12, C49, and C72 along with the launch site at UTEP. Wind runs from 21 August 2020 are shown for C12 UTEP (bottom-left), C49 Socorro Hueco (bottom-right), and C72 Skyline Park (top-right).

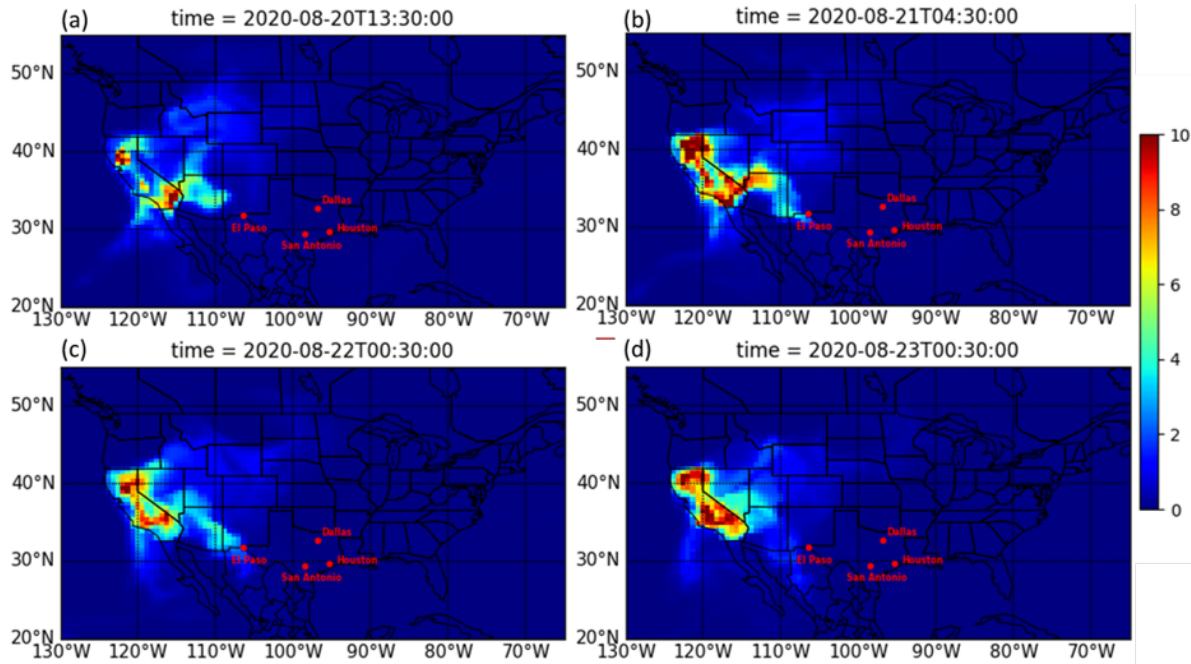
At the C49 Socorro Hueco monitor, the surface winds were stagnant throughout the morning to the late afternoon. Images from the GOES satellite (Figure 15) showed the transport of smoke from then ongoing California wildfires to throughout much of the western United States including the El Paso region. The transport of VOCs related to biomass burning may have

combined with  $\text{NO}_x$  in the local area to make for the particularly high ozone event recorded Socorro.



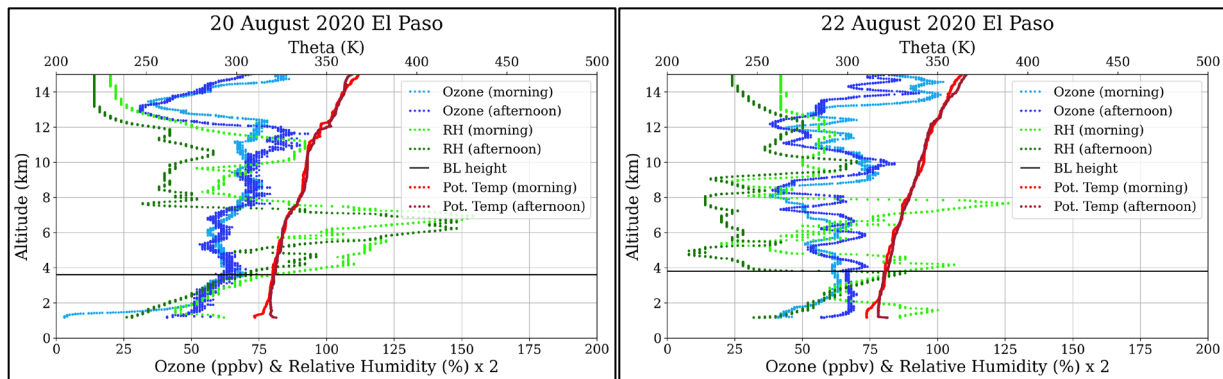
The GEOS-Chem passive tracer simulation is a useful tool to determine the air mass origins in the model, as demonstrated in our prior work investigating long-range transport of Mexican pollution (S. Wang et al. 2018). Here we designed a California tracer to track the transport of wildfire smoke to El Paso. The tracer has a fixed lifetime of 30 days, which resembles the lifetime of carbon monoxide ( $\text{CO}$ ) in the warm season and was emitted at a constant rate ( $10^{-10} \text{ kg/m}^2/\text{s}$ ) from California. The transport was driven by Modern-Era Retrospective analysis for Research and Applications, version 2 (MERRA-2) data with a native resolution of  $0.5^\circ \times 0.625^\circ$  over North America, using lateral boundary conditions updated every 3 hours generated from a global GEOS-Chem simulation with a horizontal resolution of  $2^\circ \times 2.5^\circ$ .

Figure 16 shows maps of the California tracer on four days that clearly depict the transport of the wildfire smoke to El Paso, with the most likely days for influence being 21 and 22 August (the upper right and lower left panels in the figure). On the wildfire day of 20 August, the air mass originating from southern California was traveling toward south until its first arrival at El Paso at about 04:30 MDT of 21 August (Figure 16a-b). This transport continued for the rest of the day (Figure 16c) and weakened by the end of 22 August (Figure 16d), contributing to the high  $\text{O}_3$  concentrations on both days.



**Figure 16:** Maps of the California tracer below 500m at 13:30 20 August 2020 (a), 04:30 21 August 2020 (b), 00:30 22 August 2020 (c), and 00:30 23 August 2020 (d). The time is in CDT. The color bar is for reference only, not representing the real concentrations.

Twice daily ozonesonde flights occurred on the day before (20 August 2020) and the day after (22 August 2020) and are shown in Figure 17. Both sets of profiles, particularly that those on 22 August 2020, show a positive gradient in ozone above the top of the boundary layer (marked by the black horizontal line), which is often indicative of transport.



**Figure 17:** Early morning and afternoon ozonesonde profiles on 20 August 2020 (left) and 22 August 2020 (right).

2.1.2.8 22 August 2020

The MDA8 [O<sub>3</sub>] for C49 Socorro Hueco was 73 ppbv and C12 UTEP was 72 ppbv. This was the day after the highest ozone day of the year where the C49 Socorro Hueco monitor had an MDA8 [O<sub>3</sub>] of 102 ppbv.

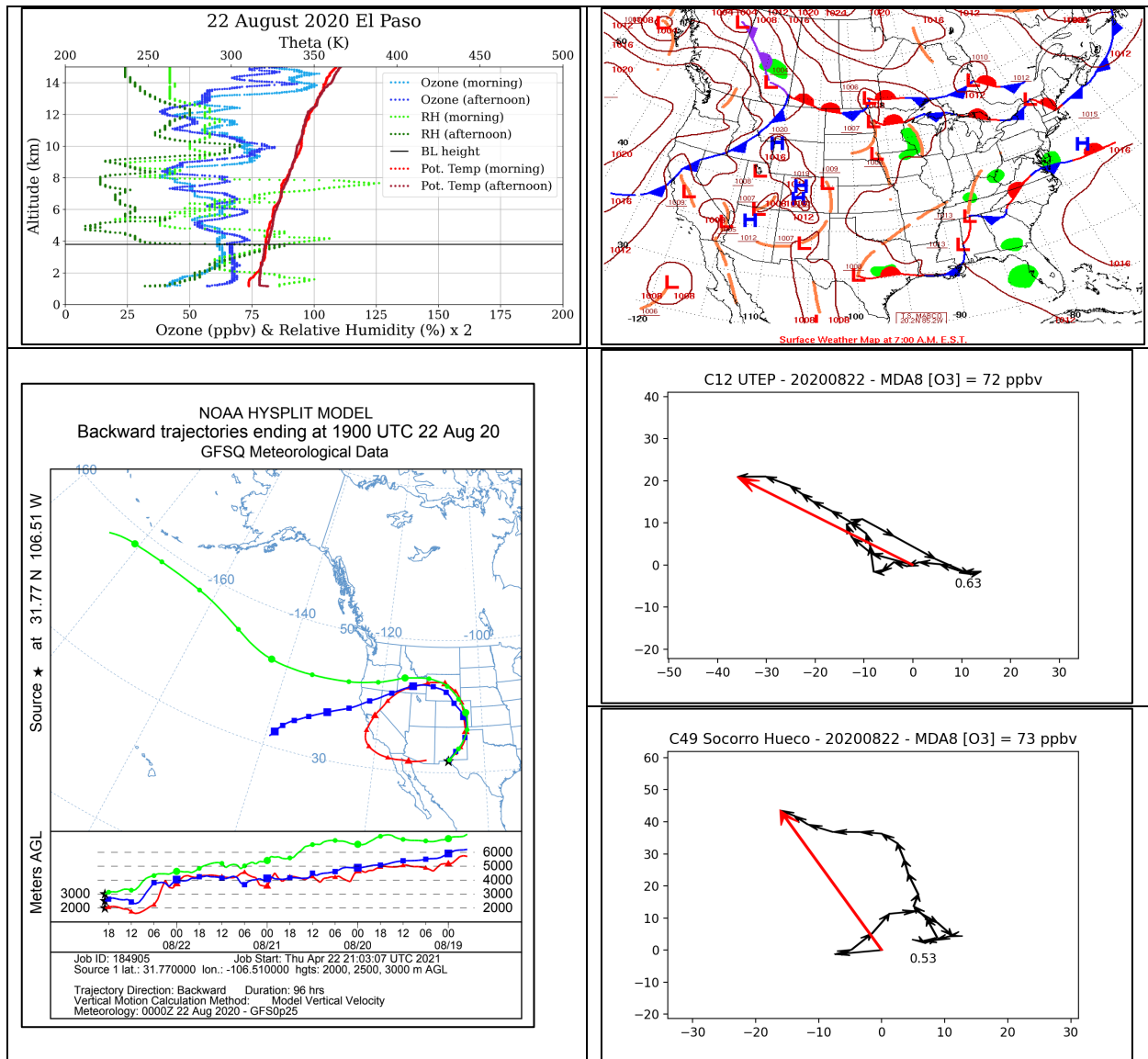


**Figure 18:** The five images shown are for August 22, 2020. Top left: Tropospheric profiles for a pair of flights (one at dawn and the other in the early afternoon) from the UTEP campus in El Paso. The black line shows the afternoon boundary layer height. Top right: Weather map. Bottom left: HYSPLIT back trajectories for altitudes 2000 m, 2500 m, and 3000 m above ground level of the afternoon flight. Wind runs are shown for the C12 UTEP monitor (middle right) and the C49 Socorro Hueco monitor (bottom right).

Ozone in the morning residual layer on this day (light blue data in the upper left panel of Figure 18) showed concentrations > 60 ppbv from 3 – 4 km. The afternoon ozone profile shows enhancements relative to the morning profile from the surface up to ~4.5 km, including a

positive gradient at the top of the boundary layer near 4 km. Such positive ozone gradients moving up from the boundary layer into the lower free troposphere are often indicative of influences from long-range transport events. The high ozone day on 21 August 2020 may have been influenced by the wildfires in California, with some residual effects contributing to continued high ozone on 22 August. At C12 UTEP, the winds were slow and there was some recirculation though the overall direction was out of the ESE. At C49 Socorro Heuco, there was a fair amount of recirculation and changing wind direction with near stagnant air throughout the late morning and early afternoon. The HYSPLIT back trajectories at 2000 m above ground level (AGL; lower left panel in Figure 18) trace the air mass history back through the wildfire region in California in the prior 3-4 days.

#### **2.1.2.9 27 August 2020**

The MDA8 [O<sub>3</sub>] was 71 ppbv at C12 UTEP, which was the only monitor in the El Paso area to exceed the ozone standard on this date. At C12 UTEP, the winds were consistently slow and out of the ESE throughout the course of the entire day (Figure 19). All of the monitors had similar prevalent wind directions (varying from ESE to SSE). The overall flow pattern may have been influenced by the Hurricane Laura (seen making landfall in western Louisiana in the weather map in the upper right panel of Figure 19). The profiles show high relative humidity in the lower troposphere. Morning residual layer ozone concentrations (see in the light blue ozone profile in the upper left panel of Figure 19) were generally 50 – 60 ppbv, with a thin layer > 70 ppbv just above 4 km AMSL. Subsequent afternoon boundary layer ozone concentrations (dark blue ozone profile in Figure 19) were around 70 ppbv, with a negative gradient seen at the top of the boundary layer near 4 km.

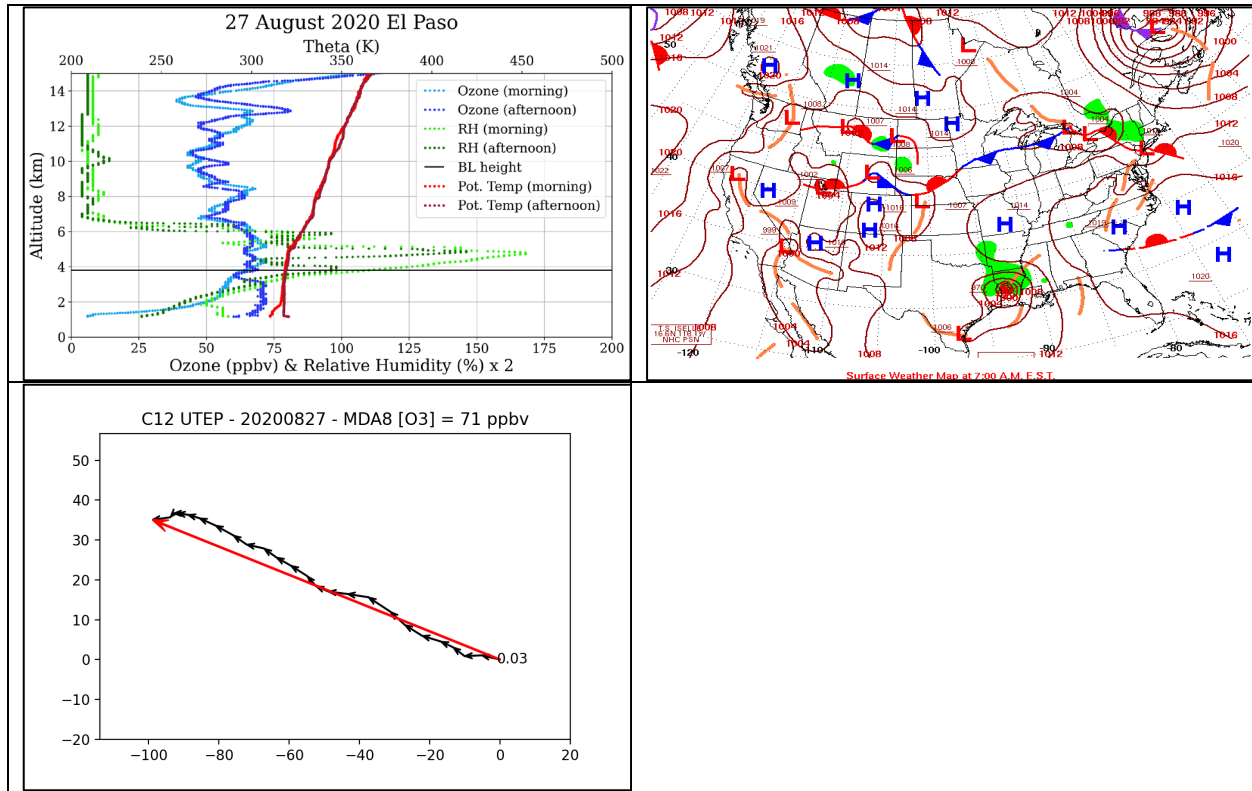


**Figure 19:** The three images shown are for 27 August 2020. Top left: Tropospheric profiles for a pair of flights (one at dawn and the other in the early afternoon) from the UTEP campus in El Paso. The black line shows the afternoon boundary layer height. Top right: Weather map. Bottom left: Wind run from the C12 UTEP monitor.

### 2.1.2.10 29 August 2020

The MDA8 ozone concentration C12 monitor was 72 ppbv on 29 August 2020. This day was one on which an ozonesonde was not flown due to the projected balloon trajectory landing site. The wind run shown in Figure 20 shows that while winds were primarily out of the WNW (atypical for a day in which the C12 monitor exceeds the ozone standard), there was a flow reversal leading to some recirculation in the late morning and early afternoon.

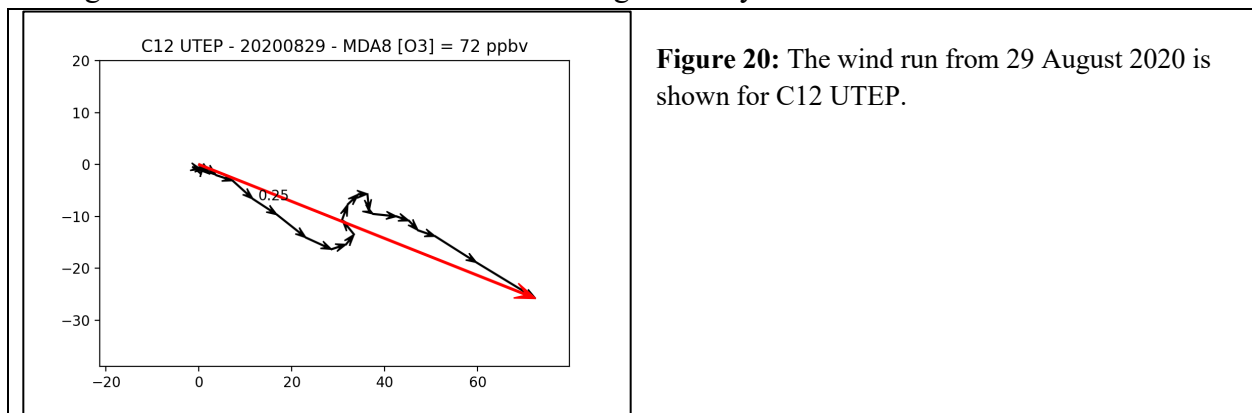
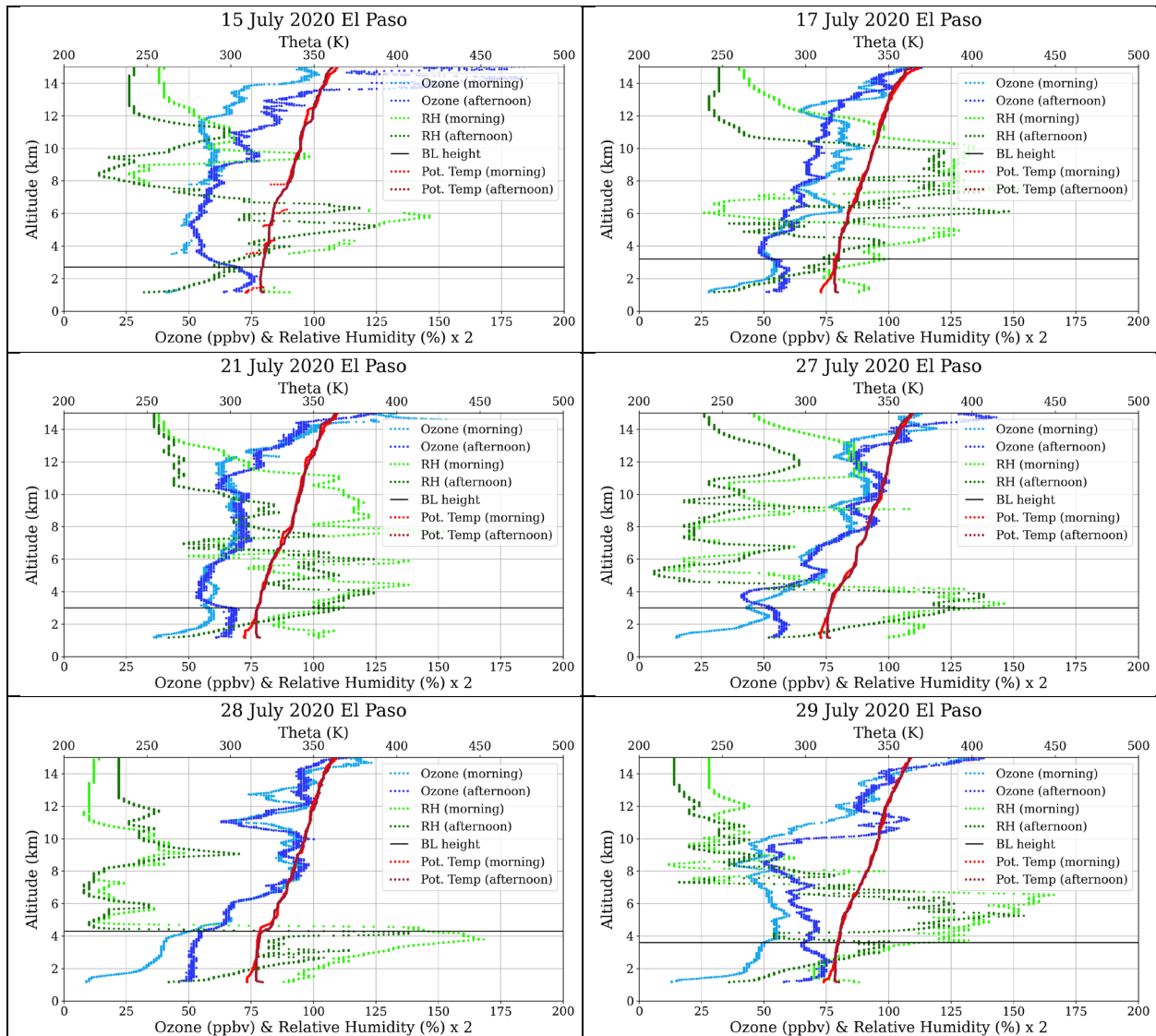


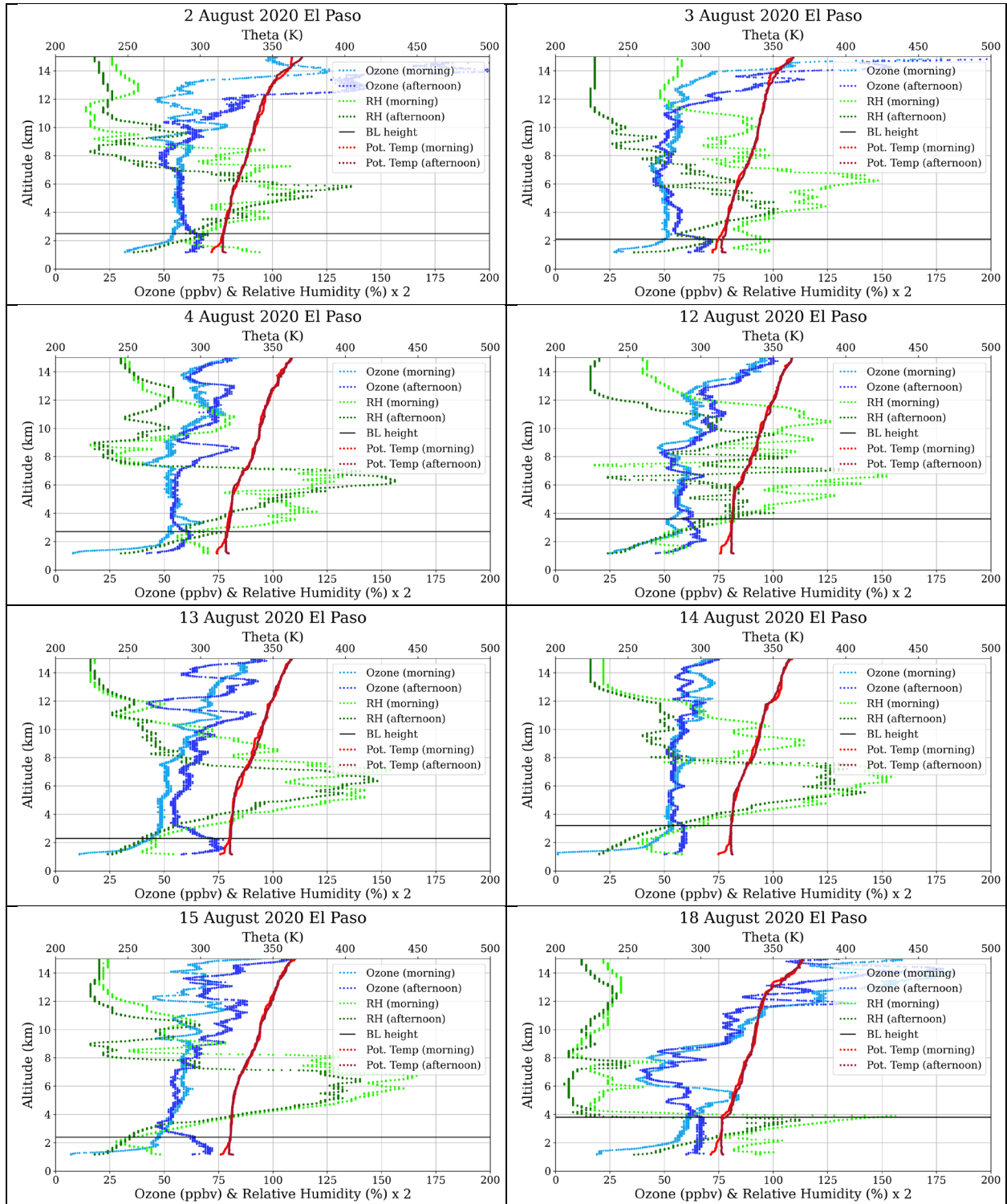
**Figure 20:** The wind run from 29 August 2020 is shown for C12 UTEP.

### 2.1.3 Profiles of 2020 El Paso Dawn and Afternoon Paired Flights

Of the 41 ozonesondes flown from El Paso in 2020, 40 of them were flown in pairs (i.e., 20 paired flight days): one flight at dawn to capture the residual layer and another flight coinciding with the peak afternoon ozone. Figure 21 shows the tropospheric profiles of 19 paired flight days and provides information about the contribution of the residual layer to the ozone that measured in the afternoon. The black line in each panel shows the boundary layer height for the afternoon flight. The afternoon boundary layer height can be found from when there are simultaneously strong gradients in the ozone concentration, the relative humidity, and where the potential temperature reaches the same value it has at the surface (Haman, Lefer, and Morris 2012). In cases where the boundary layer height of the afternoon flight was difficult to discern (e.g., 12 – 15, 20, and 27 August, and 3 September 2020), the potential temperature was used. Note that for the morning flight of 15 July 2020, gaps in the data have resulted in an uneven profile with averaging processes applied, particularly for potential temperature (light red) data.



Ozonesonde Launches for San Antonio and El Paso – Final Report  
PGA 582-20-10914-009



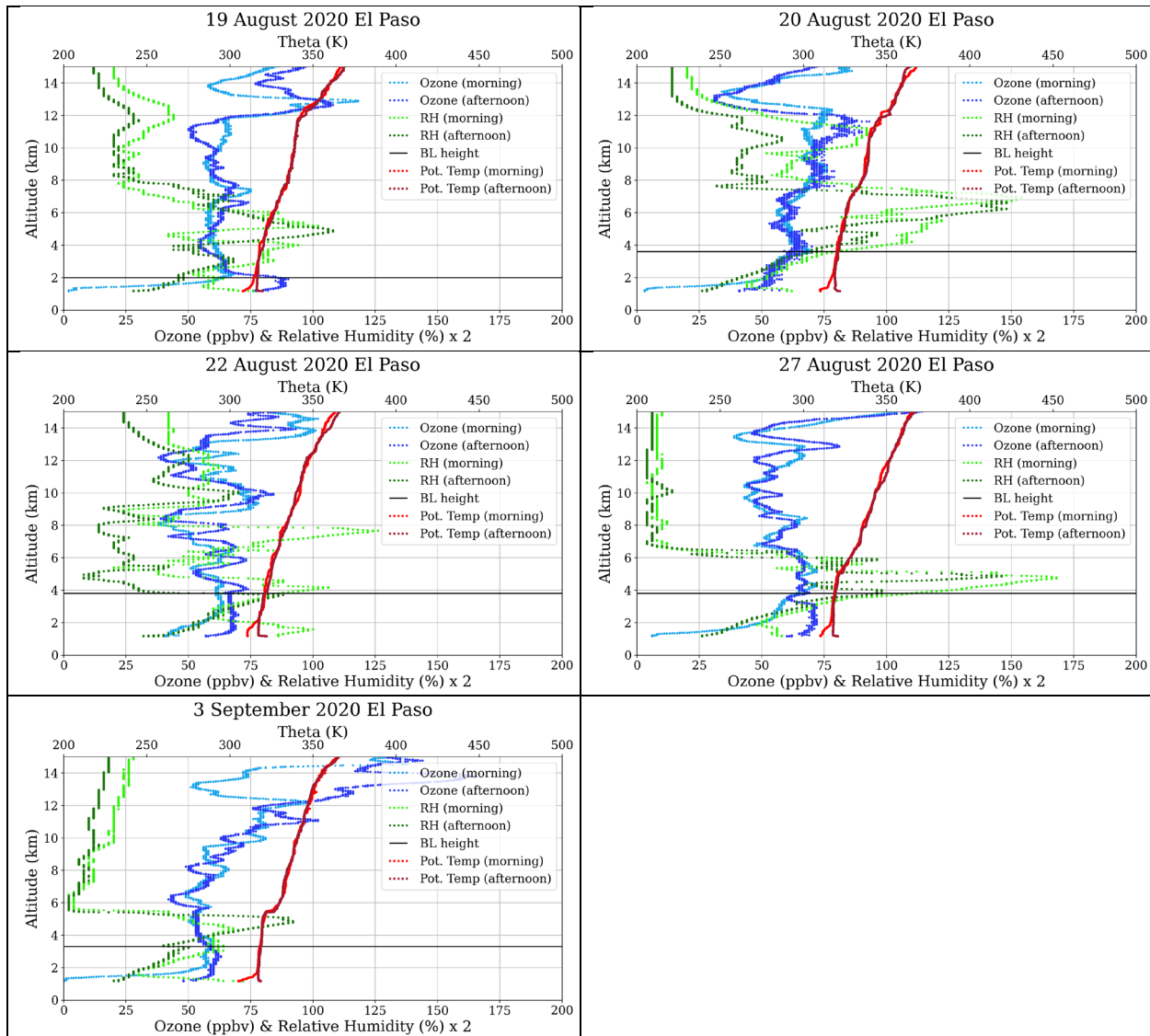


**Figure 21:** Tropospheric profiles for 19 days where flights were flown in pairs (one at dawn and the other in the early afternoon) from the UTEP campus in El Paso. The black horizontal line shows the afternoon boundary layer height. The morning ozone, RH, and potential temperature data are light blue, light green, and light red respectively, while the afternoon ozone, RH, and potential temperature data are dark blue, dark green, and dark red respectively.

The ozonesonde data shown in Figure 21 indicates several factors contributing to high ozone in El Paso. First, the amount of ozone observed within the afternoon boundary layer increases, while the ozone concentrations above the afternoon boundary layer generally do not increase. The selective increase within the afternoon boundary layer strongly suggests that local ozone production is a major factor in determining peak ozone. The magnitude of the local ozone production can be quantified by examining the difference between morning and afternoon concentrations at the top of the afternoon boundary layer. Second, ozone within both the morning and afternoon boundary layers is often titrated due to local NO<sub>x</sub> emissions, yielding a non-

uniform ozone profile within the boundary layer, and suggesting that there are observable limits to the amount of mixing occurring within the afternoon boundary layer. Third, two ozonesonde flights found a layer of higher ozone above the afternoon boundary layer: August 18 and 22. These days could have boundary layer ozone influenced by ozone transported into the area and mixed down into the boundary layer. On Aug 20, there is very little difference between morning and afternoon ozone within the boundary layer, strongly suggesting that transported ozone comprises much of the local ozone on that day, since local ozone production is low. Fourth, an elevated layer of moist air above the afternoon boundary layer seems to coincide with low vertical variation in ozone concentrations. If the moist layer is absent, the ozone concentrations have greater vertical variation. Fifth, layers of air with extremely low humidity at altitude may be indicative of stratospheric influences. Data from July 28 shows both low humidity and high ozone within the same layer of air; the abrupt decrease in humidity above 4 km altitude corresponds to a strong increase in ozone and potential temperature. It is possible that the higher afternoon ozone includes a contribution from the stratosphere on July 28, but if so, the contribution was limited, since July 28 was not an exceedance day, and only one site in the El Paso area had MDA8 ozone over 50 ppbv.

## **2.2 2019 OZONESONDE CAMPAIGN FROM EL PASO**

During 31 July – 6 September 2019, there were a total 27 ozonesonde launches from El Paso at the UTEP campus. We chose to be aggressive early in the campaign based on the extended period of high ozone days in early August 2019. There were five days in August 2019 for which at least one monitor in the El Paso area exceeded of the 8-hour ozone standard.

Further results from the 2019 ozonesonde flights from El Paso that are not included here are available in the final report of “Ozonesonde Launches in San Antonio and El Paso,” PIs James Flynn, Paul Walter, Marilyn Wooten, and Rosa Fitzgerald, PGA Number 582-19-93513-06.

### **2.2.1 Exceedance Days in El Paso Region During 2019 Campaign**

There were five days in August 2019 that had a maximum daily 8-hour average (MDA8) ozone concentration that was above the National Ambient Air Quality Standard (NAAQS) of MDA8 [O<sub>3</sub>] > 70 ppbv: 5 August, 7 August, 8 August, 10 August, and 15 August 2019. In four of those cases El Paso monitors were in exceedance of the ozone standard and for the other case the Socorro, TX monitor (C49 Socorro Hueco) was in exceedance of the ozone standard.

#### **2.2.1.1 5 August 2019**

The highest measured MDA8 ozone concentration during the sampling period of 83 ppbv occurred at C12 UTEP on 5 August 2019. Wind speeds all throughout the troposphere were very slow (< 5 m/s from the surface to the tropopause as reported by the GPS data from the

ozonesonde flight that day) and favorable for photochemically produced ozone to remain in the local area. The image on the left in Figure 22 shows the path of the afternoon flight. The red arrow shows where the sonde passed an altitude of 55,909 feet (17 km) while still in El Paso city limits. The middle image shows the HYSPLIT back trajectories at 500 meters above ground level (AGL) for 3 different monitors. The table on the right shows the maximum daily 8-hour average (MDA8) ozone concentration for different monitors in the area.

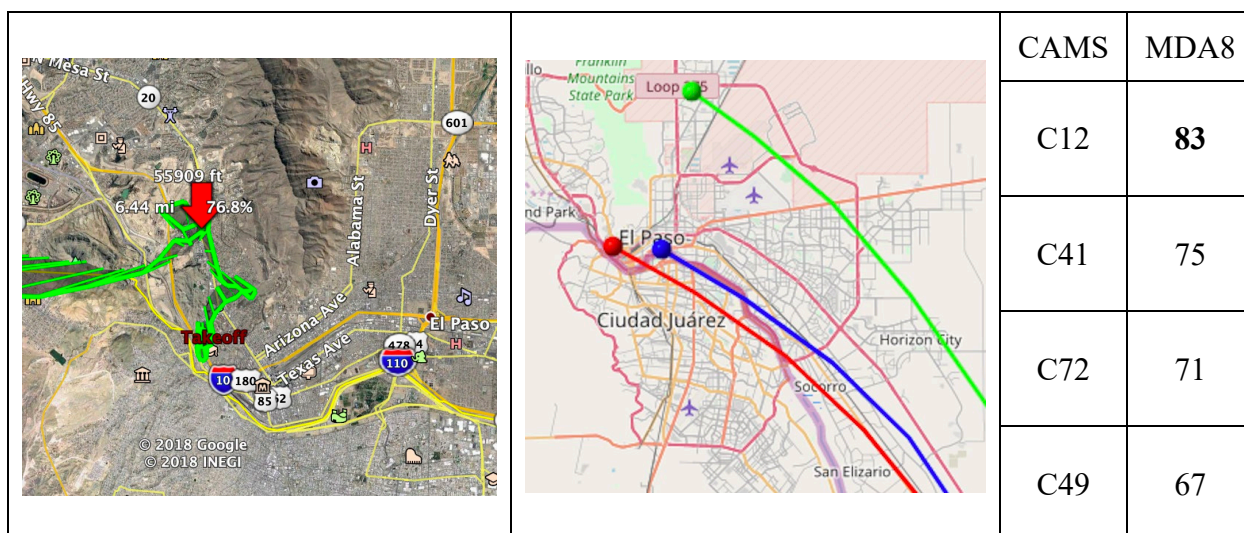


**Figure 22:** The image on the left shows the path of the afternoon flight on 5 August 2019. The middle image shows the HYSPLIT back trajectories at 500 m above ground level from C12 (red), C41 (blue), and C72 (green). CAMS 49 (Socorro) is located southeast of El Paso. The table on the right shows the MDA8 ozone concentrations for different monitors in the region.

Figure 23 shows the dawn and afternoon profiles as well as 24-hour wind run for the C12 UTEP monitor. The afternoon profile shows a high ozone concentration (~90 ppbv) near the surface that falls off ~1 km AGL while above that surface level ozone enhancement the relative humidity increases. The enhanced surface level ozone is likely the result of local effects of nearby transport or local photochemical production. The potential temperature increase above the boundary layer suggests that the high ozone feature located at about 6 km AMSL is isolated from the boundary layer air and unlikely to be a factor influencing the high ozone concentrations seen in the boundary layer this day. The residual layer in the morning ozone profile (light blue) and the lower free tropospheric ozone concentrations suggest 70 – 75 ppbv of ozone available for entrainment in the growing morning boundary layer, providing an elevated baseline (already in exceedance of the MDA8 ozone standard) that was further augmented by local ozone production. Afternoon boundary layer ozone seen in the ozonesonde profile indicate concentrations ~15 ppbv higher than the morning residual layer and lower free tropospheric values. The upwind surface monitor for this day at Socorro (C49) shows an MDA8 value 16 ppbv lower than the UTEP monitor (C12), suggesting that sources between C49 and C12 resulted in production of ~15 ppbv

of ozone. The wind run shows winds out of ESE, which is common for a day when the C12 UTEP monitor exceeds the MDA8 ozone standard.

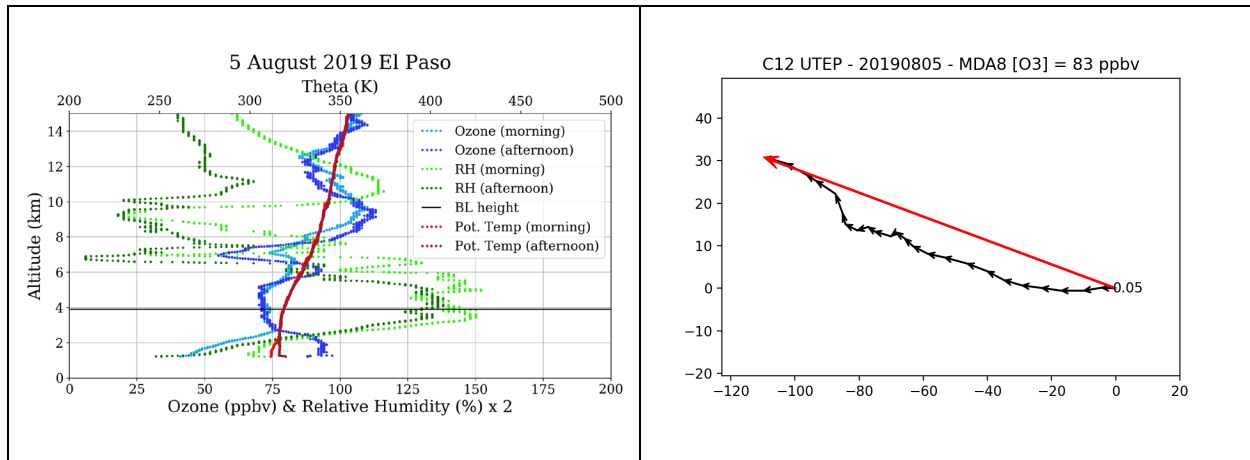


**Figure 23:** Left: The dawn and afternoon profiles from 5 August 2019. For the afternoon profile, the ozone concentration is high (~90 ppbv) near the surface and then decreases ~1 km AGL and the relative humidity is high, making UT/LS contributions unlikely. In this case, contributions to the high ozone levels are more likely from nearby, local sources, although the elevated ozone in the morning residual layer and in the lower free troposphere made conditions ripe for an ozone exceedance day at the surface. Right: The wind run for 5 August 2019 for the C12 UTEP monitor.

### 2.2.1.2 7 August 2019

In Figure 24, the dawn and afternoon profiles are shown on the image on the top left. There is a sizable gap in ozone concentrations between the dawn residual layer and the afternoon boundary layer, with the morning residual layer peaking near 70 ppbv at ~3 km AMSL and the afternoon boundary layer peaking at a slightly lower altitude near 90 ppbv, a great than typical 20 ppbv enhancement. The increase just above the boundary layer is suggestive of a change in source direction at these altitudes between the morning and afternoon profiles. Such a shift is observed in the wind runs at the surface shown in Figure 24, with northwesterly winds in the morning at C12 UTEP briefly switching to southerly winds in the late morning and early afternoon, with the afternoon sounding occurring near 1900 UTC, just before the winds shift back to northwesterly. Looking at the profile of winds in the boundary layer from the morning and afternoon sondes, we find a shift from an average of NW in the morning profile to an average of SE in the afternoon profile. We also find a wind shift from S/SE in the morning profile to S/SW in the afternoon profile at 4 – 6 km AMSL altitude.

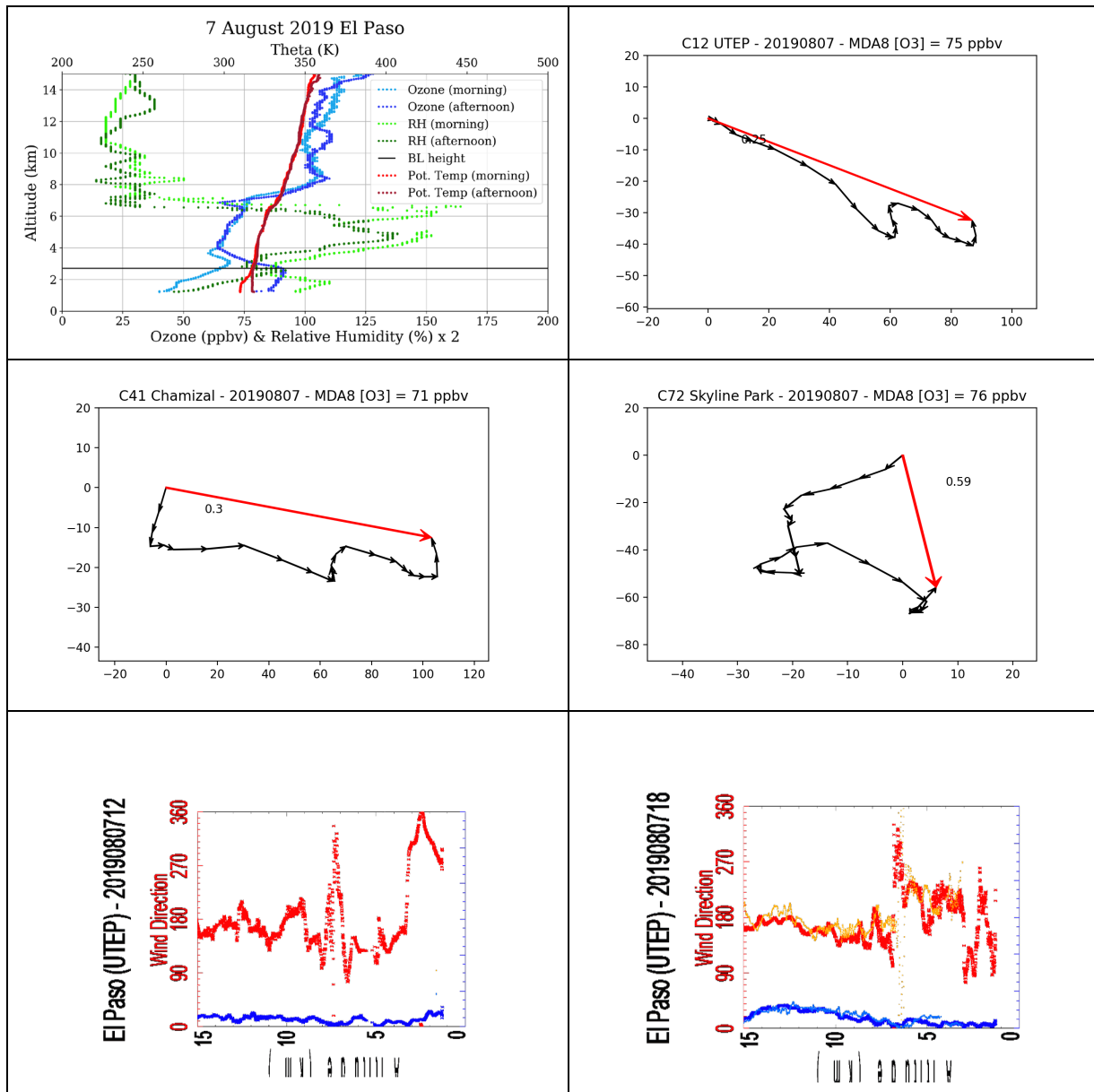


**Figure 24:** The image on the top left shows the profiles of dawn and afternoon ozonesondes for 7 August 2019. The 24-hour wind runs are shown for the C12 UTEP monitor (top right), C41 Chamizal monitor (middle left), and C72 Skyline Park monitor (middle right). The bottom two panels show the morning (left) and afternoon (right) wind speed (blue) and wind direction (red) profiles. Wind speeds are generally low throughout the troposphere at both times this day. A wind shift occurs below ~6 km.

### 2.2.1.3 8 August 2019

We did not launch ozonesondes on 8 August 2019, which was an exceedance day for the CAMS 49 Socorro Hueco monitor. In Figure 25, the monitor locations are shown on the image on the top left. The table on the top right shows the maximum daily 8-hour average (MDA8) ozone concentration for different monitors in the area. The wind runs for the C12 UTEP monitor

(bottom left) and C49 Socorro Hueco monitor (bottom right) are shown. Slow surface winds at the CAMS 49 Socorro Hueco monitor were out of the W and then SW throughout the afternoon when the ozone concentration was at its peak. The prevailing winds at the C12 UTEP monitor, which had an MDA8 O<sub>3</sub> that was 12 ppbv lower, did not exceed the ozone standard, where instead out of the NW and thus had less local urban influences.

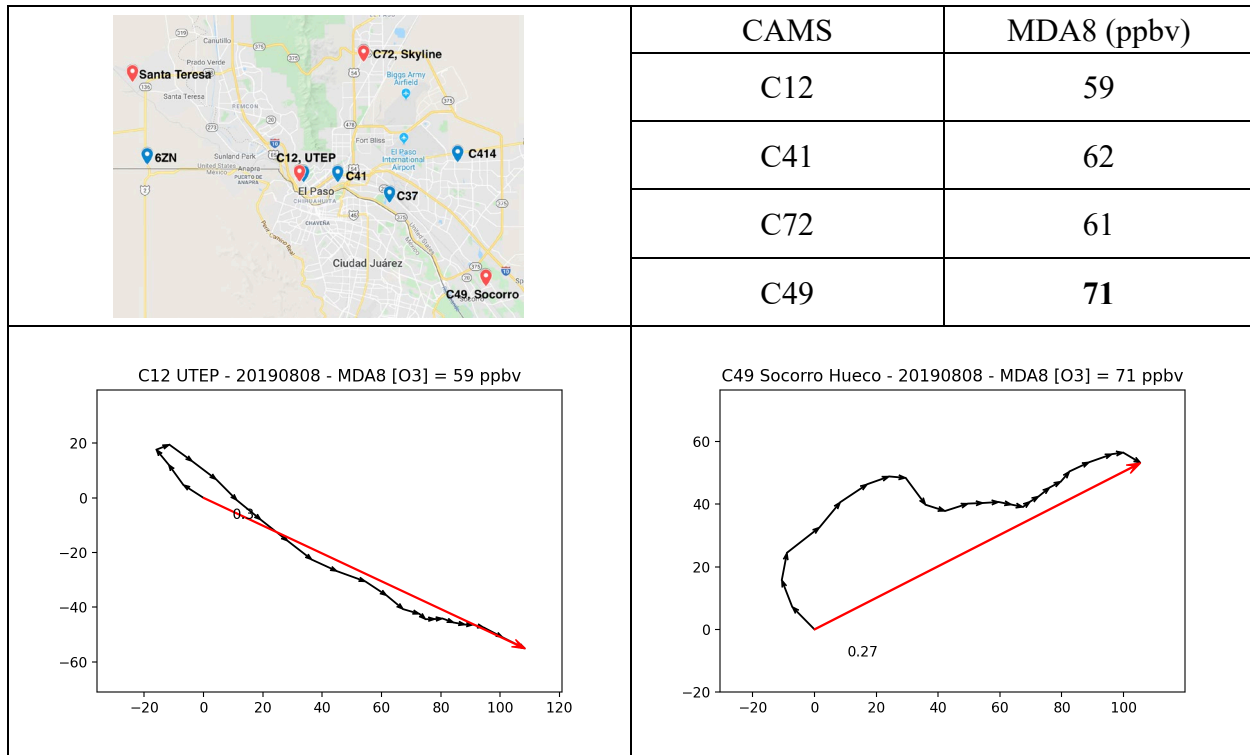


**Figure 25:** The image on the top left shows map of monitors in the greater El Paso area. The table on the top right shows the MDA8 ozone concentrations. The 24-hour wind runs are shown for the C12 UTEP monitor (bottom left) and the C49 Socorro Hueco monitor (bottom right).

### 2.2.1.4 10 August 2019

Having more clear skies than were initially projected, 10 August 2019 was also in exceedance of the ozone standard for El Paso. One ozonesonde was launched on this day in the early evening, and its profile is shown in Figure 26 (top left). The 24-hour wind runs are shown for C12 UTEP (top right), C41 Chamizal (bottom left), and C72 Skyline Park (bottom right). The C72 Skyline Park monitor, which had an MDA8 O<sub>3</sub> of 78 ppbv, observed southerly winds throughout the morning and afternoon. The C12 UTEP monitor observed NW winds that changed to stagnant and then southerly in the later morning and early afternoon. The negative gradient in the ozone concentration above the boundary layer suggests the ozone enhancement in the boundary layer was the result of nearby transport or local photochemical production.

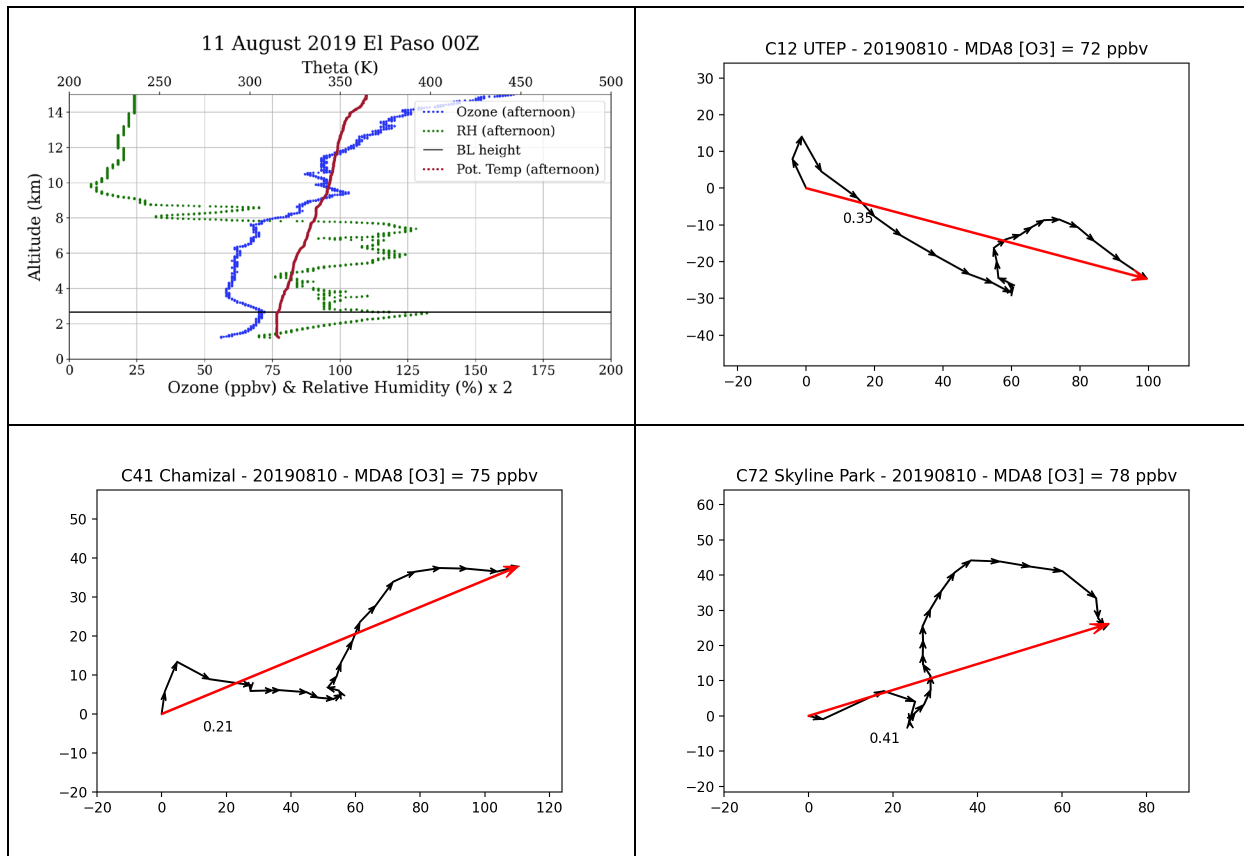


**Figure 26:** The image on the left shows the profile of the flight in the early evening on 10 August 2019. The 24-hour wind runs are shown for the C12 UTEP monitor (top right), the C41 Chamizal monitor (bottom left), and the C72 Skyline Park monitor (bottom right).

### 2.2.1.5 15 August 2019

In Figure 27, the wind runs are shown for the C12 UTEP monitor (left) and the C41 Chamizal monitor (right). The C12 UTEP wind runs show stagnant recirculating air, and the C41 Chamizal wind runs show slow southerly winds in the later morning and afternoon. The C12 monitor at UTEP reached a 1-hour ozone maximum around 1 pm MST of 89 ppbv with an 8-hour average of 75 ppbv. The C41 monitor at Chamizal reached a 1-hour ozone maximum around 4 pm MST of 83 ppbv with an 8-hour average of 71 ppbv. Four of the six monitors in the El Paso area registered 8-hour exceedances this day. The generally stagnant wind conditions and mid-day southerly flow appear to have been contributing factors.

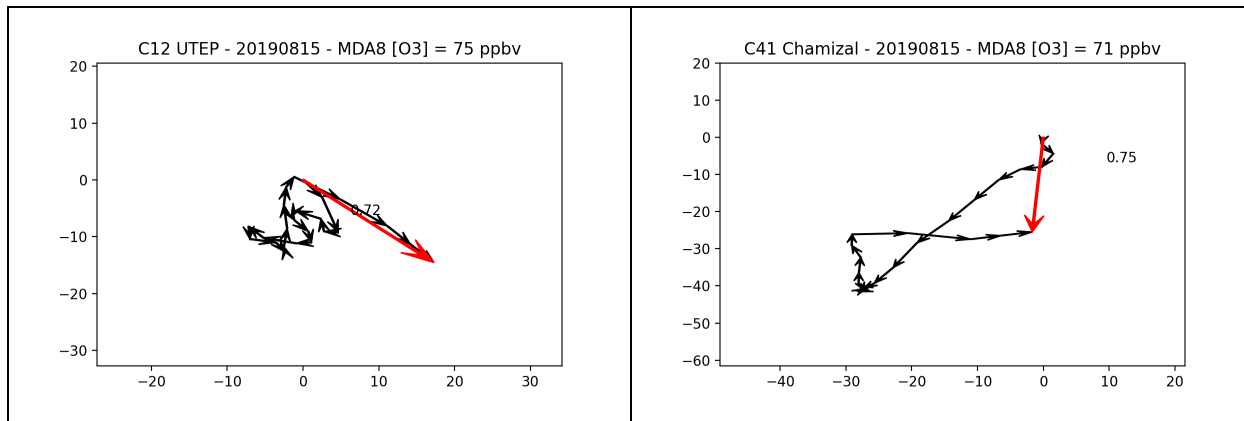


**Figure 27:** The 24-hour wind runs for 15 August 2019 for the C12 UTEP monitor (left) and the C41 Chamizal monitor (right).

### 2.2.2 Flight on 29 August 2019: Landed in Juarez

We do not launch when we believe there is a high likelihood of it landing in an urban area. On the 29 August 2019 afternoon flight, however, the balloon popped earlier than expected and landed safely at a private residence in Juarez.

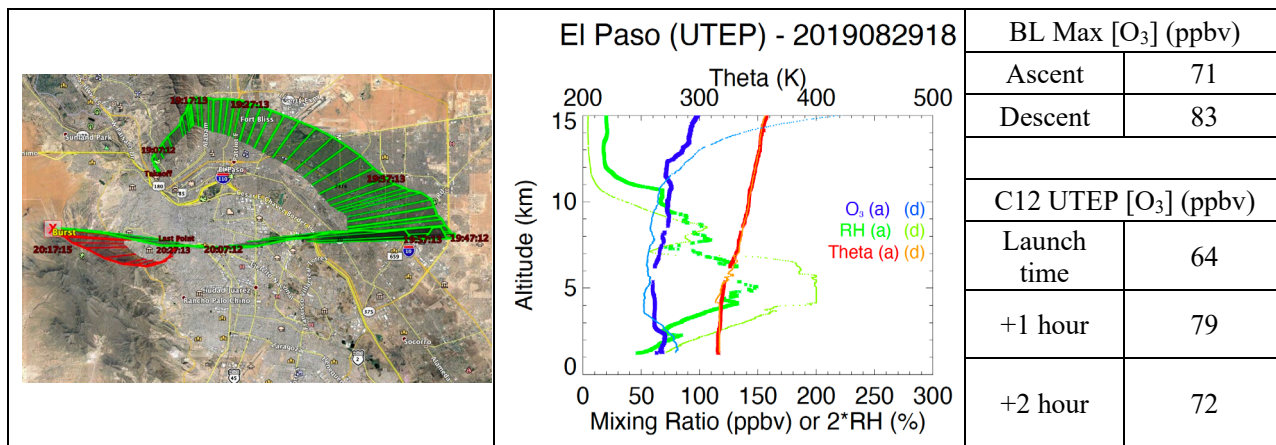


**Figure 28:** The image on the left shows the path of the afternoon flight on 29 August 2019 that landed in Juarez. The middle image shows the tropospheric profiles of ozone (blue), relative humidity (green) and potential temperature (red). The thicker lines correspond to the ascent and the thinner lines correspond to the descent. The top table on the right shows the peak ozone concentration found in the boundary layer during ascent and descent. The bottom table on the right shows the hourly averaged ozone concentrations at CAMS 12 UTEP at the time of launch as well as one and two hours after the launch.

In Figure 28, the image on the left shows the flight path with green being the ascent and red being the descent. The middle image shows the tropospheric profile of the ozone (blue), relative humidity (green), and potential temperature (red). The thick lines show the ascent data and the thin lines show data of the descent. The table on the top right shows the peak ozone concentration values in boundary layer for the ascent and descent. The boundary layer descent

over Juarez showed ozone was elevated by ~12 ppbv compared to the boundary layer conditions seen during the launch from UTEP, with the descent occurring about 90 minutes after launch (which occurred at just before 1900 UTC/1200 MST). The table on the bottom right shows the hourly ozone concentrations at the C12 (UTEP) monitor at the time of launch and one and two hours after the time of launch. The ozone was higher in those hours after the launch and thus some or perhaps all of the higher ozone that we see on the descent (~2 hours after the launch) may be attributable to local production of ozone continuing during the day rather than from differences between locations.

### 2.2.3 Possible Influence of Border-crossing Traffic to El Paso

On 10 August 2019 (an ozone exceedance day) the wind direction shifted throughout the afternoon. In Figure 29, the table on the left shows the hourly ozone concentrations and the wind directions from the C12 UTEP, C41 Chamizal, and C72 Skyline Park monitors.

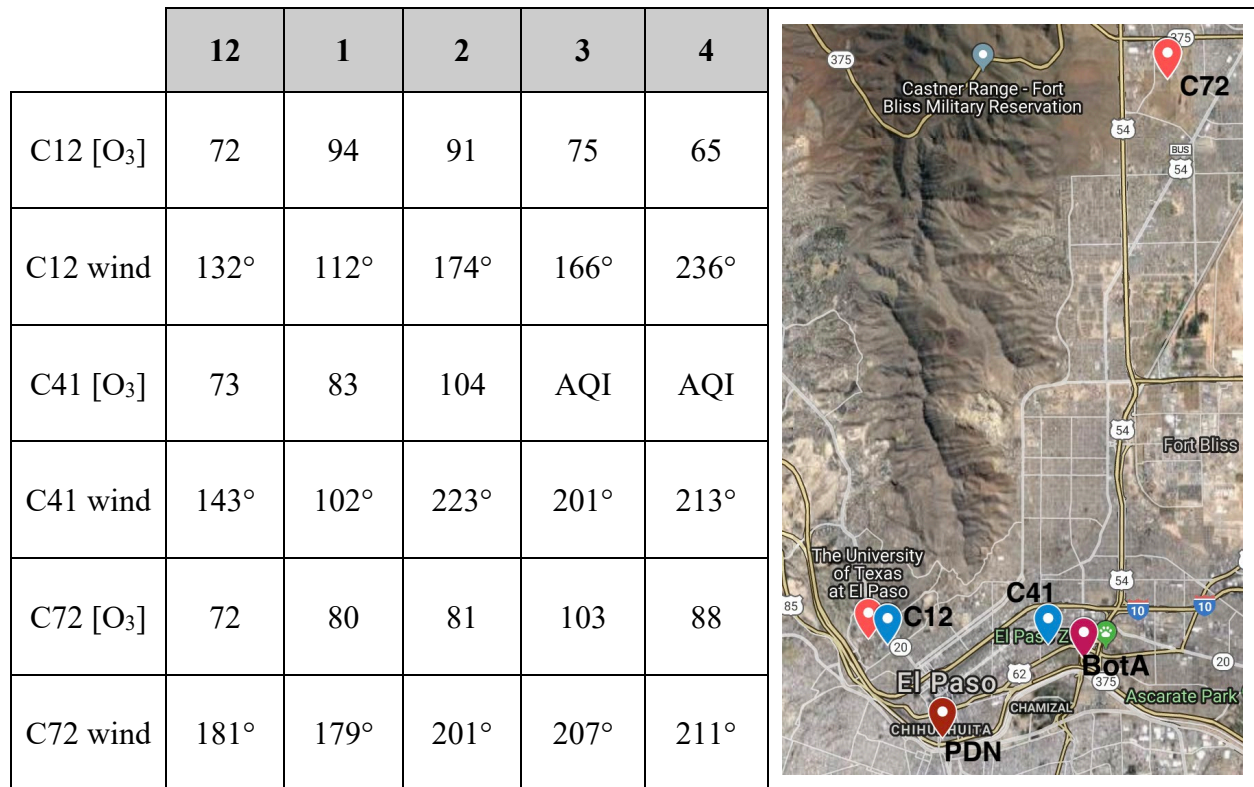


**Figure 29:** The table on the left shows the hourly ozone concentration and resultant wind direction for C12 UTEP, C41 Chamizal, and C72 Skyline Park on 10 August 2019. The top row shows the local time (MDT). The image on the right shows the locations of those monitors as well as the locations of Ports of Entry: Paso del Norte (PDN) and Bridge of the Americas (BotA).

The top row of the table in Figure 29 shows the hour in local (MDT) time. The image on the right shows the location of those monitors as well as the locations of the ports of entry Paso del Norte (PDN) and Bridge of the Americas (BotA). For the 1 pm MDT hour, the C12 ozone

concentration increased by 22 ppbv from the previous hour under southerly winds. From the 1-2 pm MDT period, the wind direction at C41 Chamizal shifts, coinciding with an ozone increase of 21 ppbv in a single hour. The C72 Skyline Park ozone concentration also increased by 22 ppbv from 2 to 3 pm MDT. That delay of an hour in comparison to C41 Chamizal may reflect the time for a plume to be transported to C72 Skyline Park 15 km to the north.

### **2.3 2017 OZONESONDE CAMPAIGN FROM EL PASO**

In 2017, there were 58 ozonesonde launches from the El Paso metropolitan area in support of a field study designed to better understand ozone pollution events. Figure 30 shows a map of the locations of the launch sites during the 2017 campaign. Logistically it is challenging to have launches from multiple sites due to the need to have a team that is mobile and able to safely transport helium. During the 2017 campaign we had those capabilities whereas in 2019 and 2020, we did not. One advantage of have mobile capabilities to launch from different sites is you can launch from the site that is forecasted to be high. Furthermore, in some cases, the balloon trajectories will be such that you can launch safely (based on the projections for where the balloon is expected to land and the need to avoid the airport early in the flight) from some sites and not others. During the 2019 campaign, the lack of mobility meant that we could not safely launch on some high ozone days. The 2019 campaign had the advantage of twice-daily launches to capture the residual layer with a flight at dawn and peak ozone with a flight in the afternoon. In the 2017 campaign, there was typically only one flight on a launch day that captured peak ozone in the afternoon.

Table 2 lists the number of launches from each site in 2017. There were 58 ozonesonde launches in total during the campaign, the first 8 of which were a part of an ozonesonde workshop on 15 – 18 May 2017 that included ~40 participants from the University of Texas at El Paso, New Mexico State University, Trinity University, St. Edward's University, and Southwestern University. During the rest of the campaign, launches typically occurred on moderate and high ozone days and coincided with peak ozone in the afternoon.

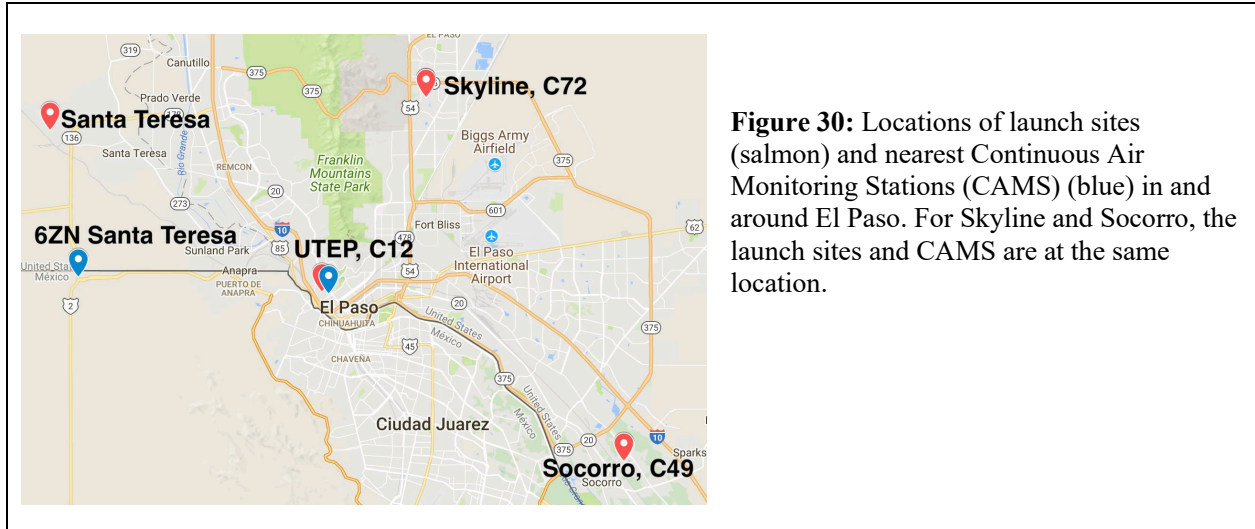
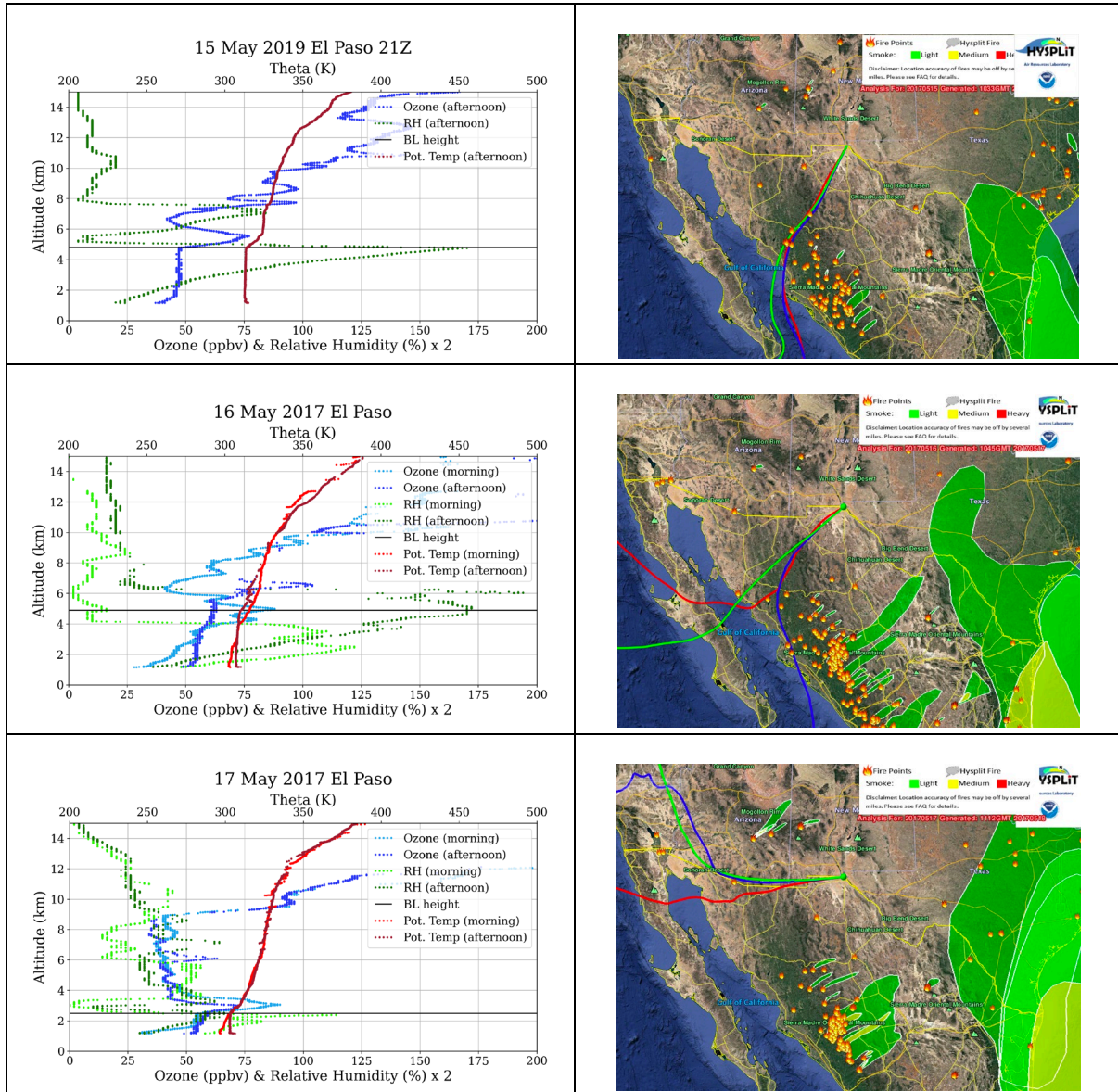


**Table 2:** Launch site locations and the number of ozonesondes from each location for the El Paso area in 2017.

| Ozonesondes in El Paso Area in 2017 |                      |                     |      |      |        |           |         |       |
|-------------------------------------|----------------------|---------------------|------|------|--------|-----------|---------|-------|
|                                     |                      | Number of Soundings |      |      |        |           |         |       |
| Launch Site                         | Latitude & Longitude | May                 | June | July | August | September | October | Total |
| Santa Teresa                        | 31.87° N, 106.70° W  | 0                   | 5    | 3    | 7      | 5         | 2       | 22    |
| UTEP                                | 31.77° N, 106.51° W  | 11                  | 1    | 0    | 4      | 0         | 0       | 16    |
| Skyline                             | 31.89° N, 106.43° W  | 0                   | 5    | 7    | 1      | 2         | 2       | 17    |
| Socorro                             | 31.67° N, 106.29° W  | 0                   | 1    | 1    | 0      | 1         | 0       | 3     |
| Total                               |                      | 11                  | 12   | 12   | 12     | 8         | 4       | 58    |

### 2.3.1 15 – 18 May 2017 (Indications of long-range transport)

The initial 8 flights during the El Paso Ozonesonde Workshop provided an interesting case study of meteorological and anthropogenic phenomena and their influences on ozone concentrations in the greater El Paso region. A combination of the sounding profiles, thermal returns from MODIS, and HYSPLIT trajectories allow for identifying cases for which the long-range transport of biomass burning may influence ozone concentrations in El Paso.



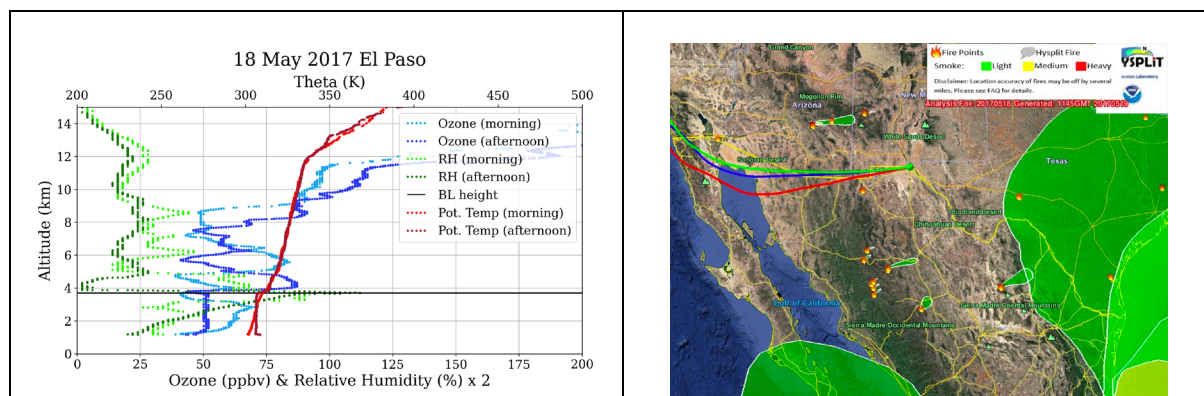


**Figure 31:** The tropospheric ozonesonde profiles from 15-18 May 2017 are shown in the left-hand column. Most profiles, except for the afternoon 16 May 2017 profile show an enhancement of ozone above the boundary layer that may be an indication of long-range transport. The right-hand column shows HYSPLIT back trajectories at the time of each afternoon flight that are overlaid on MODIS fires and smoke for the same day.

The left-hand column of Figure 31 shows the tropospheric ozonesonde profiles of an afternoon sounding on 15 May 2017 and twice-daily (dawn and afternoon) soundings on 16-18 May 2017 from the UTEP campus. The right-hand column of Figure 31 shows HYSPLIT back trajectories for starting at the approximate launch time of each afternoon sounding. Overlaid on top of the back trajectories are the MODIS fire and smoke returns for the same corresponding day as the profiles in the column on the left. With the exception of 16 May, each set of HYSPLIT back trajectories were generally taken at the location of the ozone enhancement above the afternoon boundary layer: 15 May (21Z), 4.8 km (green), 5.2 km (blue), 5.6 km (green) AMSL; 16 May (18Z), 2.5 km (red), 3.5 km (blue), 4.5 km (green) AMSL; 17 May (18Z), 2.5 km (red), 2.9 km (blue), 3.3 km (green) AMSL; 18 May (18Z), 4 km (red), 4.5 km (blue), 5 km (green) AMSL. The HYSPLITs were generated using the NAM 12 km meteorology, the highest resolution available.

There is a sizable ozone enhancement above the boundary layer on each day aside from the afternoon of 16 May; an ozone enhancement coinciding with dry air is present above the residual layer of the dawn flight on 16 May. There is a strong cap on the afternoon boundary layer on 15 May, 17 May, and 18 May as seen by the high lapse rate in the potential temperature just above the boundary layer for the afternoon profiles (dark red curves). The strong cap on those days reduces the likelihood of mixing of air in the lower free troposphere down into the boundary layer. Also, a strong cap can be indicative of heating resulting from the presence of smoke particles in the air just above the boundary layer.

Volatile organic compounds (VOCs) transported from the biomass burning in Mexico or other locations may have influenced the El Paso airshed. If wildfire smoke were to have reached the surface, we would expect elevated levels of  $PM_{2.5}$ . Even if the smoke did not reach the surface, we would expect reduced visibility if smoke were present aloft above the boundary layer.  $PM_{2.5}$  levels were not elevated in El Paso on 15 May 2017 but were greatly elevated on 16 May 2017

reaching a peak of 176.3  $\mu\text{g}/\text{m}^3$  at the C41 Chamizal monitor, and were similarly elevated at the C12 UTEP and C37 Ascarate Park monitors (the C49 Socorro Hueco monitor did not have  $\text{PM}_{2.5}$  on 16 May 2017). The visibility at the C37 Ascarate Park monitor reached a low of 1.29 miles during the same time (the 2 pm MST hour) at which the  $\text{PM}_{2.5}$  levels peaked at 166  $\mu\text{g}/\text{m}^3$ . The peak hourly  $\text{PM}_{2.5}$  levels and the lowest hourly visibility during 15-18 May 2017 are shown in Table 3. The series of profiles during 15-18 May 2017 along with the elevated  $\text{PM}_{2.5}$  levels and reduced visibility on 16 May 2017 suggest contributions from biomass burning mixed into that afternoon’s boundary layer on that day.

**Table 3:** The peak hourly  $\text{PM}_{2.5}$  concentrations during 15-18 May 2017 are shown for the C12 UTEP, C37 Ascarate Park, and C41 Chamizal monitors. Also shown is the lowest hourly visibility at the C37 Ascarate Park monitor. On 16 May 2017, the peak hourly  $\text{PM}_{2.5}$  concentrations and the lowest hourly visibility all occur during the same hour (i.e., the 2 pm MST hour).

|             | Peak hourly $\text{PM}_{2.5}$ ( $\mu\text{g}/\text{m}^3$ ) |              |              | Lowest Visibility (miles) |
|-------------|--|--------------|--------------|---------------------------|
|             | C12  | C37          | C41          | C37                       |
| 15 May 2017 | 9.5  | 17.8         | 17.3         | 12.44                     |
| 16 May 2017 | <b>109.1</b>   | <b>166.0</b> | <b>176.3</b> | <b>1.29</b>               |
| 17 May 2017 | 8.1  | 17.0         | 15.3         | 14.21                     |
| 18 May 2017 | 10.3   | 15.4         | 12.3         | 14.45                     |

### 2.3.2 Simultaneous flights on 19 July 2017

On three occasions, balloons were simultaneously released on opposite sides of the Franklin Mountains to investigate the impact of topography and local production on ozone concentrations. Figure 32 shows one such case with the profiles of two simultaneous soundings that took place at 18:20 UTC on 19 July 2017, one from Santa Teresa (31.87°N, 106.7°W) and one from Skyline (31.89°N, 106.43°W). The two launch sites are on opposite sides of the Franklin mountains (see Figure 30 to view the launch site locations).

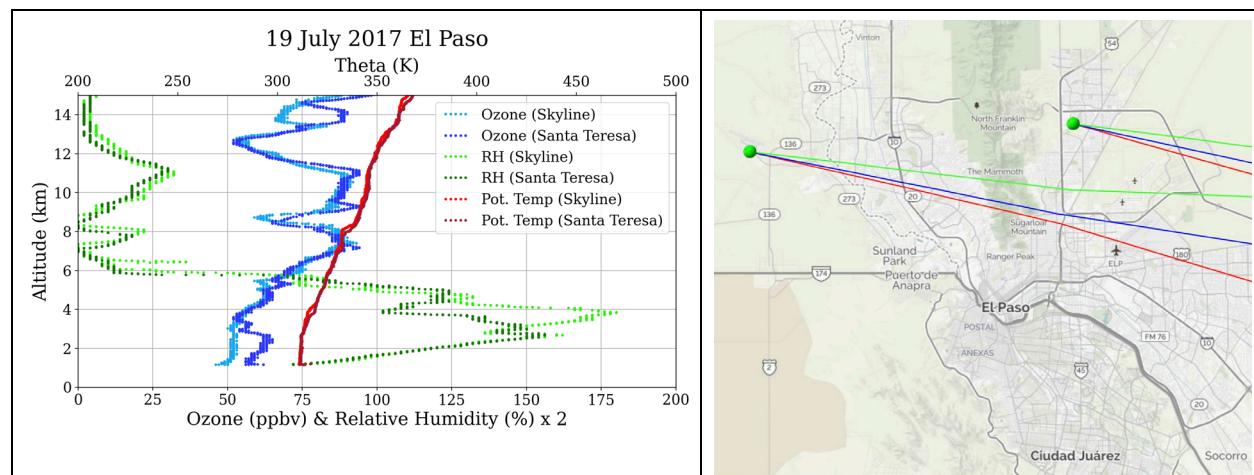
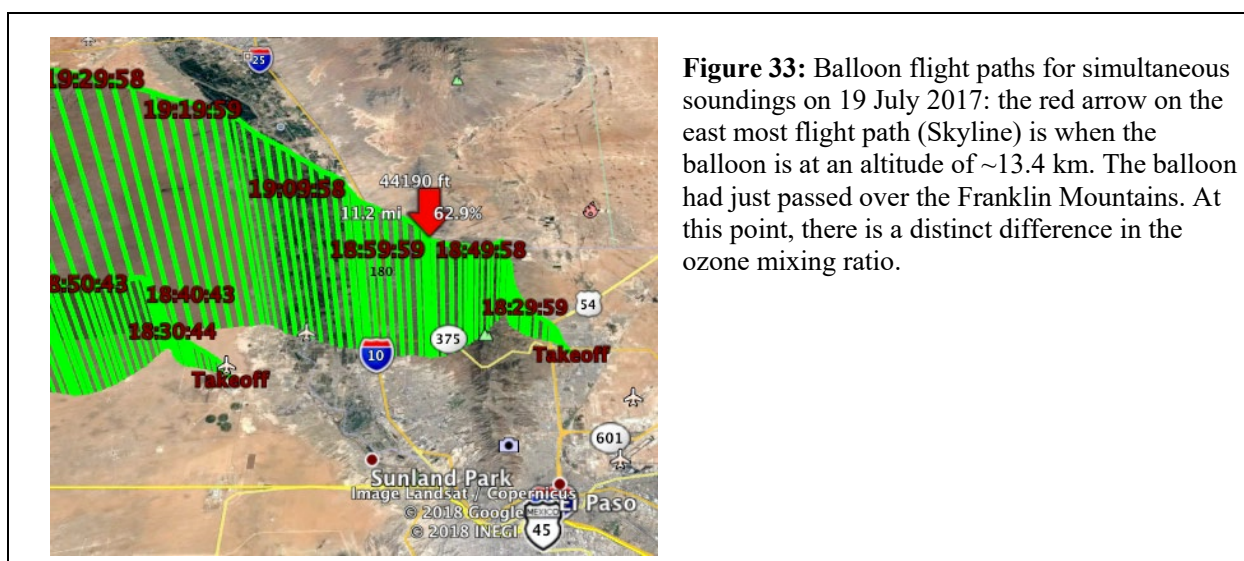


**Figure 32:** Left: Profiles from 19 July 2017 of two simultaneous soundings show an ozone enhancement in the boundary layer for Santa Teresa but not for Skyline and have differences at 13.3 – 14.5 km. Right: HYSPLIT Back trajectories at 500 m (red), 1000 m (blue), and 1500 m (green) for simultaneous soundings on 19 July 2017: boundary layer air at Santa Teresa was influenced by the El Paso plume whereas Skyline was not.

We see an enhancement of boundary layer ozone for the Santa Teresa profile (dark blue) that is not present for the Skyline profile (light blue). Figure 32 shows the HYSPLIT back trajectories of boundary layer air at altitudes 500 m (red), 1000 m (blue), and 1500 m (green) above ground level. The boundary layer air above Santa Teresa was influenced by the plume from El Paso; the boundary layer air above Skyline was not. The ozone enhancement of 10 – 15 ppbv in the boundary layer likely can be attributed to local production in El Paso. The ~50 ppbv observed in Skyline serves as an estimate of the background ozone at both Skyline and Santa Teresa.



For the simultaneous soundings that took place on 19 July 2017 in El Paso, Figure 32 shows that above the boundary layer, the ozone mixing ratios for both flights agree well until a deviation at 13.3 – 14.5 km. Figure 33 shows the paths of the sondes during flight. For the altitude range of interest, the Skyline sonde had just passed over the Franklin Mountains. This ozone feature, therefore, may be a result of orographic impacts from the Franklin Mountains. The windward face induces rising motion yielding leeward subsidence. This may result in significant vertical transport of air thus influencing the concentrations of ozone at a specific altitude.

## 2.4 RESIDUAL LAYER INFLUENCES ON AFTERNOON OZONE IN EL PASO

Following Morris et al. (2010), we can investigate to the afternoon ozone concentration that is accounted for by the ozone that is entrained overnight in the residual layer. Figure 34 shows a plot of the peak ozone concentration in the afternoon boundary layer versus the highest ozone in the dawn residual layer for flight days in 2017, 2019, and 2020 where launches occurred twice-daily: one ozonesonde launch at dawn and the other in the afternoon. Only three such dawn/afternoon paired flight days occurred in 2017, all during the ozonesonde training workshop

in May 2017. In 2019 and 2020, the launches occurred from July – September (primarily in August).

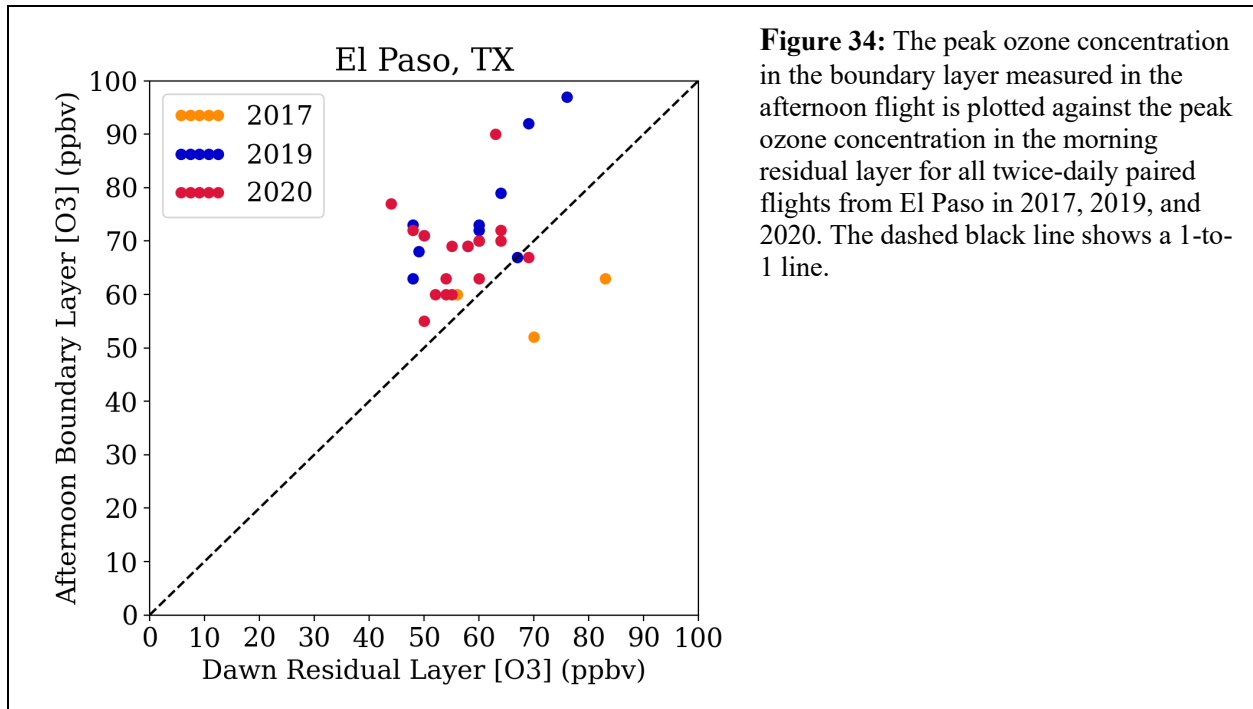


**Figure 34:** The peak ozone concentration in the boundary layer measured in the afternoon flight is plotted against the peak ozone concentration in the morning residual layer for all twice-daily paired flights from El Paso in 2017, 2019, and 2020. The dashed black line shows a 1-to-1 line.

There is uncertainty associated with each data point in Figure 34 resulting from (1) uncertainty in choosing the boundary layer height and (2) assigning the correct value for the residual layer ozone concentration. For the dawn residual layer concentration, we chose the highest ozone concentration from the morning ozone profile that is below the afternoon boundary layer height. Our sample is biased in that we launched primarily on days when the ozone concentration was expected to be relatively high. The four days that had the highest measured ozone concentrations in the afternoon boundary layer all coincided with ozone concentrations in the residual layer (dawn flight) reaching in excess of 60 ppbv.

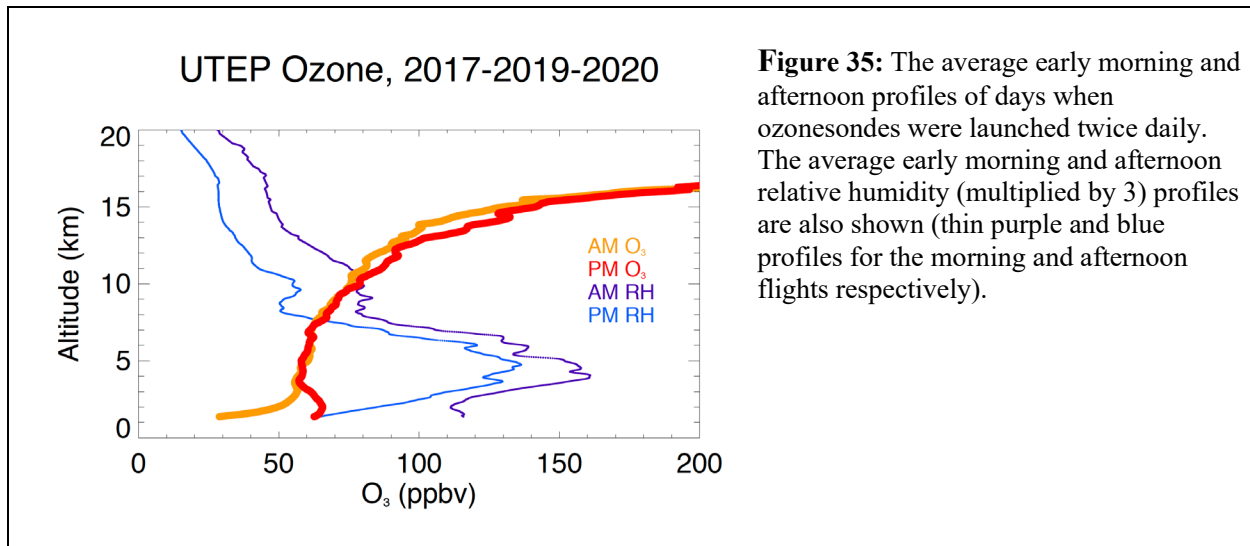
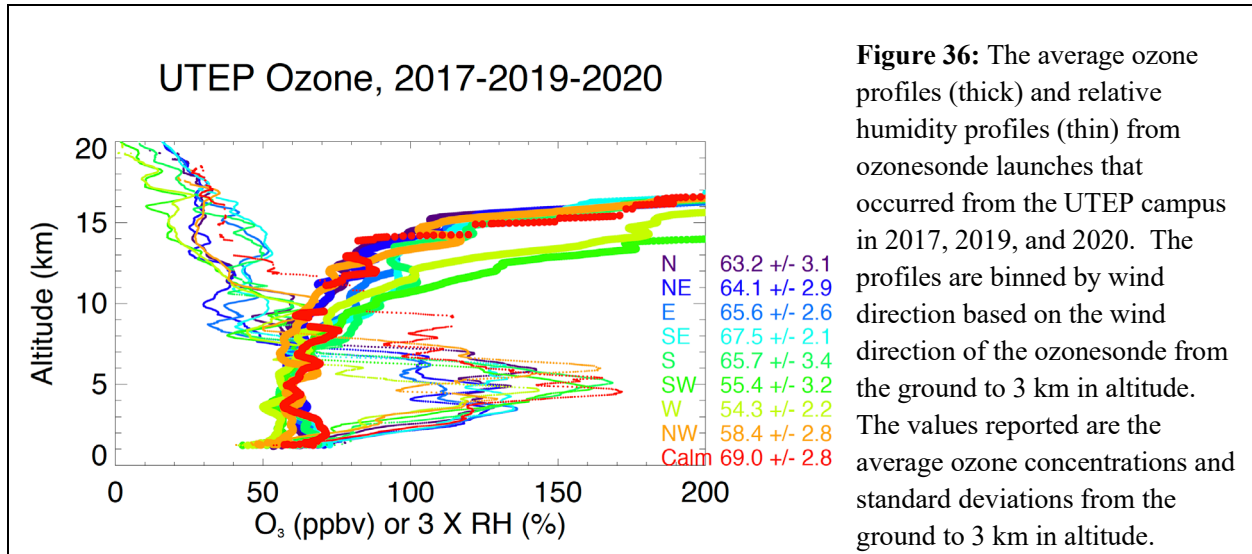


Figure 35 shows average morning and afternoon profiles of ozone and relative humidity (the RH is multiplied by 3 in the figure) on days where twice daily launches occurred in 2017, 2019, or 2020. In the boundary layer, the average peak afternoon ozone (shown in red) is ~65 ppbv, while in the residual layer, the average ozone (shown in orange) is ~55 ppbv at the same altitude. The mean ozone concentration from 3 to 7 km AMSL is nearly uniform ranging from 58 to 60 ppbv. The same range is also where the relative humidity is the highest in the troposphere. The mean RH data suggest the average cloud deck forms in the 3 – 7 km altitude range over El Paso, with afternoon RH lower than morning RH as the atmosphere warms. The difference between the mean afternoon boundary layer ozone profile and the mean morning ozone profile as well as the mean lower free tropospheric ozone profile (either morning or afternoon) suggests local production leading to average enhancements of ~10 ppbv of ozone. On days with moist air in the 3 – 7 km altitude range (such as shown for the morning and afternoon averages in Figure 35), stratospheric influences are unlikely.

## 2.5 AVERAGE AFTERNOON PROFILES BY WIND DIRECTION

Upwind sources can have a large effect on ozone concentrations in the El Paso region. Figure 36 shows the average ozone profiles of ozonesondes launched from the UTEP campus in 2017, 2019, and 2020 based on wind direction. The data shown at the right of the figure indicate the mean boundary layer ozone (here taken to be the average below 3.0 km AMSL)  $\pm$  one standard deviation. The highest ozone at UTEP occurs when winds are calm or southeasterly, with southerly and easterly winds producing the next highest mean boundary layer ozone concentrations. Lower ozone is found when winds are out of the southwest, west, or northwest, areas with sparse population.

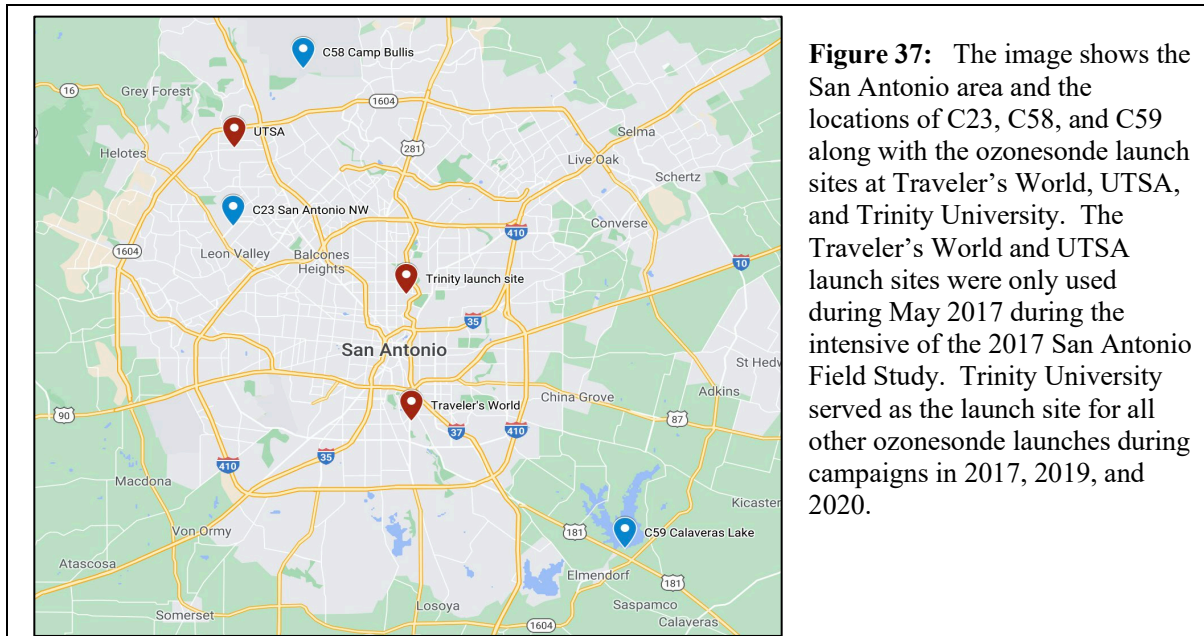


**Figure 36:** The average ozone profiles (thick) and relative humidity profiles (thin) from ozonesonde launches that occurred from the UTEP campus in 2017, 2019, and 2020. The profiles are binned by wind direction based on the wind direction of the ozonesonde from the ground to 3 km in altitude. The values reported are the average ozone concentrations and standard deviations from the ground to 3 km in altitude.

### 3. SAN ANTONIO

There were ozonesonde campaigns from San Antonio in 2017, 2019, and 2020. During 2017 there were 52 ozonesondes launched from San Antonio, 27 in May as part of the San Antonio Field Study, and 28 later in the summer and fall at the Trinity University campus. During 26 July – 31 October 2019, there were 32 ozonesonde launches from San Antonio at the Trinity University campus. During 15 July – 15 October 2020, there were 40 ozonesonde launches from San Antonio at the Trinity University campus. Bexar County, which includes San Antonio, was deemed out of compliance with the Environmental Protection Agency (EPA) NAAQS ozone standard in 2018.

There were two days in August 2020 and 4 days in October 2020 in exceedance of the NAAQS ozone standard.



### 3.1 2020 OZONESONDE CAMPAIGN FROM SAN ANTONIO

#### 3.1.1 Listing of All 2020 San Antonio Flights

Table 4 shows all days during the sampling period. Some days we are unable to fly due to unfavorable balloon trajectory forecasts. For safety reasons and in accordance with flight protocols developed in conjunction with the FAA, we avoid flying on days when the pre-flight balloon trajectory forecasts indicates that the payloads are likely to land in a metropolitan area.

Ozonesonde Launches for San Antonio and El Paso – Final Report  
 PGA 582-20-10914-009

**Table 4:** Maximum daily 8-hour average (MDA8) ozone concentrations (ppb) at three surface monitors in the San Antonio area, 15 July – 15 October 2020, with ozonesonde flights noted.

| Flight(s) | Date      | Morning flight number | Afternoon flight number | Final TCEQ Daily Air Quality Forecast | C23 San Antonio Northwest | C58 Camp Bullis | C59 Calaveras Lake |
|-----------|-----------|-----------------------|-------------------------|---------------------------------------|---------------------------|-----------------|--------------------|
|           | 7/15/2020 |                       |                         |                                       | 33                        | 41              | 29                 |
|           | 7/16/2020 |                       |                         |                                       | 33                        | 43              | 29                 |
| 1, 2      | 7/17/2020 | SA088 <sup>t</sup>    | SA089 <sup>t</sup>      |                                       | 33                        | 40              | 29                 |
|           | 7/18/2020 |                       |                         |                                       | 33                        | 38              | 32                 |
|           | 7/19/2020 |                       |                         |                                       | 37                        | 37              | 33                 |
|           | 7/20/2020 |                       |                         |                                       | 45                        | <b>56</b>       | 45                 |
|           | 7/21/2020 |                       |                         |                                       | 50                        | 52              | 40                 |
|           | 7/22/2020 |                       |                         |                                       | 40                        | 49              | 32                 |
|           | 7/23/2020 |                       |                         |                                       | 35                        | 42              | 33                 |
|           | 7/24/2020 |                       |                         |                                       | 38                        | 43              | 40                 |
|           | 7/25/2020 |                       |                         |                                       | 32                        | 34              | 30                 |
|           | 7/26/2020 |                       |                         |                                       | 32                        | 37              | 28                 |
|           | 7/27/2020 |                       |                         |                                       | 45                        | 43              | 32                 |
|           | 7/28/2020 |                       |                         |                                       | 34                        | 42              | 28                 |
|           | 7/29/2020 |                       |                         |                                       | 32                        | 38              | 28                 |
|           | 7/30/2020 |                       |                         |                                       | 27                        | 32              | 23                 |
|           | 7/31/2020 |                       |                         |                                       | 34                        | 38              | 35                 |
|           | 8/1/2020  |                       |                         |                                       | <b>57</b>                 | <b>61</b>       | 50                 |
| 3, 4      | 8/2/2020  | SA090                 | SA091                   |                                       | <b>58</b>                 | <b>60</b>       | 51                 |
| 5, 6      | 8/3/2020  | SA092                 | SA093                   | *                                     | <b>60</b>                 | <b>63</b>       | 49                 |
|           | 8/4/2020  |                       |                         |                                       | <b>55</b>                 | <b>70</b>       | 47                 |
|           | 8/5/2020  |                       |                         |                                       | 44                        | 53              | 39                 |
|           | 8/6/2020  |                       |                         |                                       | 36                        | 43              | 33                 |
|           | 8/7/2020  |                       |                         |                                       | 37                        | 44              | 35                 |
|           | 8/8/2020  |                       |                         |                                       | 27                        | 33              | 24                 |
|           | 8/9/2020  |                       |                         |                                       | 24                        | 31              | 22                 |
|           | 8/10/2020 |                       |                         |                                       | 25                        | 32              | 24                 |
|           | 8/11/2020 |                       |                         |                                       | 28                        | 35              | 26                 |
|           | 8/12/2020 |                       |                         |                                       | 25                        | 34              | 25                 |
|           | 8/13/2020 |                       |                         |                                       | 27                        | 37              | 23                 |
|           | 8/14/2020 |                       |                         |                                       | 31                        | 42              | 28                 |
|           | 8/15/2020 |                       |                         |                                       | 40                        | 51              | 31                 |

Ozonesonde Launches for San Antonio and El Paso – Final Report  
 PGA 582-20-10914-009

|        |           |       |       |   |           |           |           |
|--------|-----------|-------|-------|---|-----------|-----------|-----------|
| 7, 8   | 8/16/2020 | SA094 | SA095 |   | 42        | 48        | 35        |
|        | 8/17/2020 |       |       |   | <b>57</b> | <b>70</b> | <b>60</b> |
| 9      | 8/18/2020 | SA096 | ***   |   | <b>64</b> | <b>70</b> | <b>68</b> |
| 10, 11 | 8/19/2020 | SA097 | SA098 |   | <b>66</b> | <b>71</b> | <b>73</b> |
| 12, 13 | 8/20/2020 | SA099 | SA100 | * | <b>71</b> | <b>67</b> | <b>65</b> |
| 14, 15 | 8/21/2020 | SA101 | SA102 |   | 52        | <b>65</b> | 50        |
|        | 8/22/2020 |       |       |   | <b>60</b> | <b>60</b> | <b>55</b> |
| 16, 17 | 8/23/2020 | SA103 | SA104 |   | <b>58</b> | <b>64</b> | 54        |
|        | 8/24/2020 |       |       |   | <b>62</b> | <b>68</b> | NV        |
|        | 8/25/2020 |       |       |   | 53        | <b>60</b> | 53        |
|        | 8/26/2020 | ***   | ***   |   | 41        | 43        | 39        |
|        | 8/27/2020 | ***   | ***   |   | <b>55</b> | <b>64</b> | 44        |
|        | 8/28/2020 | ***   | ***   |   | 39        | 51        | 30        |
|        | 8/29/2020 | ***   | ***   |   | 34        | 46        | 27        |
| 18, 19 | 8/30/2020 | SA105 | SA106 |   | 29        | 36        | 26        |
|        | 8/31/2020 |       |       |   | 32        | 38        | 31        |
|        | 9/1/2020  |       |       |   | 35        | 40        | 35        |
|        | 9/2/2020  |       |       |   | 38        | 47        | 30        |
|        | 9/3/2020  |       |       |   | 30        | 35        | 28        |
|        | 9/4/2020  |       |       |   | 24        | 29        | 24        |
|        | 9/5/2020  |       |       |   | 33        | 34        | 33        |
|        | 9/6/2020  | ***   | ***   |   | 47        | 53        | 40        |
|        | 9/7/2020  |       |       |   | 32        | 40        | 30        |
|        | 9/8/2020  |       |       |   | 27        | 30        | 27        |
|        | 9/9/2020  |       |       |   | 19        | 19        | 20        |
|        | 9/10/2020 |       |       |   | 13        | 15        | 15        |
|        | 9/11/2020 |       |       |   | 35        | 35        | 42        |
|        | 9/12/2020 | ***   | ***   |   | 49        | 41        | 47        |
|        | 9/13/2020 |       |       |   | 34        | 37        | 42        |
|        | 9/14/2020 |       |       |   | 39        | 43        | 46        |
|        | 9/15/2020 |       |       |   | 34        | 38        | 47        |
|        | 9/16/2020 |       |       |   | 43        | 42        | 45        |
|        | 9/17/2020 |       |       |   | 36        | 40        | 42        |
|        | 9/18/2020 |       |       |   | 46        | 50        | <b>57</b> |
| 20, 21 | 9/19/2020 | SA107 | SA108 |   | 51        | <b>57</b> | <b>58</b> |
|        | 9/20/2020 |       |       |   | 51        | <b>57</b> | <b>56</b> |
|        | 9/21/2020 |       |       |   | 28        | 33        | 27        |
|        | 9/22/2020 |       |       |   | 23        | 25        | 25        |
|        | 9/23/2020 |       |       |   | 23        | 26        | 26        |
| 22     | 9/24/2020 | ***   | SA109 |   | 33        | 34        | 40        |
|        | 9/25/2020 | ***   | ***   |   | 48        | <b>57</b> | 45        |
|        | 9/26/2020 | ***   | ***   |   | 41        | 47        | 41        |

Ozonesonde Launches for San Antonio and El Paso – Final Report  
 PGA 582-20-10914-009

|        |            |       |       |   |    |    |    |
|--------|------------|-------|-------|---|----|----|----|
| 23     | 9/27/2020  | SA110 | ***   |   | 32 | 37 | 29 |
|        | 9/28/2020  |       |       |   | 39 | 45 | 42 |
| 24, 25 | 9/29/2020  | SA111 | SA112 |   | 40 | 46 | 42 |
| 26, 27 | 9/30/2020  | SA113 | SA114 | * | 52 | 59 | 50 |
| 28, 29 | 10/1/2020  | SA115 | SA116 |   | 66 | 72 | 59 |
| 30, 31 | 10/2/2020  | SA117 | SA118 |   | 61 | 70 | 51 |
|        | 10/3/2020  |       |       |   | 51 | 60 | 49 |
|        | 10/4/2020  | ***   | ***   |   | 57 | 55 | 52 |
| 32     | 10/5/2020  | ***   | SA119 |   | 59 | 70 | 57 |
| 33, 34 | 10/6/2020  | SA120 | SA121 | * | 64 | 77 | 58 |
| 35, 36 | 10/7/2020  | SA122 | SA123 |   | 71 | 74 | 66 |
|        | 10/8/2020  | ***   | ***   |   | 55 | 62 | 44 |
|        | 10/9/2020  | ***   | ***   |   | 25 | 29 | 29 |
| 37     | 10/10/2020 | SA124 | ***   |   | 55 | 66 | 52 |
|        | 10/11/2020 |       |       |   | 47 | 57 | 41 |
|        | 10/12/2020 | ***   | ***   |   | 42 | 48 | 53 |
| 38     | 10/13/2020 | ***   | SA125 |   | 70 | 75 | 54 |
| 39, 40 | 10/14/2020 | SA126 | SA127 |   | 36 | 44 | 34 |
|        | 10/15/2020 |       |       |   | 42 | 38 | 43 |

Notes: The San Antonio 2020 campaign sampling period was from 15 July - 15 October 2020, with training flights (“t”) on 17 July 2020. The final projection from the TCEQ Daily Air Quality Forecast that was available for a potential flight at dawn is shown, where a \* denotes that it was an Ozone Action Day. Launch days with \*\*\* denotes that forecast balloon trajectories were unsuitable for a launch. Cell shading corresponds to the AQI category for that ozone concentration (“Good”, “Moderate”, etc.) for concentrations greater than 54 ppb.

### 3.1.2 Exceedance Days in San Antonio During 2020 Campaign

There were six days during the 2020 ozonesonde campaign where at least one monitor in the San Antonio area exceeded the ozone standard.

#### 3.1.2.1 19 August 2020

Winds were out of the NW in the morning and then out of the NE in the afternoon. The high monitor for ozone was C59 Calaveras Lake (MDA8 [O<sub>3</sub>] of 73 ppbv). The wind direction is consistent with the path of the front that came through San Antonio early that morning. The back trajectories show contributions from continental air, which is typically higher in background ozone than marine air from the Gulf of Mexico. Lower free-tropospheric ozone values, as indicated by the ozone profile data, were in the mid to upper 50’s from 3 – 5 km, while boundary layer values exceeded 70. The enhancement of ~15 ppbv in the boundary layer suggest impacts from boundary layer transport and local production.

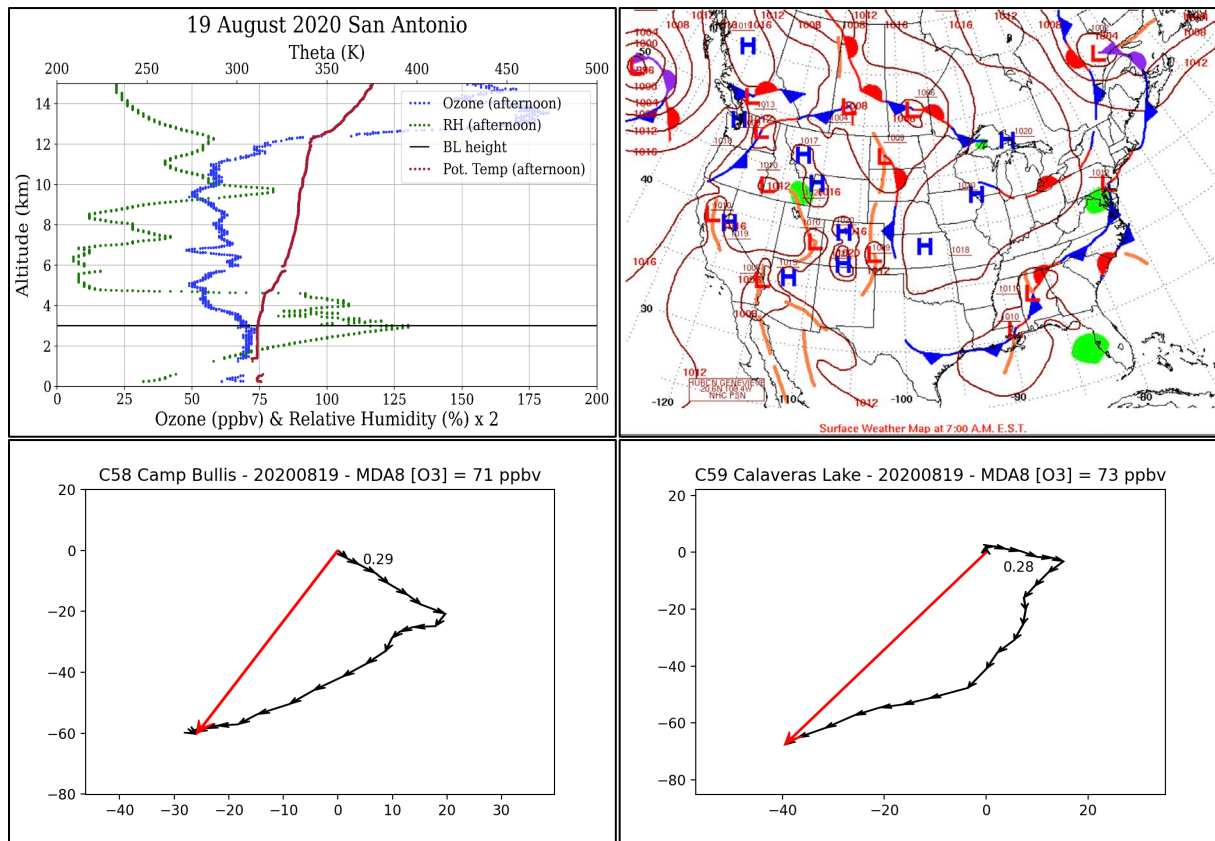


**Figure 38:** The four images shown are for 19 August 2020. Top left: Tropospheric profiles for a pair of flights (one at dawn and the other in the early afternoon) from the Trinity University campus in San Antonio. The black line shows the afternoon boundary layer height, for which the top of the boundary could potentially be closer to 5 km AMSL. Top right: Weather map. The 24-hour wind runs are shown for C58 Camp Bullis (bottom-left) and C59 Calaveras Lake (bottom-right).

### 3.1.2.2 20 August 2020

On this day, the surface monitors reported winds out of the N/NE. The high monitor for ozone was C23 Northwest (MDA8 [O<sub>3</sub>] of 71 ppbv). From the weather map, there are signs that a weak front that had passed through the day before, then stalled just south of San Antonio leading to stagnant conditions. The HYPPLIT back trajectories show influences of continental air contributing to the background ozone. The boundary layer may have had contributions from the Houston area. Surface monitor data from Houston on 19 August showed elevated ozone south of Houston (the Lake Jackson and Oyster Creek monitors near Galveston recorded 1-hour peaks of 88 and 103 ppbv), although monitors on the north side of Houston (closer to the location of the back trajectories) indicate significantly lower ozone values (in the 40s and 50s). The wind run shows light winds out of the N/NNE in the morning and out of the E/ESE in the afternoon.

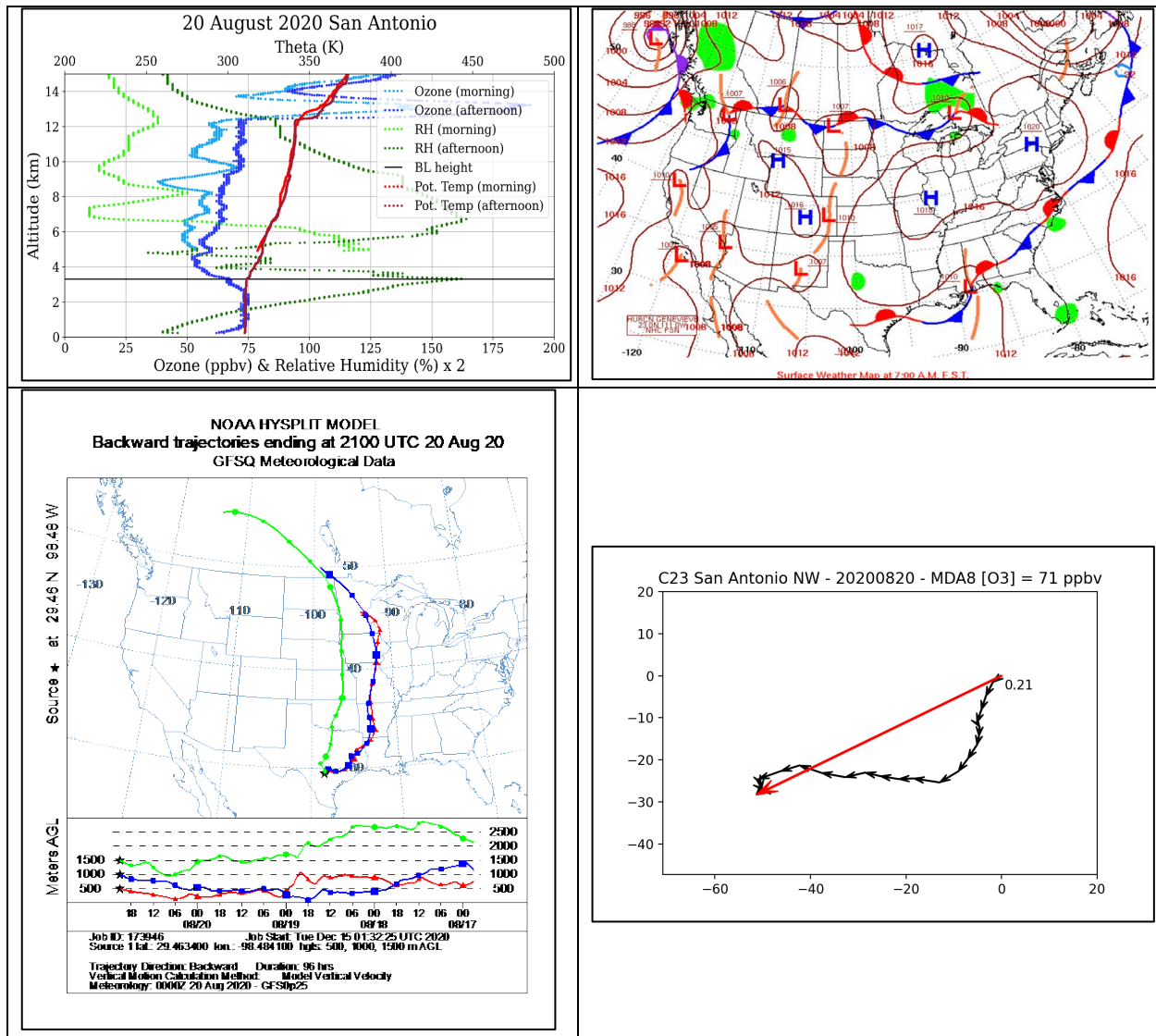


**Figure 39:** The four images shown are for 20 August 2020. Top left: Tropospheric profiles for a pair of flights (one at dawn and the other in the early afternoon) from the Trinity University campus in San Antonio. The black line shows the afternoon boundary layer height. Top right: Weather map. Bottom left: HYSPLIT back trajectories for the boundary layer of the afternoon flight which show continental air contributed to the background in San Antonio. Bottom right: Wind runs for C23 San Antonio Northwest.

### 3.1.2.3 1 October 2020

Figure 40 shows the dawn and afternoon ozonesonde profiles in the top-left. The high monitor for ozone on this day in the San Antonio area was C58 Camp Bullis (MDA8 [O<sub>3</sub>] of 72 ppbv). The 24-hour wind run for the C58 Camp Bullis monitor (bottom-right) shows recirculated air with winds out of the NW in the morning shifting to out of the SE in the afternoon. A cold front passed through on this day, three days after the prior cold front. The boundary layer height is 2 km AMSL and the potential temperature lapse rate above the boundary layer shows strong stability. Ozone within the boundary layer increased by about 25 ppbv, from values near 50

ppbv in the morning residual layer to values  $> 75$  ppbv in the afternoon boundary layer. Just above the boundary layer (from 2 – 3 km), ozone values  $< 35$  ppbv. The ozone profile observations suggest the ozone enhancement on this day are likely due to local production, with the recirculating wind conditions amplifying more typical afternoon enhancements of 10 – 15 ppbv.

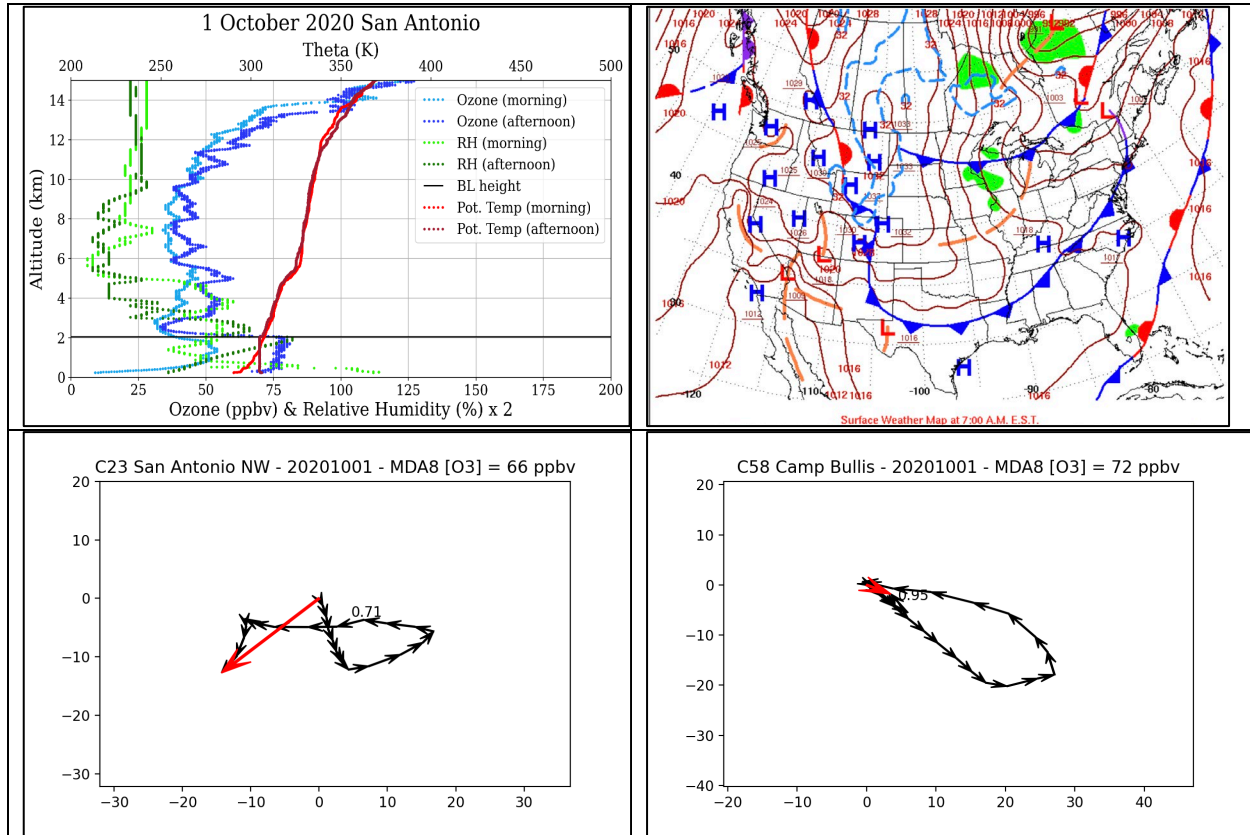


**Figure 40:** The four images shown are for 1 October 2020. Top left: Tropospheric profiles for a pair of flights (one at dawn and the other in the early afternoon) from the Trinity University campus in San Antonio. The black line shows the afternoon boundary layer height. Top right: Weather map. Bottom: The 24-hour wind runs for the C23 San Antonio NW monitor (left) and the C58 Camp Bullis monitor (right).

### 3.1.2.4 6 October 2020

The MDA8 [O<sub>3</sub>] of 77 ppbv at C58 Camp Bullis made this the highest day for San Antonio surface monitor ozone during the 2020 ozonesonde campaign. While some data was missing from the morning ozonesonde flight from Trinity University, we do see that the ozone concentration in the afternoon boundary layer (below ~ 2 km) is nearly identical to that found in the morning residual layer (top-left of Figure 41), suggesting that dynamical processes (vertical mixing) could explain much of the afternoon boundary layer profile.

Ozonesonde Launches for San Antonio and El Paso – Final Report  
 PGA 582-20-10914-009

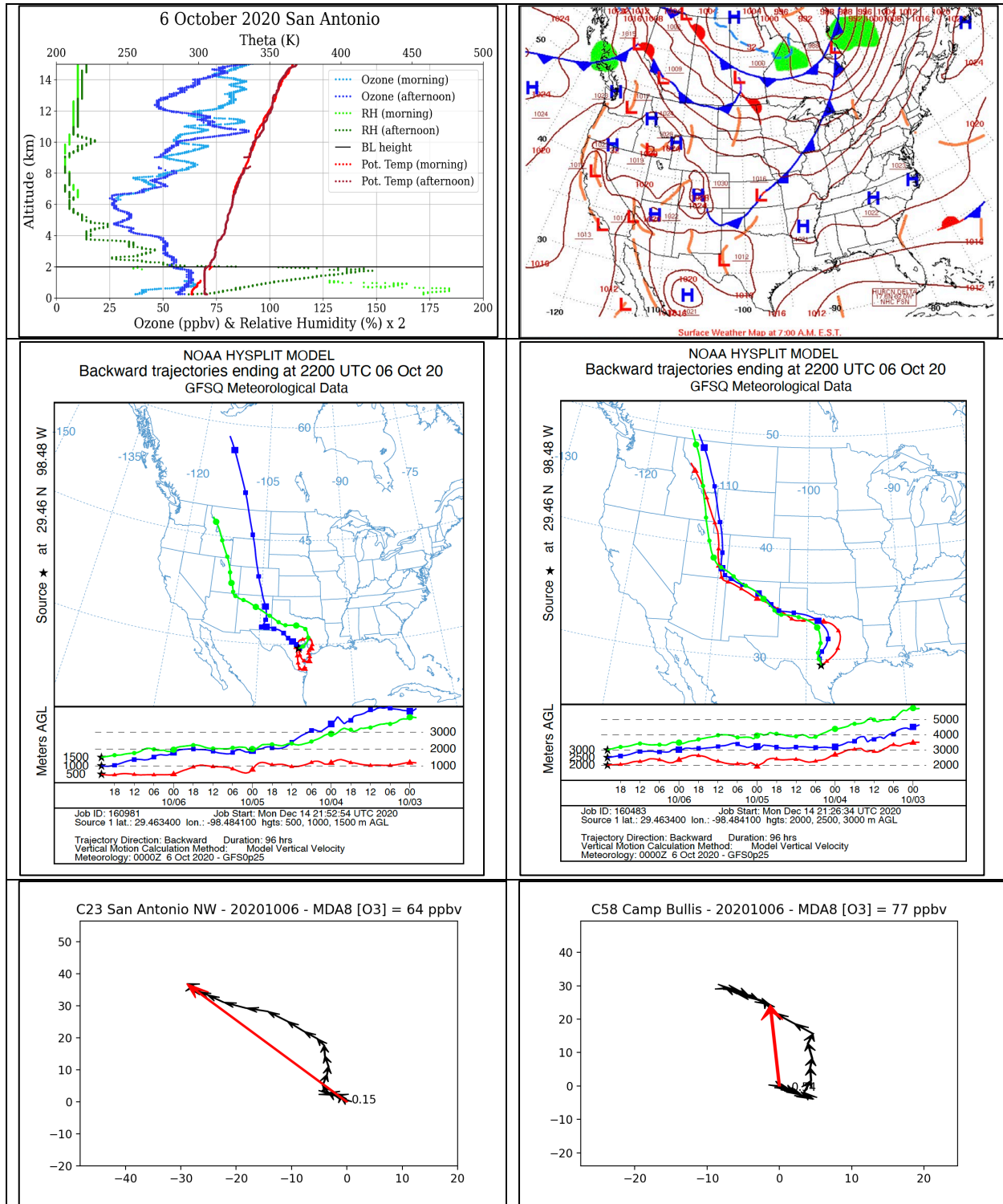


**Figure 41:** The four images shown are for 6 October 2020. Top left: Tropospheric profiles for a pair of flights (one at dawn and the other in the early afternoon) from the Trinity University campus in San Antonio. The black line shows the afternoon boundary layer height. Top right: Weather map. Middle: HYSPLIT back trajectories for trajectories starting in the boundary layer (left) and lower free troposphere (right). Bottom: The 24-hour wind runs for the C23 San Antonio NW monitor (left) and the C58 Camp Bullis monitor (right).

There was a front that made its way into Central Texas on October 4. Downward mixing of air from the upper troposphere/lower stratosphere may have impacted the ozone profile in the free troposphere. A slight ozone enhancement just above the afternoon boundary layer near 2.5 km corresponds with a RH minimum (RH near 12.5%). When combined with the HYSPLIT back trajectories that show that the air that contributed to the San Antonio airshed had continental influences passed over the Rocky Mountains, this ozone/RH feature in the profile data suggests some UT/LS influences were possible on this day. The 24-hour wind run for the C58 Camp Bullis monitor (bottom-right) shows signs recirculating air with slow winds out of the NW in the early morning shifting to out of the S and then out of the SE in the afternoon.

### **3.1.2.5 7 October 2020**

Still in post-frontal conditions, the MDA8 [O<sub>3</sub>] was 74 ppbv at C58 Camp Bullis and 71 ppbv at C23 San Antonio NW on 7 October 2020. Figure 42 shows the dawn and afternoon ozonesonde profiles (top-left). Ozone in the morning residual layer peaks near 60 ppbv, with lower free tropospheric ozone concentrations in the 50 – 55 ppbv range. The afternoon boundary layer height was 1.8 km AMSL, with boundary layer ozone near 80 ppbv, a significant enhancement of 20 – 25 ppbv over the morning residual layer concentrations. The 24-hour wind runs at C23 San Antonio NW (bottom-left) and C58 Camp Bullis (bottom-right) show signs of recirculating air with winds out of the NW in the early morning shift to easterly in the afternoon.

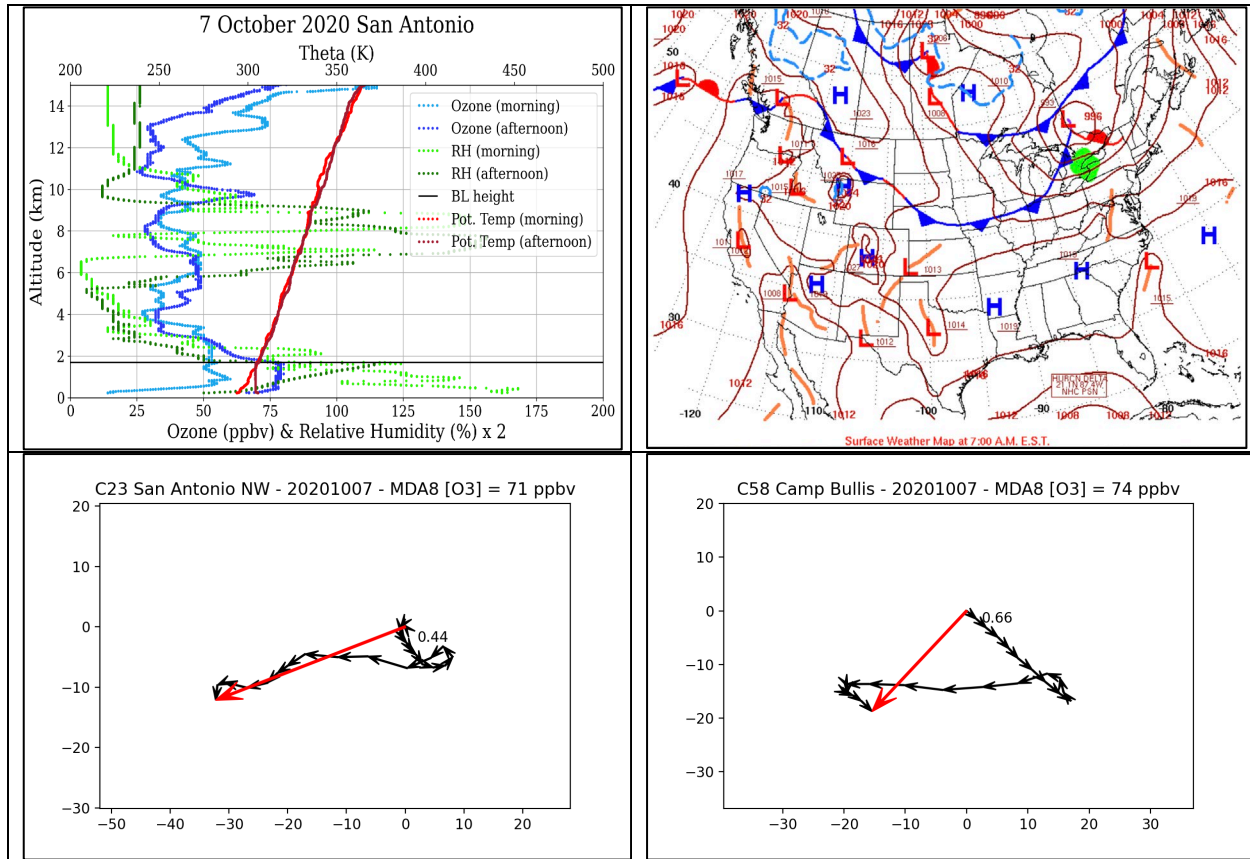


**Figure 42:** The four images shown are for 7 October 2020. Top left: Tropospheric profiles for a pair of flights (one at dawn and the other in the early afternoon) from the Trinity University campus in San Antonio. The black line shows the afternoon boundary layer height. Top right: Weather map. Bottom: The 24-hour wind runs for the C23 San Antonio NW monitor (left) and the C58 Camp Bullis monitor (right).

### 3.1.2.6 13 October 2020

The MDA8 [O<sub>3</sub>] was 75 ppbv at C58 Camp Bullis and the weather map in the top-right of Figure 43 shows San Antonio was in post-frontal conditions as a cold front passed through the day before on October 12. The afternoon boundary layer height was ~1.9 km AMSL. Dry layers with enhanced ozone appear in the profile near 3 and 4.5 km AMSL, suggesting possible descent of UT/LS air behind the cold front. The 24-hour wind run at C58 Camp Bullis (bottom-right) show signs of recirculating air with winds out of the NW in the early morning shift to out of the SE in the afternoon.

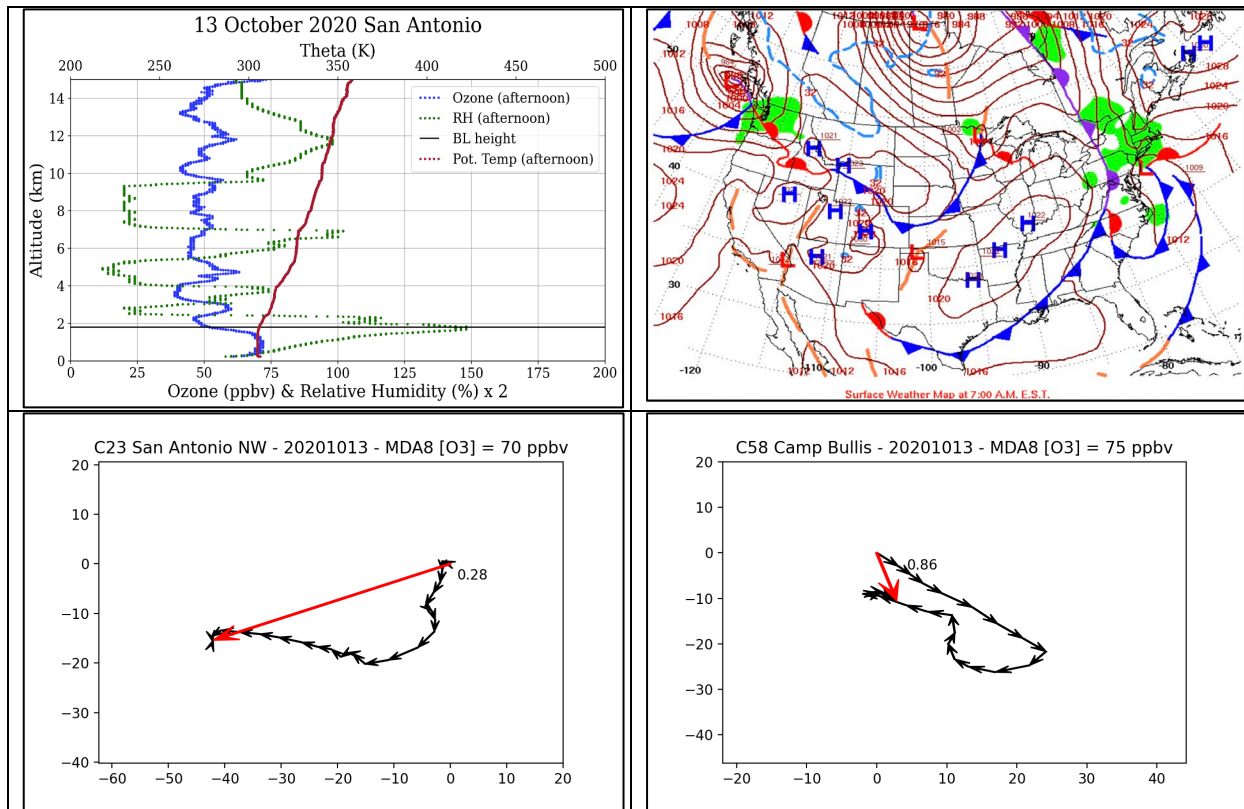


**Figure 43:** The four images shown are for 13 October 2020. Top left: Tropospheric profiles for the afternoon flight from the Trinity University campus in San Antonio. The black line shows the afternoon boundary layer height. Top right: Weather map. Bottom: The 24-hour wind runs for the C23 San Antonio NW monitor (left) and the C58 Camp Bullis monitor (right).

The C58 Camp Bullis monitoring site lies in a shallow valley where the hills on each side may make winds running along the NW/SE axis more common (Figure 44). On three of the four days in October 2020 with post-frontal conditions where the C58 Camp Bullis monitor exceeded the ozone standard, surface winds were out to the NW in the morning and SE in the afternoon. The morning winds out of the NW may transport continental air into San Antonio. Continental air often has higher background ozone than the marine air carried by southerly winds into San Antonio. The afternoon wind shift allows the San Antonio urban plume to be recirculated back into the city and into the NW quadrant to the C58 Camp Bullis monitor in the afternoon.

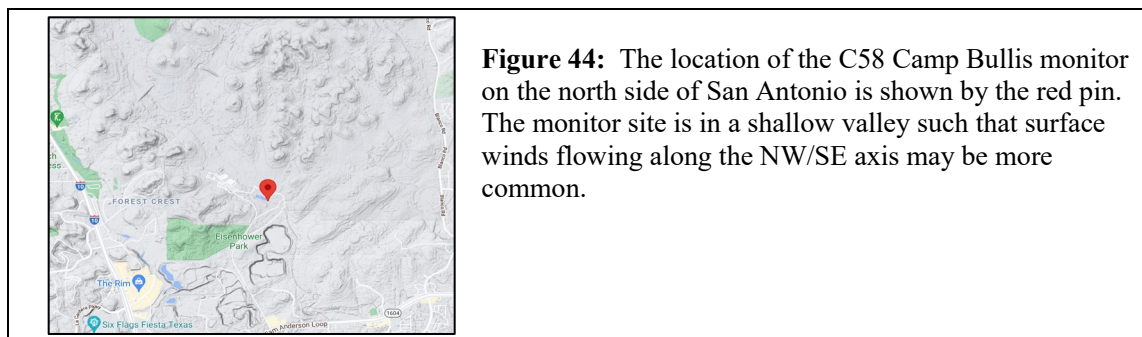
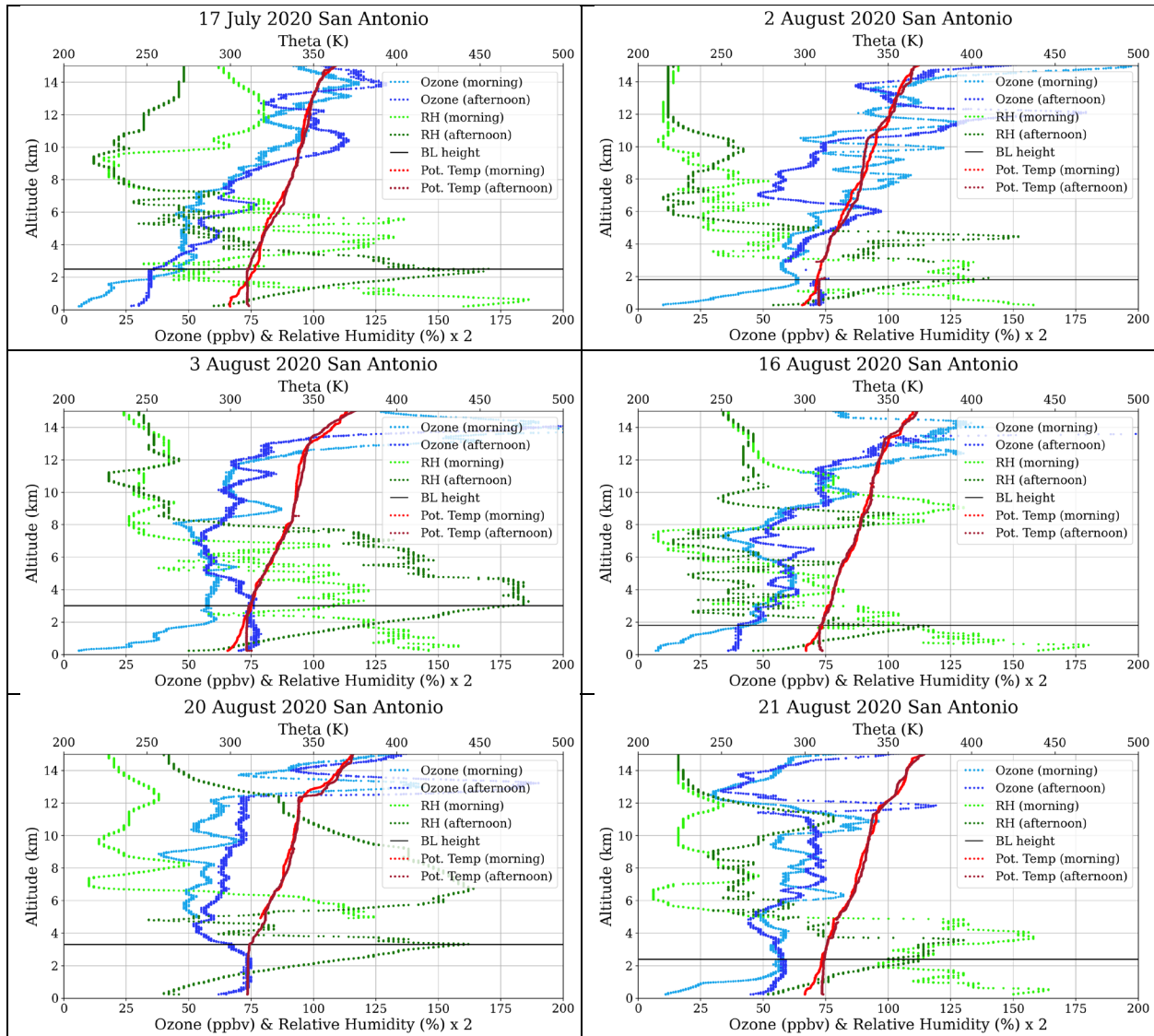


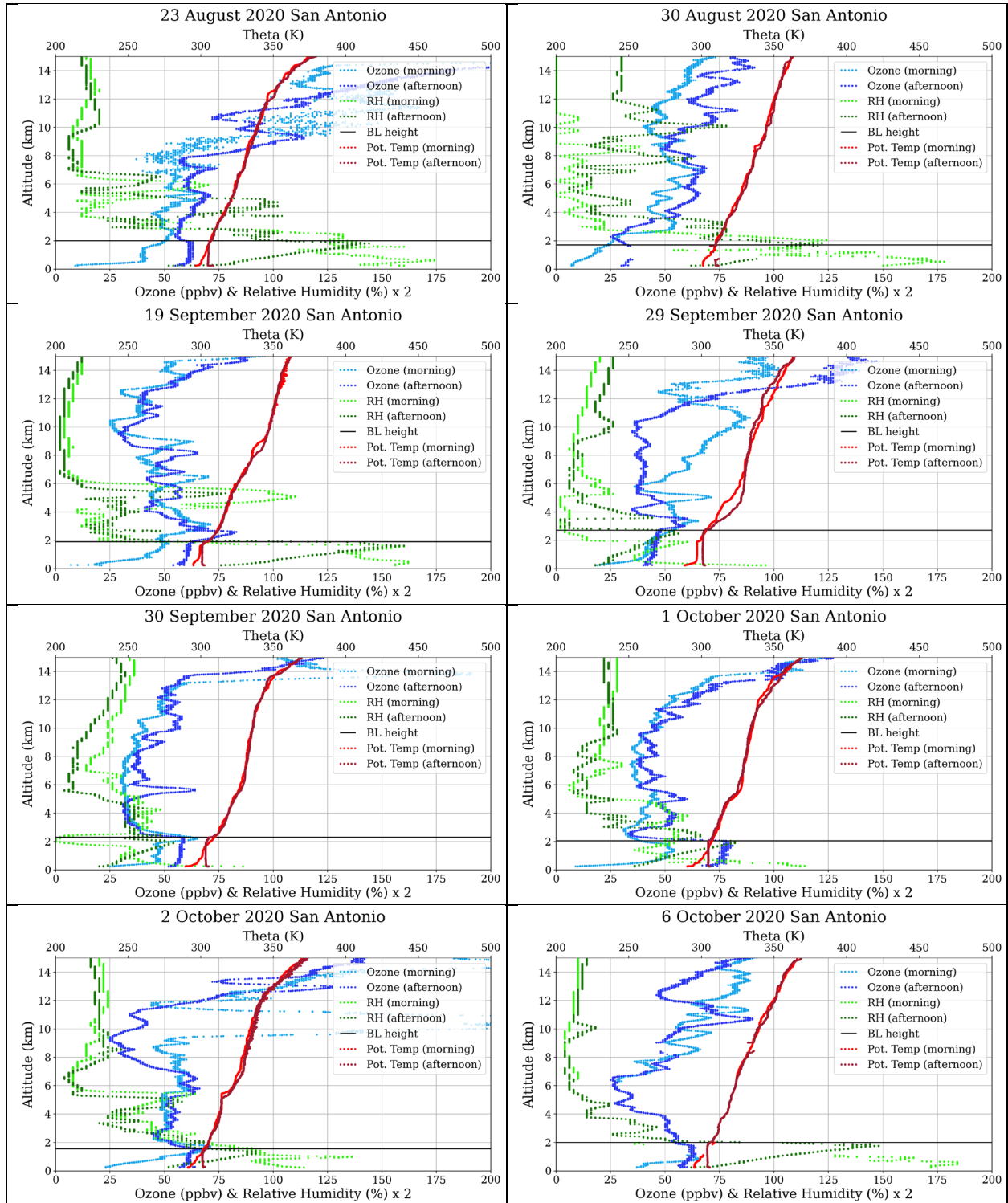
**Figure 44:** The location of the C58 Camp Bullis monitor on the north side of San Antonio is shown by the red pin. The monitor site is in a shallow valley such that surface winds flowing along the NW/SE axis may be more common.

### 3.1.3 Profiles of 2020 Dawn and Afternoon Paired Flights

Of the 40 flights from San Antonio, 34 of them were flown in twice-daily pairs (i.e., 17 days with paired flights): one flight at dawn to capture the residual layer and another flight in the afternoon, roughly coinciding with the time of peak surface ozone concentrations. Figure 45 shows the tropospheric profiles for 15 of the paired-flight days and provides information about the contribution of the residual layer to the ozone measured that afternoon.



Ozonesonde Launches for San Antonio and El Paso – Final Report  
 PGA 582-20-10914-009



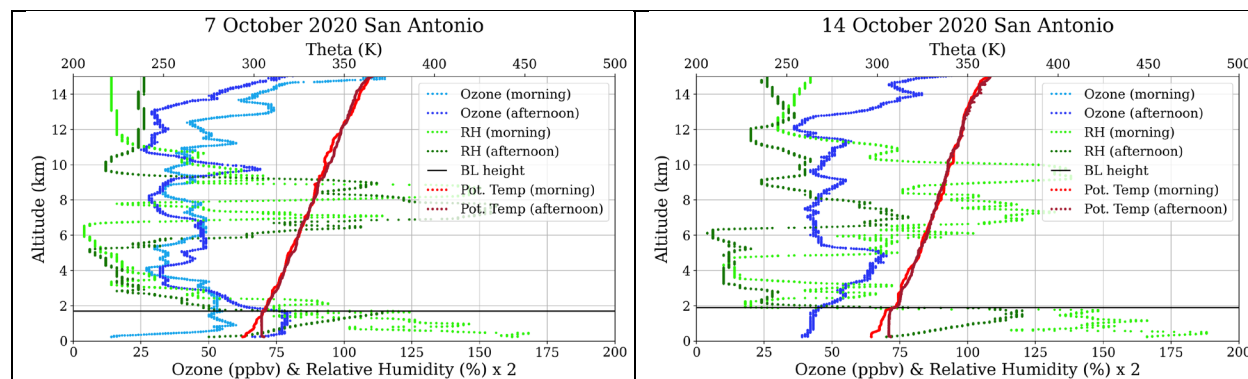


**Figure 45:** Tropospheric profiles for 16 days where flights were flown in pairs (one at dawn and the other in the early afternoon) from the Trinity University campus in San Antonio. The black horizontal line shows the afternoon boundary layer height. The morning ozone, RH, and potential temperature data are light blue, light green, and light red respectively, while the afternoon ozone, RH, and potential temperature data are dark blue, dark green, and dark red respectively.

The distinction between a positive and negative ozone gradient above the afternoon boundary layer on high ozone days may represent two different scenarios. A positive gradient may be necessary but not sufficient indication for influence by ozone transported into the area. A negative gradient may show that the local production is the dominant influence for ozone in the city, and that little contribution from distant sources is likely. An uncertainty in this method of distinguishing the two cases is the quantification of the top of the afternoon boundary layer—sometimes it looks like the BL top could be in more than one place. Deciding where to place the BL top can determine whether the ozone is positive or negative. Additional, more detailed analysis of the daily data from San Antonio will be the subject of future work.

### 3.2 2019 OZONESONDE CAMPAIGN FROM SAN ANTONIO

During 26 July – 20 October 2019, there were 32 ozonesonde launches from San Antonio at the Trinity University campus.

In contrast to the synoptic conditions in 2020, a high pressure in the southeast US separated from the Bermuda High led to a flow pattern that consisted of strong winds coming from the Gulf of Mexico throughout much of August – October 2019 (Figure 46). The marine air led to low background ozone contributions, as seen in the dawn ozonesonde flights. The residual layer over San Antonio typically exhibited lower ozone concentrations than what was observed for high ozone days in El Paso. Further, the strong winds off the Gulf prevented fronts from making it all the way to San Antonio during August and September 2019. There were no days in exceedances of the NAAQS ozone standard in August and September 2019, with 10 days that had moderate ozone levels in the range of MDA8 O<sub>3</sub> 55 – 70 ppbv.

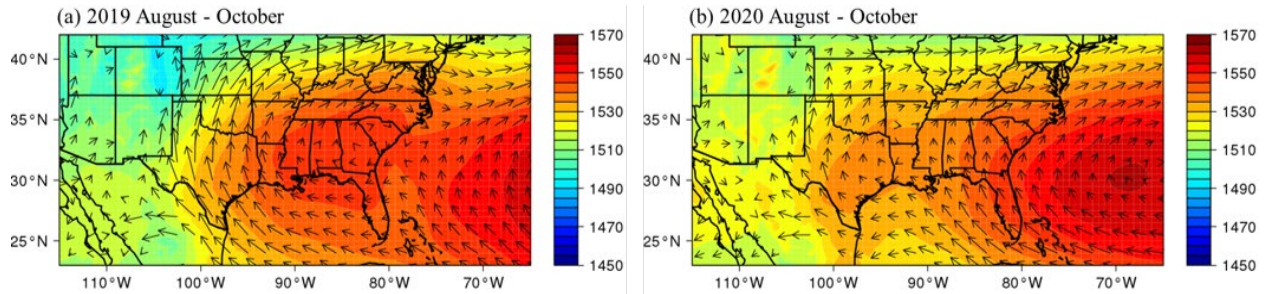


**Figure 46:** Mean geopotential height and wind vectors at 850 hPa from August to October in 2019 (a) and 2020 (b). Data source is MERRA2.

Bernier et al. (2019) found that synoptic meteorological processes, such as the low-level jet and the location of the Bermuda High, influence the circulation pattern into the Houston area and thus impact surface level ozone. It appears that a high-pressure system may impact the San Antonio area in a similar way and likely contributed to the steady strong flow from the Gulf of Mexico into the San Antonio area that was observed in August and September 2019.

Further results from the 2019 ozonesonde flights from San Antonio that are not included here are available in the final report of “Ozonesonde Launches in San Antonio and El Paso,” PIs James Flynn, Paul Walter, Marilyn Wooten, and Rosa Fitzgerald, PGA Number 582-19-93513-06.

### 3.2.1 Exceedance Day in San Antonio During 2019 Campaign

The only day in San Antonio during the campaign that was in exceedance of the NAAQS ozone standard was 26 July 2019, which was the day of our first training flight and for which there was only an afternoon flight. The MDA8 for ozone was 76 ppbv.

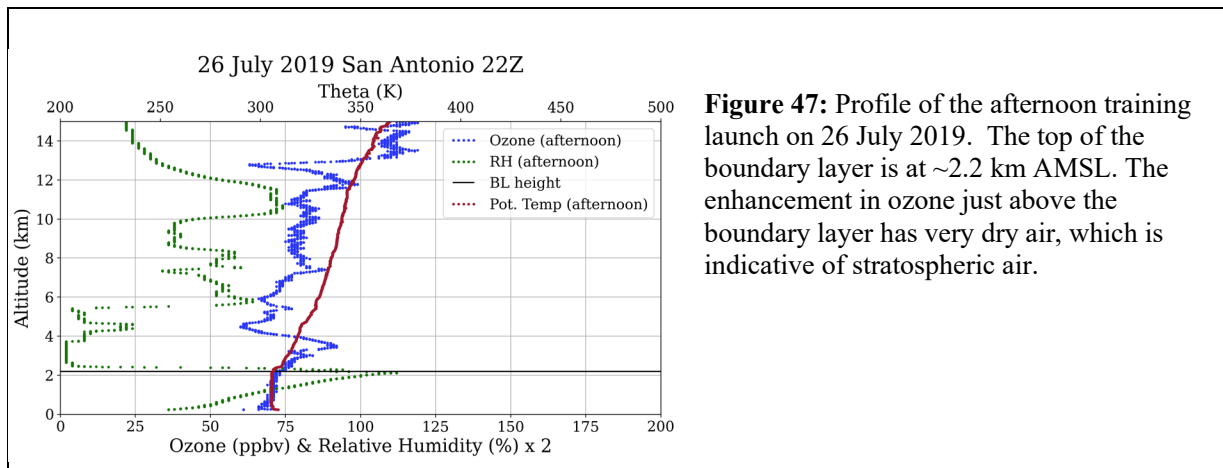


**Figure 47:** Profile of the afternoon training launch on 26 July 2019. The top of the boundary layer is at ~2.2 km AMSL. The enhancement in ozone just above the boundary layer has very dry air, which is indicative of stratospheric air.

Figure 47 shows the profile for the sounding. The top of the boundary layer is at ~2.2 km. Just above the top of the boundary layer, from 3 – 4 km, an enhanced layer of ozone (~90 ppbv) in very dry air (RH < 5%) is found. Such air masses are consistent with long-range transport or descending air masses from the UT/LS. The positive gradient in ozone moving up from the

boundary layer suggests such influences could have contributed to the boundary layer ozone concentrations seen in the afternoon, with entrainment of this aloft higher ozone layer during the morning growth of the boundary layer.

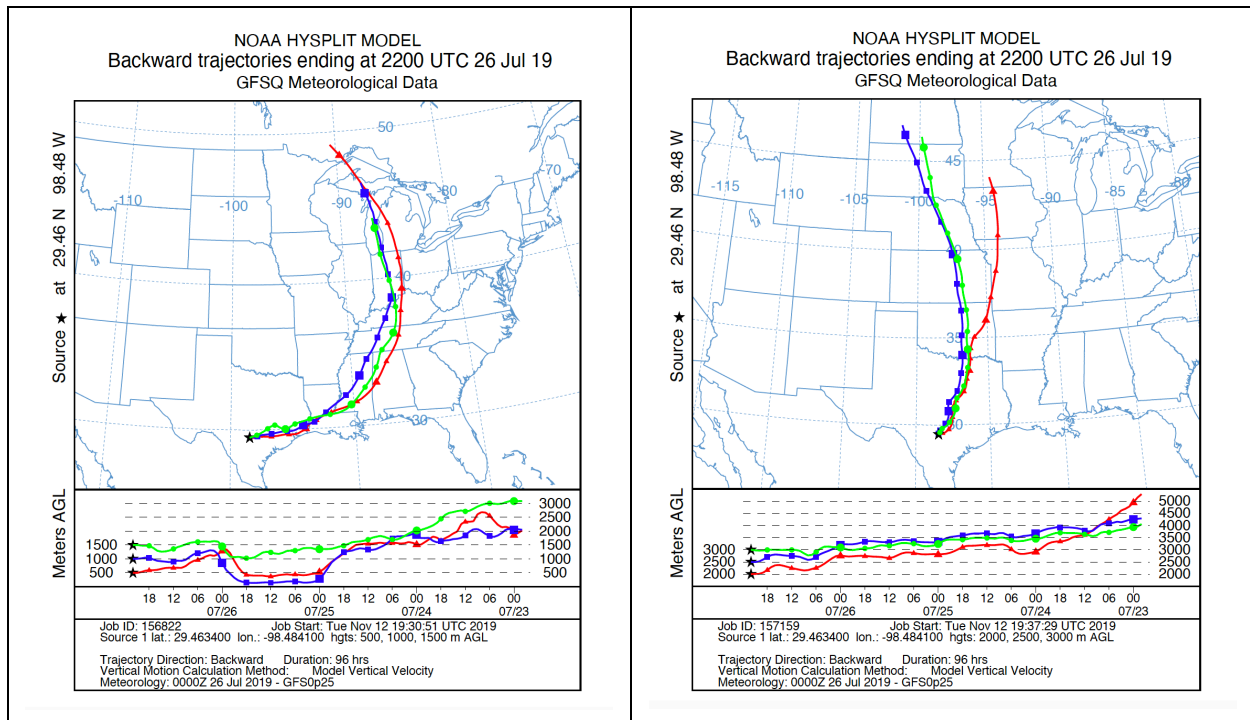


**Figure 48:** Left: NOAA HYSPLIT back trajectories show that the boundary layer air mass may have included contributions from continental air and the Houston area, both of which are consistent with elevated levels of boundary layer ozone. Right: NOAA HYSPLIT back trajectories show that the lower free troposphere air mass had contributions from descending air that is consistent with potential contributions from STE.

Figure 48 shows the NOAA HYSPLIT back trajectories for air contributing to the boundary layer (left image) and the lower free troposphere (right image) in San Antonio at the time of the flight. The HYSPLIT boundary layer back trajectories from the time of launch show that the San Antonio airshed was influenced by continental air and air from the Houston area, which would thus be expected to contribute to having a relatively high background ozone. Both 25 and 26 July were days on which Houston and San Antonio had several monitors that exceeded the 8-hour ozone standard. In Houston, five monitors recorded MDA8 values of 73 – 82 ppbv on 25 July, while in San Antonio, the San Antonio NW site recorded MDA8 values of 76 and 75 ppbv on the 25<sup>th</sup> and 26<sup>th</sup> respectively. The HYSPLIT back trajectories of air masses contributing to the lower free troposphere (trajectories starting 2000 – 3000 m AGL) show strongly descending air (as indicated by the altitude time series in the bottom panel of Figure 48), which is consistent with UT/LS influences.

Figure 49 shows a cold front passed through San Antonio on the evening on July 22 and that a stable high-pressure system remained in place over Central Texas through July 26. The post-

frontal conditions and UT/LS influences may have contributed to 26 July 2019 being an ozone exceedance day for San Antonio.

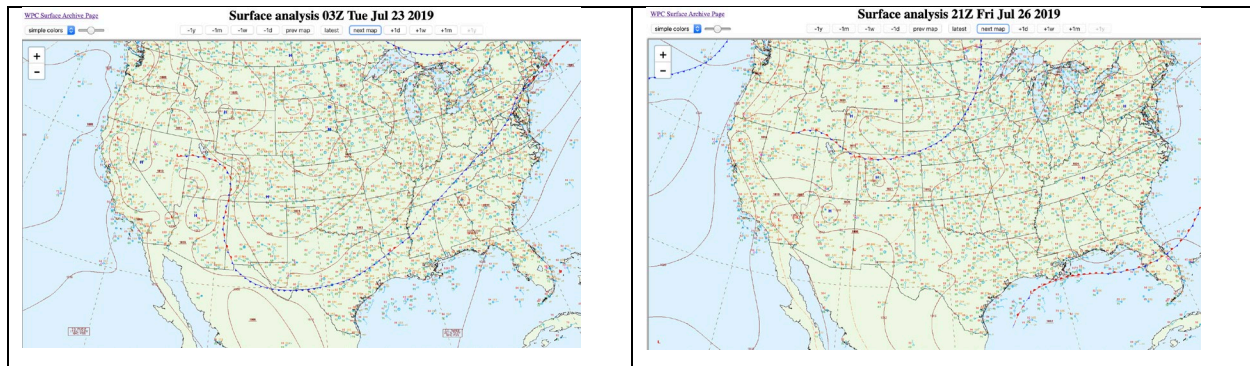


**Figure 49:** Left: NOAA surface analysis shows that a cold front passed through San Antonio the evening of 22 July 2019. Right: NOAA surface analysis at the time of the flight on 26 July 2019, which was day in which San Antonio was in exceedance of the ozone standard, shows slow easterly winds in the San Antonio area.

The 24-hour wind runs for the C23 San Antonio NW and the C58 Camp Bullis monitors are shown in Figure 50. The slow winds in the morning out of the N at C23 San Antonio and NW at C58 Camp Bullis may brought enhanced background ozone from continental air masses, a common occurrence in post-frontal conditions, and that air may have contributed a higher background to San Antonio than what is observed with southerly flow of marine air from the Gulf of Mexico. In the late morning and afternoon, the surface winds changed directions such that the urban plume was transported to the respective monitors.

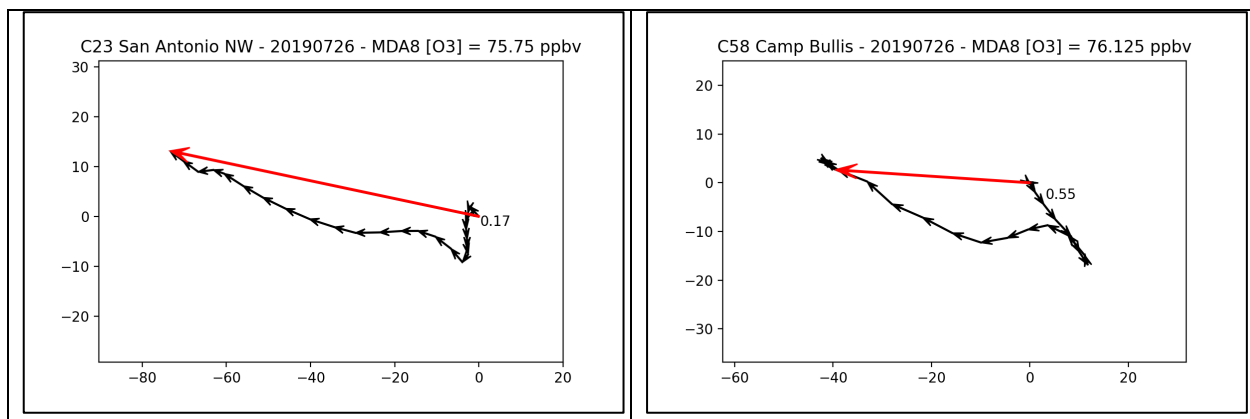


**Figure 50:** The 24-hour wind runs are shown for C23 San Antonio NW and C58 Camp Bullis (right) for 26 July 2019.

As a continued part of ozonesonde training, we flew two sondes on the next day, 27 July 2019, which was the second highest ozone day of the campaign with an MDA8 of 67 ppbv. The morning sounding shows an ozone residual layer near 700 m AMSL with about 55 ppbv of ozone, and a second layer in the lower free troposphere between 1.5 – 2.5 km with about 70 ppbv of ozone. Just above that layer, near 3.5 km, is a third layer of elevated ozone, with

concentrations up to ~90 ppbv in a very dry air mass, likely the result of descending air behind the earlier frontal passage. That same dry layer persists near 3.5 km in the afternoon profile, with boundary layer ozone well mixed below 2 km in the 65 – 70 ppbv range. A lower ozone feature appears between these two levels, with ozone dropping to near 50 ppbv in the relatively humid layer between 2 and 3 km.

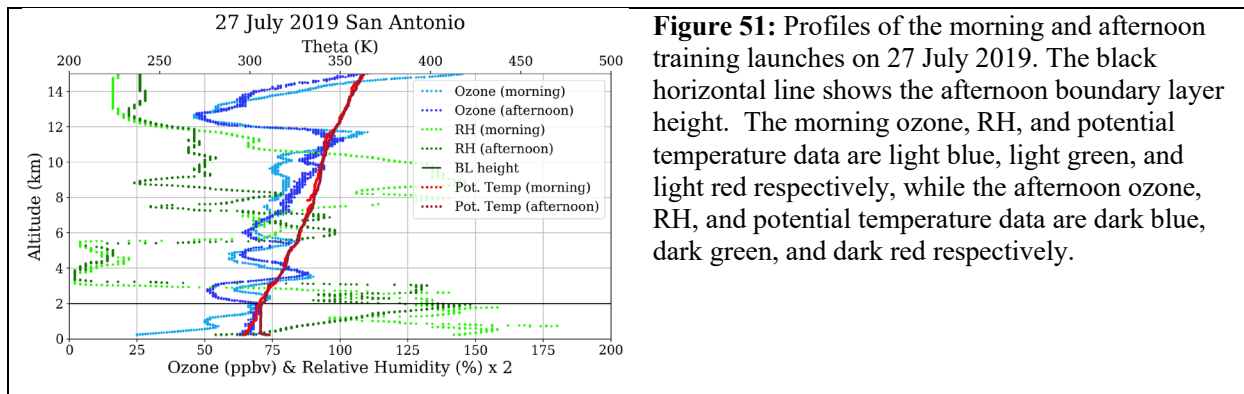


**Figure 51:** Profiles of the morning and afternoon training launches on 27 July 2019. The black horizontal line shows the afternoon boundary layer height. The morning ozone, RH, and potential temperature data are light blue, light green, and light red respectively, while the afternoon ozone, RH, and potential temperature data are dark blue, dark green, and dark red respectively.

### 3.3 2017 OZONESONDE CAMPAIGN FROM SAN ANTONIO

In 2017, there were 55 ozonesonde launches from San Antonio. As part of the May 2017 San Antonio Field Study (SAFS), researchers from the University of Houston launched 27 ozonesondes from San Antonio in collaboration with St. Edward’s University. The program was designed to measure, characterize, and explain the differences in the boundary layer (BL) and lower free troposphere (LFT) ozone profiles and associated meteorology the May intensive. During the May intensive of the San Antonio Field Study (SAFS), flights were scheduled twice-daily. The dawn launches were typically located at Traveler’s World RV Resort, which is 6 km south of downtown San Antonio. The site was in a predominately residential section of San Antonio, with I-37 1.5 km to the east, I-10 2 km to the north, and I-35 3 km to the west. The morning launches in this series occurred prior to sunrise in order to capture the residual layer before daytime mixing. The afternoon launches were typically from the southwest corner of the UTSA campus approximately 20 km northwest of downtown San Antonio, along Loop 1604. An additional 28 ozonesonde launches later in the summer and fall in San Antonio were conducted by Trinity University in collaboration with St. Edward’s University. The launches from Trinity University were once per day in the afternoon. The timing of the San Antonio flights was regulated by local air traffic considerations, with weekday flights required to be released before 7:30 am or after 4:30 pm local time. Weekend flights could be released at any time of the day.

The vertical profiles of ozone and meteorological data generated by these launches complement the existing ground monitoring network by adding a vertical component, allowing insight into transported ozone, either horizontally from other regions or vertically from events such as stratospheric intrusions into the troposphere behind cold fronts. While limited to discrete

profiles, ozonesondes provide the most cost-effective approach to gathering this data when compared to other techniques, such as Lidar or aircraft flights.

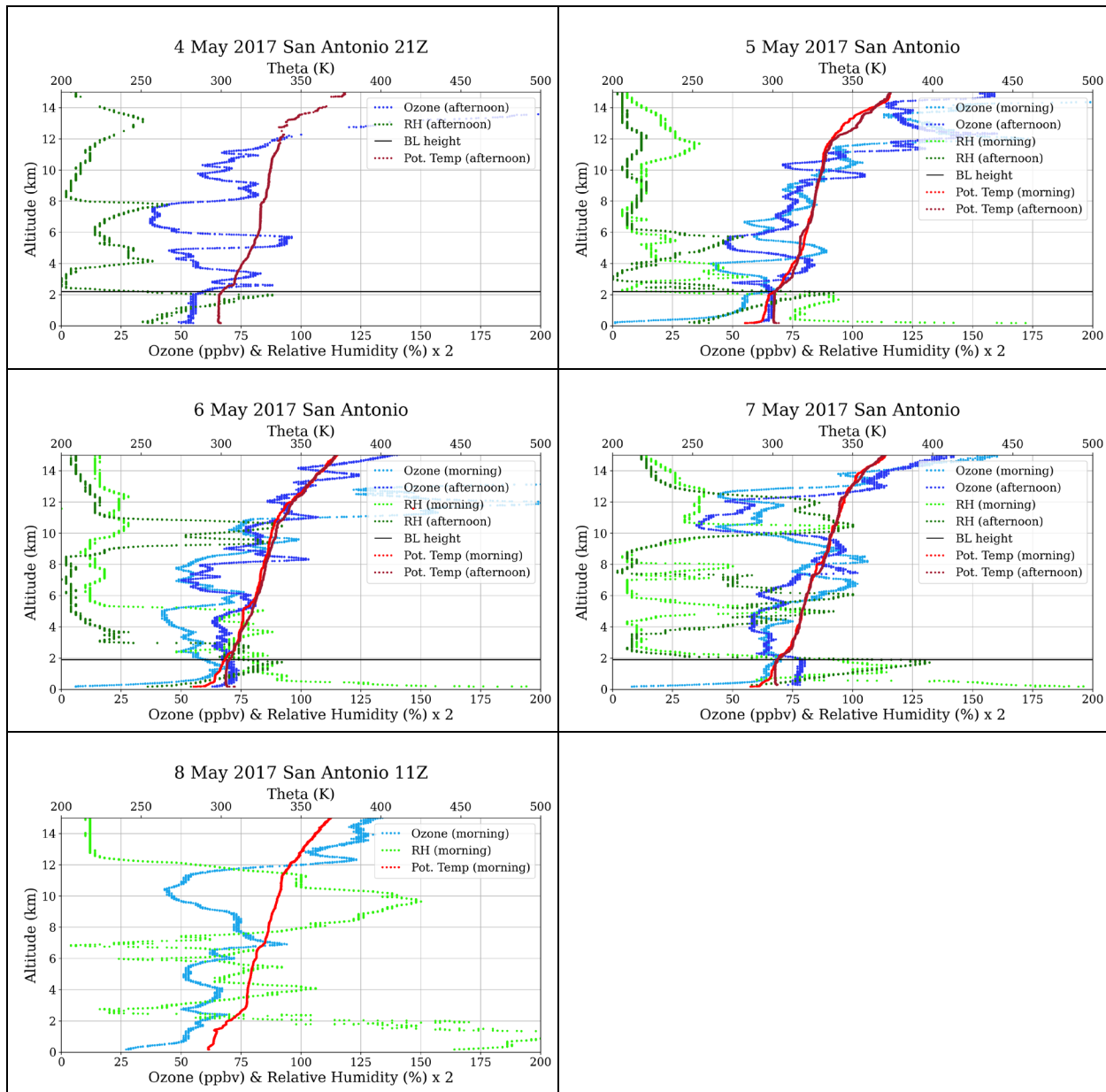


**Figure 52:** Tropospheric profiles from San Antonio occurring from 5 – 8 May 2017. The background ozone leftover in the residual layer increases on 6 – 7 May. The boundary layer shows increasing ozone concentrations each day. The final day in the series, 7 May 2017, had an MDA8 ozone concentration in exceedance of the ozone standard of 70 ppbv. The 7 May 2017 profile shows higher relative humidity in the boundary layer than previous days, with very dry air just above the boundary layer.

The morning profile on 7 May 2017 shows ozone concentrations near the surface of < 10 ppbv, indicative of overnight surface deposition and strong titration of ozone. Such morning profiles often indicate that ozone production after sunrise can be rapid given the large reservoir of NO<sub>2</sub>

that has formed overnight as ozone concentrations decreased. It is notable that the layer from 2.5 – 4.5 km is very dry, again suggestive of descending air from the UT/LS behind the front. Ozone concentrations from the residual layer up to nearly 4 km are nearly constant around 65 ppbv.

The afternoon profile on 7 May 2017 shows that dry layer continuing to move downward with nearly the same concentrations as seen in the morning profile between 2 – 3.5 km. Ozone concentrations in the well-mixed afternoon boundary layer are in the 75 – 80 ppbv range, an enhancement of 10 – 15 ppbv from the morning profile. This appears to be a case in which local production enhanced an elevated background that resulted from descending air behind a cold front.

The morning profile of 8 May 2017 shows the dry air mass seen on prior days is less prevalent. Ozone concentrations in the residual layer are around 55 ppbv, with a peak concentration ~70 ppbv in a narrow dry layer around 2.5 km. The gradient in ozone near the surface is not nearly as strong as on the prior day.

Early in the May 2017 intensive field campaign, a series of launches from 4 – 8 May 2017 sampled post-frontal conditions in San Antonio, with the profiles shown in Figure 52. A cold front passed through the San Antonio area on the evening of 3 May, leading to northwesterly winds during 4 – 5 May. The first profile in this series occurred in the afternoon of 4 May with clear sky conditions at launch. This profile features the lowest afternoon boundary layer concentrations during this series, with relatively strong winds at altitudes below 2 km of 10-15 m/s from the N or NW leading to dilution of ozone and locally emitted precursors. In the middle and lower free troposphere, there are notable layers of ozone at altitudes of 2.5, 3.5, and 5.5 km. Ozone in the very dry (RH < 5%) 2 – 4 km layer peaks at 85 – 90 ppbv, an air mass suggestive of UT/LS origins.

Over the next 3 days, morning and afternoon flights were performed. There was ~55 ppbv of ozone in the residual layer on the morning profile of 5 May, with ~65 ppbv of ozone in the very dry layer in lower free troposphere at 2 – 3 km. The afternoon profile that day showed BL ozone increased to ~65 ppbv, matching what was seen in the morning lower free troposphere. The free troposphere profiles on 5 May are consistent with descending air in the troposphere, with the ozone feature at 5.5 km on 4 May appearing at just under 5 km and near 4 km in the morning and afternoon profiles.

On 6 May, a deepening layer of dry air with high ozone peaks is found between 5 and 7 km AMSL. The morning residual layer peaks near 70 ppbv, with the afternoon boundary layer peaking ~75 ppbv. Interestingly, the afternoon ozone profile appears well mixed from just above the surface to the top of the boundary layer at 2 km, with 70 – 75 ppbv of ozone extending upwards from 2 – 5 km, again in a relatively dry layer. These profiles continue to suggest

influences from descending UT/LS air reaching the lower free troposphere, where entrainment in the growing morning boundary layer is possible.

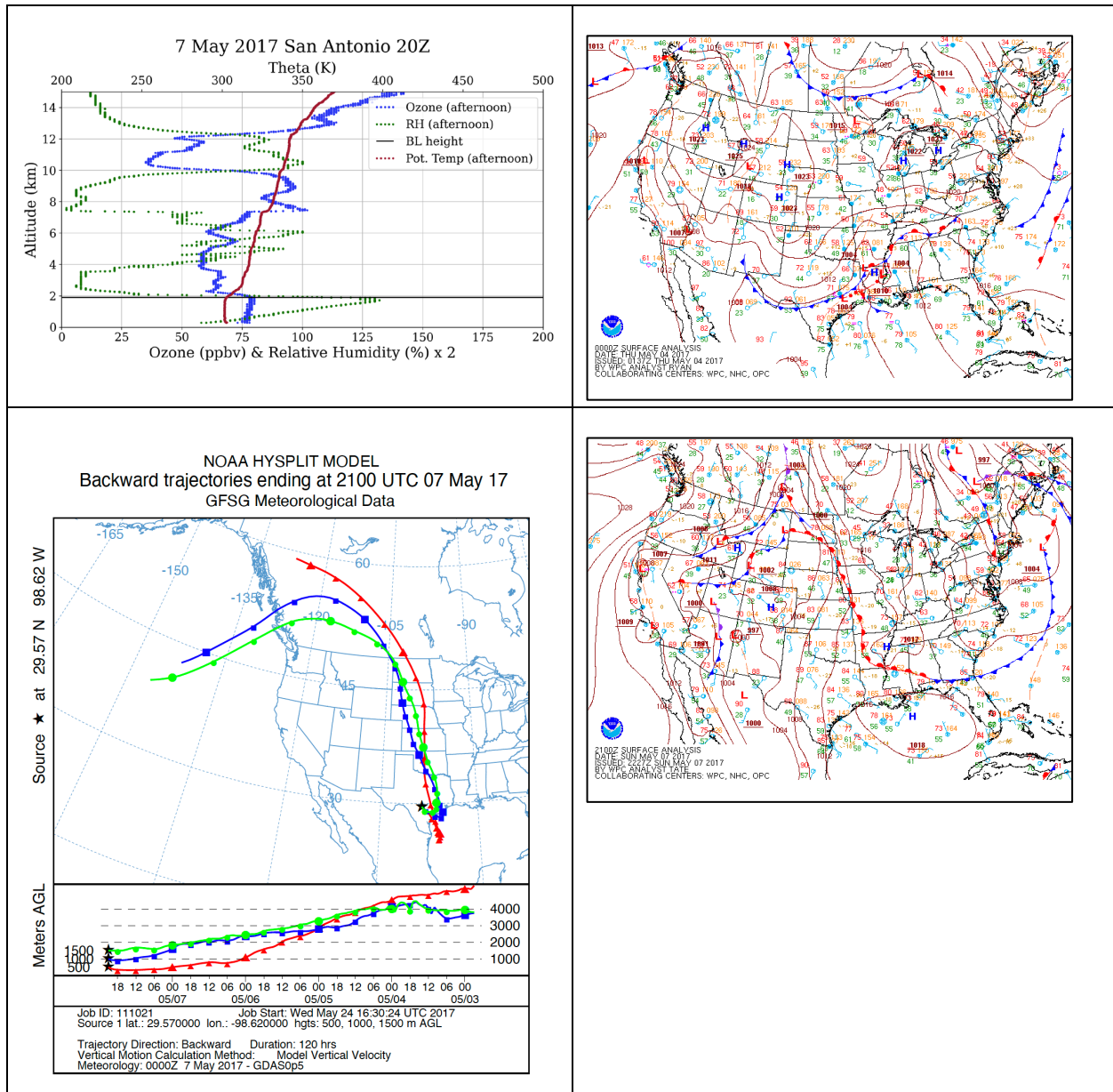


**Figure 53:** Top left: Profile of flight during the afternoon on 7 May 2017 from San Antonio. The ozone concentration in the boundary layer is 75-80 ppbv. Based on observations from the series of flights from 4 – 8 May, the dry air just above the boundary layer is likely associated with Upper-Troposphere/Lower-Stratosphere (UT/LS) air. Bottom left: HYSPLIT back trajectories show descent of the air mass that contributed to the boundary layer, consistent with UT/LS influences. Bottom left: Surface weather map for 4 May 2017 (00Z), which is when a front passed through San Antonio. Bottom right: Surface weather map for 7 May 2017 (21Z) showing post-frontal conditions and southerly flow.

The 24-hour wind runs for the C23 San Antonio NW and the C58 Camp Bullis monitors on 26 July 2017 are shown in Figure 54. At both monitors, the surface winds are nearly stagnant in the early morning hours and then there is a steady flow out of the SE all throughout the day. In the late morning and afternoon, the surface winds changed directions such that the urban plume was transported to the respective monitors.

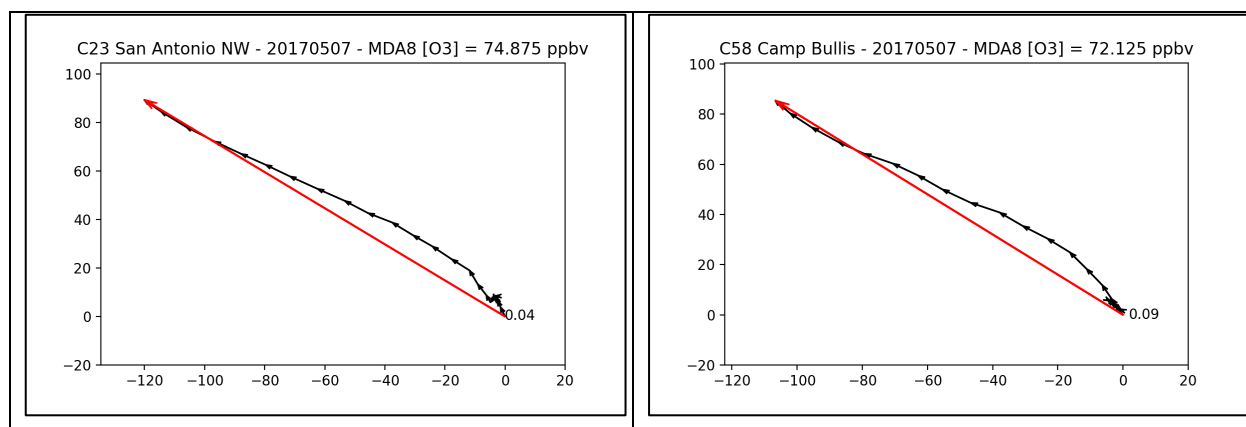


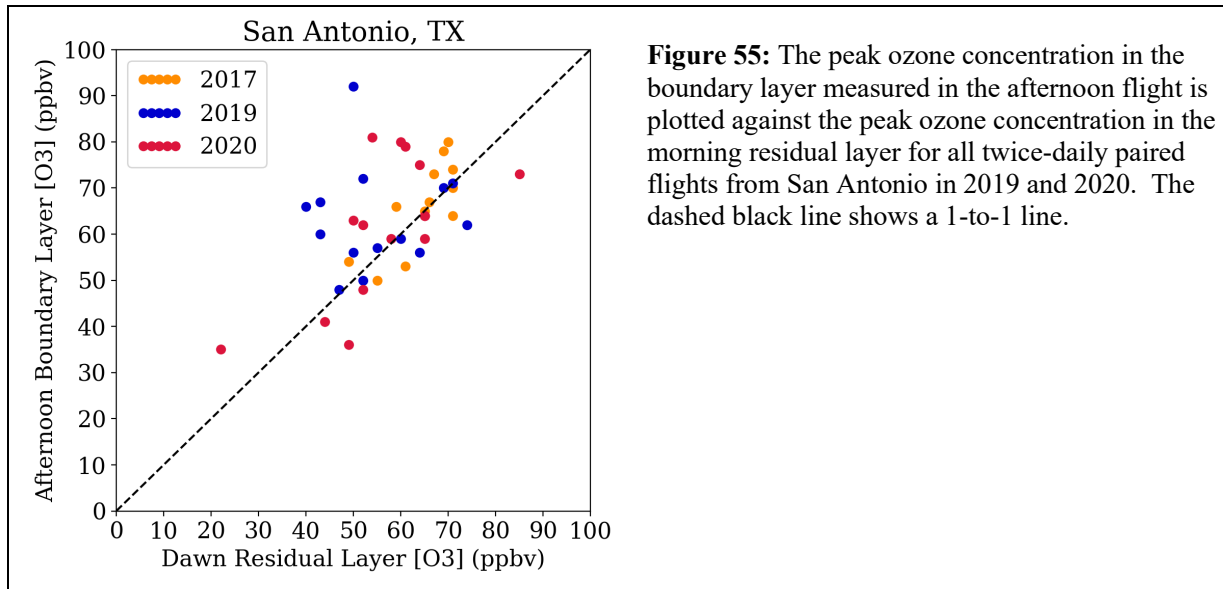
**Figure 54:** The 24-hour wind runs are shown for C23 San Antonio NW and C58 Camp Bullis (right) for 7 May 2017.

Overall, from 5 – 7 May the boundary layers of the morning and afternoon profiles show an increasing trend in ozone as the days progressed, with the maximum boundary layer ozone of 75–80 ppbv observed on the 7 May afternoon profile. The 7 May flight ended up being on one of only two ozone exceedances in the San Antonio area during the month of May 2017. Shown in Figure 53, the afternoon flight on 7 May 2017 has ozone concentrations of 75–80 ppbv in the boundary layer with a layer of high ozone/low relative humidity air riding just above. This suggests that the high ozone concentrations seen within the boundary layer may be influenced by downward mixing of Upper-Troposphere/Lower-Stratosphere (UT/LS) air that descended over the course of the previous few days. A backwards trajectory analysis seen in the HYSPLIT analysis of Figure 52 confirms significant subsidence over previous days, with strong downward motion of trajectories that end up in the boundary layer over San Antonio.

Further results from the 2017 ozonesonde flights from San Antonio are available in the final report of “Ozonesondes Launches for 2017 San Antonio Field Study,” PIs James Flynn and Gary Morris, PGA Number 582-17-71351-11. Further results of how the ozonesonde data fit within the framework of the rest of the data collected during SAFS can be found in the final report of “Analysis of San Antonio Field Study 2017 Monitoring Data,” PGA Number 582-18-82485-03.

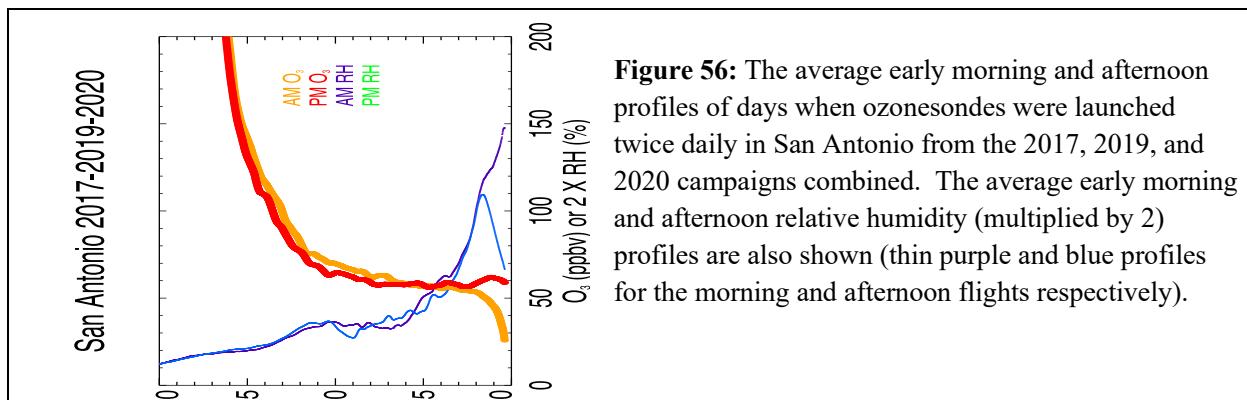
### 3.4 RESIDUAL LAYER INFLUENCE ON AFTERNOON OZONE IN SAN ANTONIO

Figure 55 shows a plot of the peak ozone concentration in the afternoon boundary layer versus the highest ozone in the dawn residual layer for flight days that occurred in twice-daily pairs: one flight at dawn and one flight in the afternoon. The twice-daily paired flights in May in 2017 during the intensive of the San Antonio Field Study while the paired flights occurred from July – October in 2019 and 2020.



**Figure 55:** The peak ozone concentration in the boundary layer measured in the afternoon flight is plotted against the peak ozone concentration in the morning residual layer for all twice-daily paired flights from San Antonio in 2019 and 2020. The dashed black line shows a 1-to-1 line.

Some of the afternoon ozone concentration was accounted for by contributions from the dawn residual layer that mixed into what became the afternoon boundary layer (Morris et al. 2010; Neu, Künzle, and Wanner 1994; Kleinman et al. 1994). There is uncertainty with each data point in Figure 55 due to (1) uncertainty in choosing the correct boundary layer height and (2) assigning the correct value for the residual layer ozone concentration. For the dawn residual layer concentration, we chose the highest ozone concentration from the morning ozone profile that is below the afternoon boundary layer height. Figure 55 shows that San Antonio afternoon ozone concentrations in excess of 70 ppbv in the boundary layer were accompanied by residual layer ozone concentrations (dawn flights) of ~50 ppbv or greater.

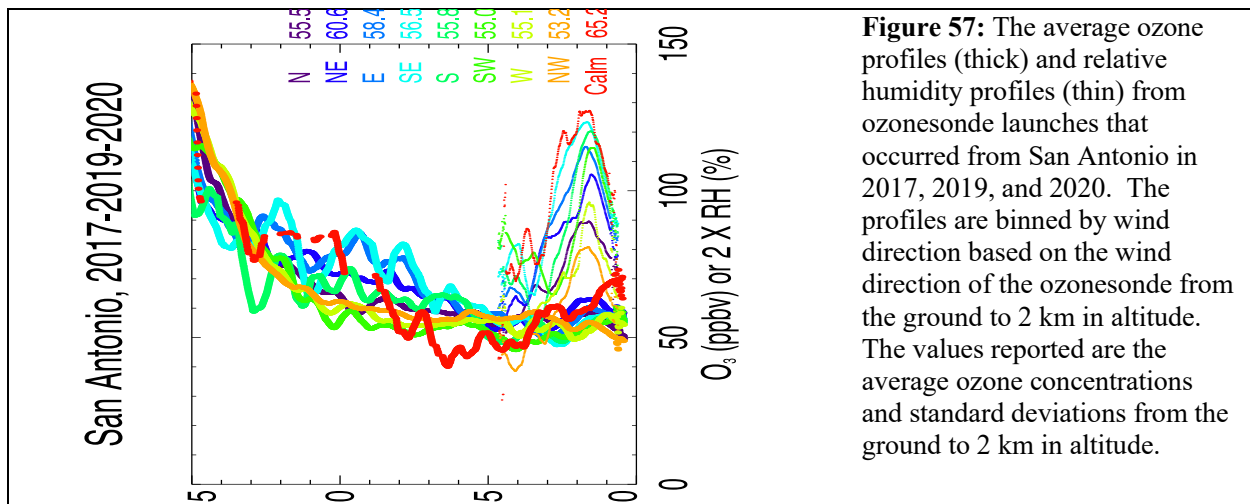


**Figure 56:** The average early morning and afternoon profiles of days when ozonesondes were launched twice daily in San Antonio from the 2017, 2019, and 2020 campaigns combined. The average early morning and afternoon relative humidity (multiplied by 2) profiles are also shown (thin purple and blue profiles for the morning and afternoon flights respectively).

Figure 56 shows average morning and afternoon profiles of ozone and relative humidity (the RH is multiplied by 2 in the figure) on days where twice daily launches occurred in 2017, 2019, or 2020. In the boundary layer, the average peak afternoon ozone (shown in red) is ~62 ppbv, while in the residual layer, the average ozone (shown in orange) is ~50 ppbv at the same altitude. The mean ozone concentration from 2 to 10 km AMSL increases slightly with altitude ranging from 55 to 62 ppbv. The mean RH data suggest the average cloud deck at the top of the boundary layer over San Antonio.

### 3.5 AVERAGE AFTERNOON PROFILES BY WIND DIRECTION

Figure 57 shows the average ozone profiles of ozonesondes launched from the sites in San Antonio in 2017, 2019, and 2020 based on wind direction. The data shown at the right of the figure indicate the mean boundary layer ozone (here taken to be the average below 2.0 km AMSL)  $\pm$  one standard deviation. The highest ozone occurs when winds are calm or northeasterly, with easterly and southeasterly winds producing the next highest mean boundary layer ozone concentrations. Lower ozone is found when winds are out of the northwest, west, or southwest, areas with sparse population.



## 4. CLUSTERING ANALYSIS OF OZONESONDES IN SAN ANTONIO AND EL PASO

The detailed case studies in previous sections provide good examples of how ozonesonde data can be used to better understand the high ozone events. In this section, we applied the K-Means clustering method to the ozonesonde data for San Antonio and El Paso to group the days with similar vertical O<sub>3</sub> distributions, which can reduce the day-to-day variability and reveal the general features. Clustering analysis has been shown to be an effective technique to discover underlying patterns by dividing objects into a number of groups or clusters based on some features of interest that are similar within each cluster but distinct between any two clusters (e.g. Li et al. 2020).

### 4.1 CLUSTERING IN SAN ANTONIO

We compiled a total of 37 flight days in 2017, 2019 and 2020 with pair-launched ozonesondes in the morning and afternoon. Days with no valid ozone data and one stormy day (15 August 2019) were removed. Before performing the clustering, features of interest need to be identified. Based on the boundary layer dynamics during the course of a day, we set the threshold of 2.5 km to separate the mixing layer (ML) and lower free troposphere (LFT) because the 37-day mean of the ML height is 2.56 km. We created the following three features in San Antonio:

- ① **O<sub>3</sub>\_AM\_RL**: Average O<sub>3</sub> below 2.5 km in the morning launches. As the residual layer (RL) makes up the bulk of the lower 2.5 km in the morning, this feature approximates the average O<sub>3</sub> in the morning RL.
- ② **O<sub>3</sub>\_PM\_LFT - O<sub>3</sub>\_AM\_LFT**: The difference of the average O<sub>3</sub> from 2.5 km to 5 km between the afternoon and morning launches. This altitude range represents the lower free troposphere (LFT).
- ③ **O<sub>3</sub>\_PM\_ML - O<sub>3</sub>\_AM\_RL**: The difference of the average O<sub>3</sub> below 2.5 km between the afternoon and morning launches. This feature represents the change in ozone between the afternoon mixing layer and the morning residual layer.

Feature 1 can capture the background O<sub>3</sub>, which is largely determined by the amount of O<sub>3</sub> in the RL since O<sub>3</sub> in the nocturnal stable boundary layer is much lower. As the stable boundary layer grows with the increasing temperature during daytime, O<sub>3</sub> in the residual layer will mix down and contribute to the ML O<sub>3</sub>. Feature 2 is designed to capture the presence of long-range transport, which normally occurs in the LFT. Feature 3 represents the net changes of O<sub>3</sub> from local photochemical production, transport and mixing.

The calculations of the features yielded a matrix of size 37×3, containing 37 days with three features on each day. Before applying this matrix to K-Means clustering, each feature is normalized to have a zero mean and unit variance. Since the K-Means clustering algorithm calculates Euclidean distance to the centroid, normalization gives each feature the same weight

to the clustering. Furthermore, the number of clusters, which is the k value, has to be predetermined. The value was determined as three by a function in the NbClust R package, which encapsulates 30 indices for selecting the value of k. The package suggested the optimal value of k to be three, but we chose k as four to yield an additional cluster which is the cleanest cluster as described below. In summary, a matrix containing 37 days with three normalized features is implemented into the K-Means clustering with k equal to 4 in San Antonio.

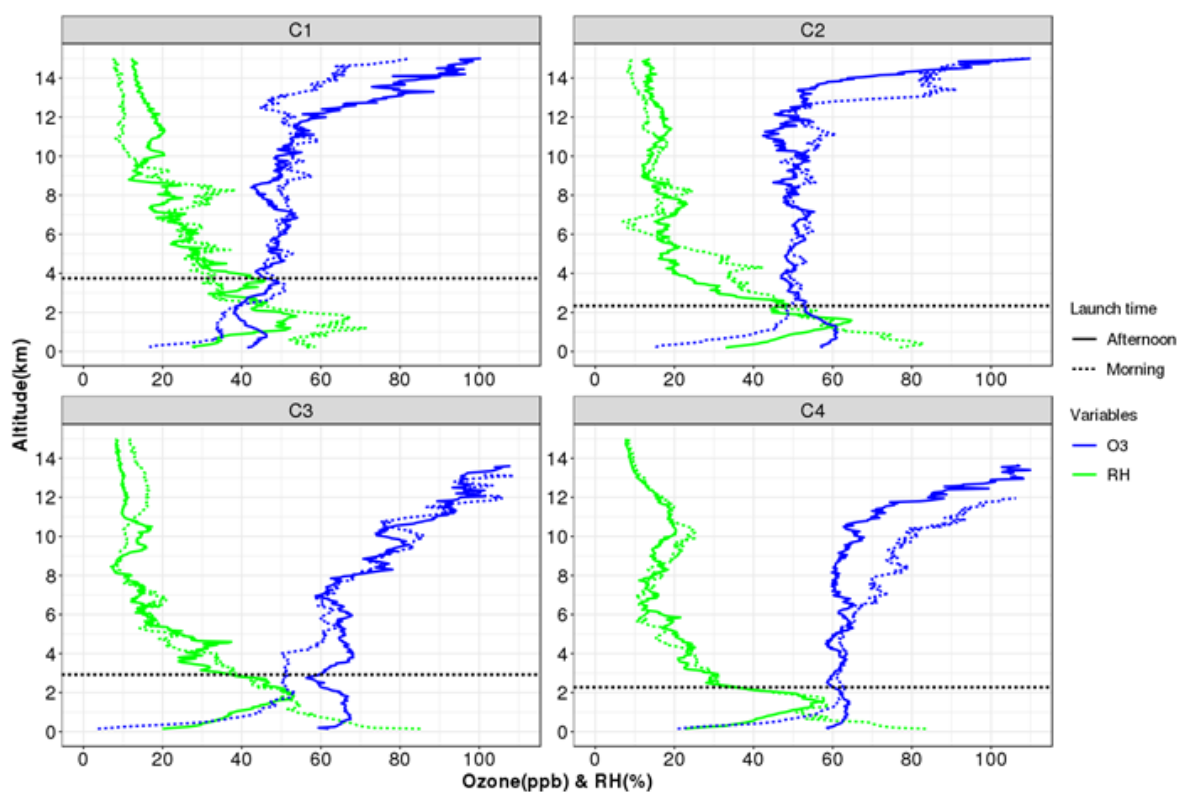


**Figure 58:** Cluster-mean O<sub>3</sub> (blue lines) and RH (green lines) profiles in the morning (dashed line) and afternoon (solid lines) launches for San Antonio. The black dashed lines indicate the mean ML height in each cluster.

The O<sub>3</sub> and RH profiles from four clusters (C1-C4) are shown in Figure 58. They were obtained from the average values of each 50 m altitude band from the surface to 15 km over all the days in each cluster. Table 5 summarizes the mean features and the number of days in each cluster. C1 is the cleanest cluster with the minimum O<sub>3</sub>\_AM\_RL value of 33.79 ppbv. Long-range transport has little influence in C1 as indicated by the similar value of O<sub>3</sub>\_AM\_LFT and O<sub>3</sub>\_PM\_LFT. O<sub>3</sub>\_PM\_ML is 6.10 ppbv higher than O<sub>3</sub>\_AM\_RL, which could be attributable to the local chemical production. C2 has a relatively higher O<sub>3</sub>\_AM\_RL value of 40.72 ppbv compared with C1. The long-range transport effects in C2 are also unlikely but the local production is the highest at about 17.10 ppbv. C3 has a similar background ozone level with C2 of 42.93 ppbv but the transport input is higher (~10 ppbv). The transport-influenced cases in May 2017 described in Section 3.3 were captured by this cluster, which confirms the clustering results. The local O<sub>3</sub>

production in this cluster is the second highest at about 13.06 ppbv. C4 has the highest O<sub>3</sub>\_AM\_RL value of about 55.08 ppbv but with a low level of O<sub>3</sub> production (7.56 ppbv), indicating the highest contribution of background O<sub>3</sub> to the ML O<sub>3</sub> in this cluster. In summary, C1 is the cleanest with both the lowest background and locally-produced O<sub>3</sub>. C2 and C3 have similar middle levels of background O<sub>3</sub>, but C2 has higher O<sub>3</sub> production in the mixing layer while C3 has higher long-range transport inputs. C4 has the highest background O<sub>3</sub> but with the second lowest O<sub>3</sub> production.

**Table 5:** Cluster-mean O<sub>3</sub>, wind direction (WD) and wind speed (WS) in the morning (AM) residual layer (RL) and lower free troposphere (LFT), and afternoon mixing layer (ML) and LFT in San Antonio and El Paso.

|                               | San Antonio |        |        |        | El Paso |        |        |        |
|-------------------------------|-------------|--------|--------|--------|---------|--------|--------|--------|
|                               | C1          | C2     | C3     | C4     | C1      | C2     | C3     | C4     |
| Days(#)                       | 4           | 9      | 8      | 16     | 15      | 6      | 5      | 3      |
| O <sub>3</sub> _AM_RL (ppbv)  | 33.79       | 40.72  | 42.93  | 55.08  | 48.21   | 52.99  | 40.80  | 60.00  |
| O <sub>3</sub> _AM_LFT (ppbv) | 49.33       | 51.20  | 54.06  | 61.79  | 60.52   | 58.39  | 56.27  | 72.66  |
| O <sub>3</sub> _PM_ML (ppbv)  | 39.90       | 57.82  | 65.78  | 62.64  | 61.06   | 63.25  | 62.23  | 80.72  |
| O <sub>3</sub> _PM_LFT (ppbv) | 45.97       | 49.72  | 63.86  | 60.54  | 59.36   | 60.84  | 62.91  | 72.46  |
| WD_AM_RL (degree)             | 168.71      | 199.56 | 106.24 | 166.64 | 175.50  | 329.79 | 105.09 | 29.77  |
| WD_AM_LFT (degree)            | 330.47      | 345.03 | 16.06  | 316.76 | 73.07   | 58.27  | 63.99  | 18.51  |
| WD_PM_ML (degree)             | 167.98      | 100.45 | 78.23  | 158.65 | 120.57  | 38.31  | 100.50 | 126.90 |
| WD_PM_LFT (degree)            | 326.77      | 299.92 | 21.82  | 292.56 | 58.69   | 48.70  | 35.43  | 172.23 |
| WS_AM_RL (m/s)                | 1.58        | 1.33   | 0.86   | 1.89   | 0.29    | 1.28   | 2.41   | 0.94   |
| WS_AM_LFT (m/s)               | 2.09        | 2.89   | 6.64   | 4.63   | 3.44    | 6.39   | 2.44   | 0.64   |
| WS_PM_ML (m/s)                | 1.76        | 1.17   | 1.99   | 2.15   | 0.79    | 1.01   | 2.98   | 0.91   |
| WS_PM_LFT (m/s)               | 2.18        | 2.26   | 4.16   | 3.50   | 2.18    | 5.15   | 2.54   | 0.22   |

Figure 59 displays the wind roses of the average winds in the morning RL and afternoon ML on all the days of each cluster. C1 is dominated by southerly winds both in the morning (~168.71°) and afternoon (167.98°), which explains the lowest background and locally produced ozone due to the clean marine air from the Gulf of Mexico. Morning wind directions in other clusters are

quite variable leading to relatively higher levels of background O<sub>3</sub>. For C1 and C2 with the highest locally-produced O<sub>3</sub>, winds are generally from the east (78°-100°) in the afternoon ML, which is consistent with the afternoon wind conditions in many exceedance cases discussed in Section 3 (e.g. 1 October 2020). C4 in the afternoon ML is also dominated by strong (2.15 m/s) southerly (158.65°) winds causing the very low O<sub>3</sub> productions. For the only transport-influenced C3, strong (~ 4.16 m/s) winds in the afternoon LFT come from the northeast (21.82°) differing from the northeasterly winds in other clusters (292°-326°). This may infer that the passage of the cold front favors the long-range transport of continental air from the northeastern states.

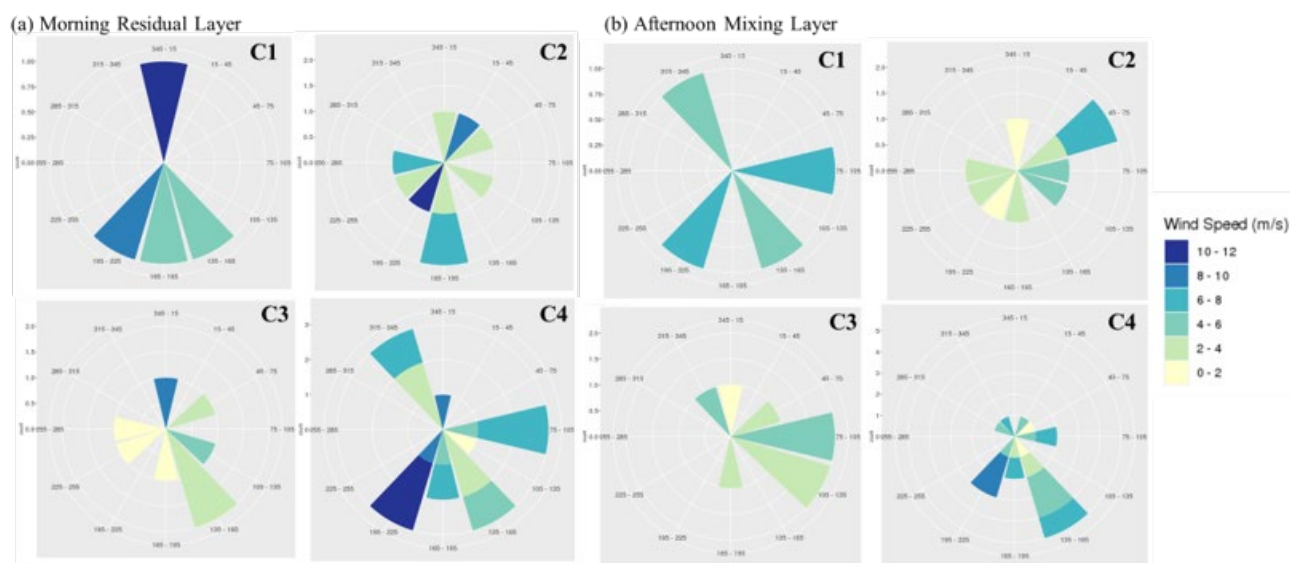


**Figure 59:** Wind roses for San Antonio of the average winds in the morning RL (a) and afternoon ML (b) on all days of each cluster.

## 4.2 CLUSTERING IN EL PASO

Of all the twice-daily (dawn and afternoon) paired ozonesonde launches in 2019 and 2020, two days (15 July and 26 August 2020) with too much missing data were removed. Although 6 August 2019 has complete O<sub>3</sub> data, it was also deleted because it always formed a one-day cluster if included. This indicates the unique O<sub>3</sub> vertical distributions on that day and cannot represent the general cases. As a result, a total of 29 days in El Paso were used for clustering analysis. The same three features are fed into K-Means algorithm but the threshold between ML and LFT was changed from 2.5 km to 4 km due to the higher elevation in El Paso. We also set k equal to four to keep consistent with San Antonio analysis.

The cluster mean O<sub>3</sub> and RH profiles in El Paso were shown in Figure 60; the average features were also listed in Table 5. C1 and C2 have similar vertical distributions of O<sub>3</sub> except that O<sub>3</sub>\_AM\_RL in C2 is about 5 ppbv higher. Their local O<sub>3</sub> production amount is also comparable

at 10-13 ppbv. C3 has the lowest value of O<sub>3</sub>\_AM\_RL about 40.80 ppbv with a relatively higher O<sub>3</sub> production of ~15 ppbv. It is also the only transport-impacted cluster with an input of 6.63 ppbv. C4 is identified with both the highest O<sub>3</sub>\_AM\_RL value of ~60 ppbv and locally-produced O<sub>3</sub> value of ~20.72 ppbv, making it the dirtiest cluster of all. There is little long-range transport influence in C4 but the positive gradient and the low RH just above ML may indicate the subsidence air from the upper troposphere or even stratosphere intrusions. In summary, C1 and C2 have a middle level of both background and locally-produced O<sub>3</sub> with no transport effects. C3 is characterized by the lowest background O<sub>3</sub> with relatively higher O<sub>3</sub> production and transport inputs. C4 is the dirtiest cluster with the highest local O<sub>3</sub> production and background O<sub>3</sub>.

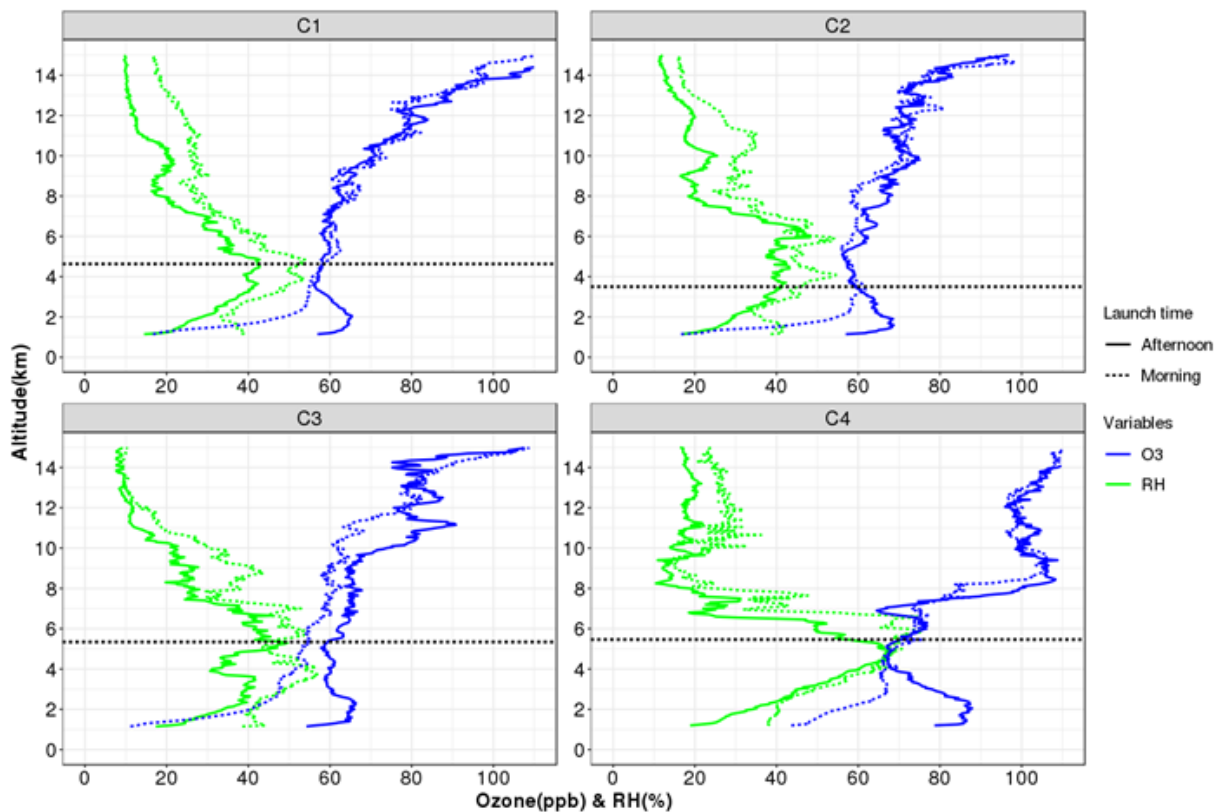


**Figure 60:** Cluster-mean O<sub>3</sub> (blue lines) and RH (green lines) profiles in the morning (dashed line) and afternoon (solid lines) launches for San Antonio. The black dashed lines indicate the mean ML height in each cluster.

The wind roses of the average winds in the morning RL and afternoon ML on all the days of each cluster in El Paso are shown in Figure 61. In the morning RL, C1 has some days with southerly or southeasterly winds, while C2 is dominated by northwesterly winds (329.79°). This explains the ~5 ppbv higher value of O<sub>3</sub>\_AM\_RL in C2 relative to C1. Southeasterly (105.09°) winds with the highest speed (~2.41) prevail in C3, causing the lowest background O<sub>3</sub>. The highest background O<sub>3</sub> in C4 may be induced by the overall northeasterly (29.77°) winds bringing polluted continental air. In the afternoon ML, Wind directions in C1-C2 are quite variable leading to a middle level of O<sub>3</sub> production. C3 is dominated by the fastest (~ 3m/s)

easterly ( $\sim 100^\circ$ ) winds, which may bring emissions from the east region causing high  $O_3$  productions. The highest  $O_3$  production in C4 can be attributable to the weak dissipation effects due to the low wind speed ( $< 2$  m/s) on all days. Similar to San Antonio, winds in the afternoon LFT of the transported-impacted C3 blow from the northeast indicating the inputs of  $O_3$  from the northeastern regions.

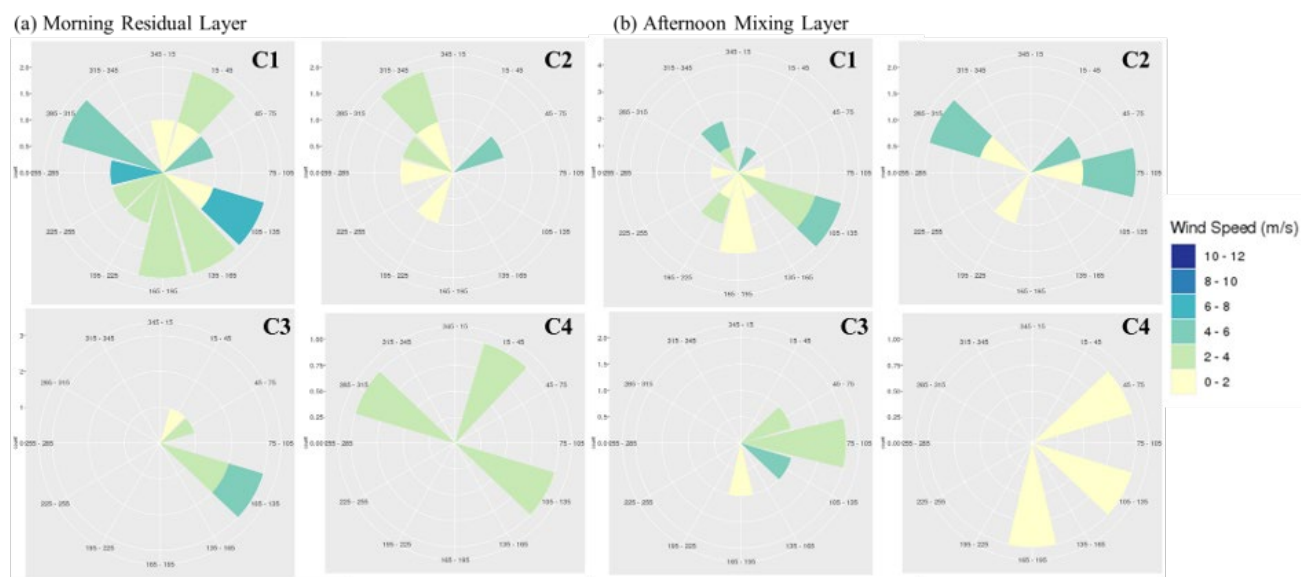


**Figure 61:** Wind roses for El Paso of the average winds in the morning RL (a) and afternoon ML (b) on all days of each cluster.

Lastly, we compared the surface MDA8  $O_3$  distributions by cluster in Figure 62. The CAMS sites used are listed in Table 1 for El Paso and Table 4 for San Antonio. MDA8  $O_3$  is generally higher in El Paso (40-85 ppbv) than that in San Antonio (25-75 ppbv). The ML  $O_3$  distributions by cluster generally match with the surface MDA8  $O_3$  in San Antonio with the lowest values in C1 and higher values in C2-C4. The maximum MDA8 value in C1 is less than 70 ppbv, indicating it is not likely to have an exceedance day in this cluster. However, there is a mismatch between the ML and surface MDA8  $O_3$  in C3 of El Paso. This may be caused by the very high wind speed (3 m/s) in C3. The fresh emissions and  $O_3$  can be quickly transported to the downwind area, mixed up therein, and then captured by the balloon at a relatively higher layer ( $\sim 2$  km in Figure 60). The sample sizes for all clusters are relatively small; larger sample sizes could change the results, including the cluster characteristics.

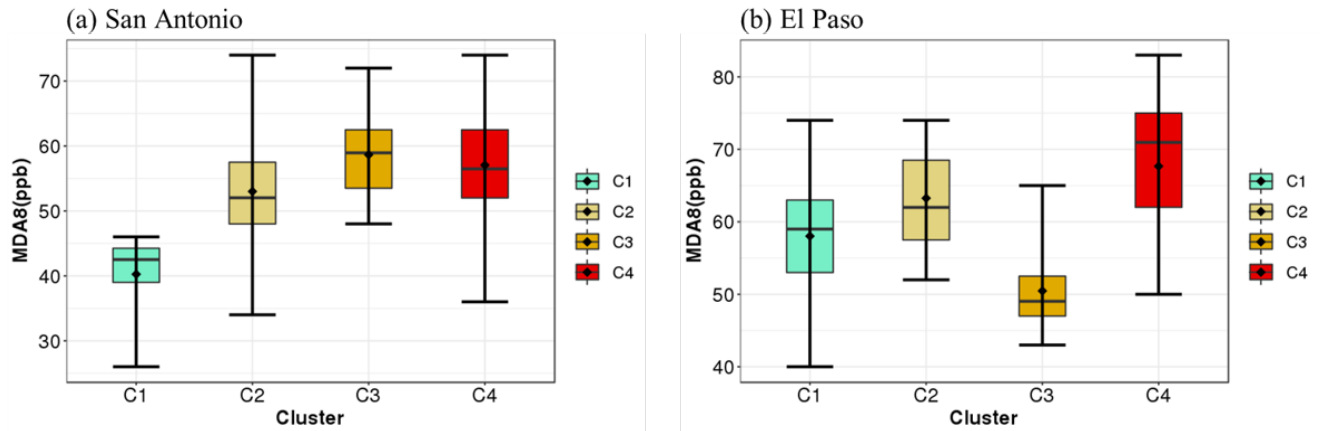


**Figure 62:** Boxplots of surface MDA8 O<sub>3</sub> at the CAMS sites in San Antonio (a) and El Paso (b) of each cluster.

In conclusion, we applied the K-Means clustering technique based on three well-designed features to the multiple-year ozonesondes data in San Antonio and El Paso. Four clusters were obtained in both regions with distinct O<sub>3</sub> and wind features. O<sub>3</sub> in each cluster is characterized by the different contributions from long-range transport, background, and locally-produced O<sub>3</sub> despite the comparable O<sub>3</sub> levels between two certain clusters. This indicates that ozonesonde data can provide insights towards a better understanding of O<sub>3</sub> variability and contains helpful information for air quality policy makers. The good match between ML and surface O<sub>3</sub> at the CAMS sites further verifies the effectiveness of ozonesonde data serving as a complement of surface monitoring networks, allowing for a three-dimensional depiction of O<sub>3</sub> distribution. The clustering analysis presented here is built upon limited sample days between July and October. Additional vertical distributions from other months different from the patterns discerned here are expected considering the seasonality of synoptic conditions in Texas (Bernier et al. 2019). To reveal these patterns, more launches in other seasons are necessary.

## **5. CONCLUSIONS AND RECOMMENDATIONS FOR FUTURE WORK**

### **5.1 EL PASO**

The dawn launches provide ozone profiles of the residual layer that can contribute to that day's afternoon peak ozone in the boundary layer as mixing occurs throughout the morning. For the days during the 2019 and 2020 campaigns that exceeded the ozone standard, the winds were typically slow overnight and during the day, enhancing the contributions of air from the previous day being to the ozone found in the residual layer. The high background ozone present in the residual layer accelerated and enhanced local production resulting in exceedance days. As might be expected, the atmosphere was relatively clear of clouds and moisture on exceedance days.

For the days during the 2019 and 2020 campaigns that exceeded the ozone standard, there were signs of possible transport of ozone and its precursors into either the El Paso or Socorro, TX areas. Juarez is usually upwind of the high ozone areas observed in El Paso or Socorro, TX. When Juarez is upwind, slow steady winds may lead to an increase greater than 10 ppbv to the MDA8 ozone concentration on those days, and thus influence whether the El Paso and Socorro, TX monitors are in compliance with the NAAQS ozone standard. The exceedance event on 21 August 2020 was influenced by smoke from the wildfires in California and perhaps other areas.

A series of ozonesonde launches from 15-18 May 2017 (none of these days exceeded the ozone standard in El Paso) showed most profiles had an ozone enhancement that coincided with dry air just above the boundary layer, which can be indicative of transport. For afternoon profiles where the enhancement was above the boundary layer, there was a strong cap preventing mixing down into the boundary layer. The afternoon of 16 May had a weaker cap at the top of the boundary layer and the enhancement above the afternoon boundary layer was no longer present. That same afternoon the surface measurements showed greatly elevated levels of PM<sub>2.5</sub> that also coincided with decreased visibility. This series of ozonesonde launches is an example of how ozonesonde data along with other supporting measurements can provide an indication of when there may be influences to biomass burning.

When conditions are favorable for ozone production, the transport of ozone and its precursors (e.g., NO<sub>x</sub>) into the El Paso area can lead to increases in ozone concentrations at key monitors that are in the path of the transported plume.

### **5.2 SAN ANTONIO**

In San Antonio, post-frontal environments are very effective in creating conditions for high local ozone production, particularly when the return to southerly flow of moist, cleaner air from the Gulf of Mexico does not happen quickly. During much of August and September 2019, a high-pressure system in the southeast US led to persistent and strong southerly flows from the Gulf of Mexico that prevented cold fronts from making it to San Antonio. The marine air resulted in lower background ozone as could be observed from the dawn flights, which captured the residual

layer. During the 2020 campaign, the cold fronts that did make it to San Antonio were precursors to six days in exceedance of the ozone standard.

The location of the C58 Camp Bullis monitor, which often records the highest maximum daily eight-hour ozone concentrations in San Antonio, likely plays a role in the direction of surface winds observed there. The monitor lies in a shallow valley where the hills on each side may channel the winds along a NW/SE axis. On most days during 2017, 2019, and 2020 where the C58 Camp Bullis monitor exceeded the NAAQS ozone standard, the surface winds were out to the NW in the morning and SE in the afternoon. With many such days occurring in post-frontal conditions, the morning winds out of the NW may transport continental air with a higher background of ozone and its precursors into San Antonio. The plume affecting Camp Bullis and San Antonio Northwest monitors contains both elevated background ozone from continental transport and local ozone production from San Antonio. Recirculation of this combined air mass over San Antonio brings the polluted air back over the northwestern San Antonio monitors during the afternoon of a high ozone day.

Ozonesonde profiles show that in some cases there was a positive gradient in the ozone concentration just above the afternoon boundary layer. Such cases that have an enhancement of ozone just above the boundary layer may indicate transport. The lapse rate of the potential temperature at the top of the afternoon boundary layer can provide an indication of how strong the cap is and whether mixing into the boundary layer may be possible. Supporting surface measurements may provide some indication of whether any of the air aloft was mixed to the surface and whether it may have had biomass influences.

There is limited evidence of stratospheric influence, due to low humidity and high ozone present above the boundary layer, but it is not clear that the stratospheric air is reaching the boundary layer. More work is needed to better quantify the potential impacts of transported ozone on boundary layer concentrations. This could potentially be done by incorporating modeling along with sonde profile analysis.

### **5.3 RECOMMENDATIONS FOR FUTURE WORK**

With the field campaigns from each city in 2017, 2019, and 2020, we are now beginning to build up a robust data set to observe differences between years when there may be differences in the circulation patterns. In conjunction with surface measurements, ozonesondes provide a way of obtaining a three-dimensional view of what contributes to boundary layer ozone. Being near the edge of attainment, both San Antonio and El Paso are areas worthy of ongoing and further study.

Utilizing the growing ozonesonde data set, there are a number of ways to maximize scientific returns and to better understand the factors contributing to boundary layer ozone. Future ozone sonde studies can focus upon the following topics to assist the TCEQ in identifying the causes of high ozone in Texas cities.

- *Ozonesonde data can be used to identify days impacted by biomass burning.* The TCEQ, either directly or through the AQR program, has funded field projects which utilize aerosol optical properties to identify periods which may have been impacted by biomass burning plumes. As discussed previously, these biomass burning plumes can also be associated with impacts on O<sub>3</sub>. Several of the events identified in El Paso showed abrupt transitions from increasing or moderate O<sub>3</sub> levels to much lower levels, often accompanied by abrupt changes in other gas and aerosol measurements at C12 UTEP. These changes suggest a change in air mass or mixing may have occurred. Additionally, questions have been raised regarding the altitude at which distant biomass burning plumes are transported with the suggestion that plumes are transported aloft but may or may not affect the surface conditions. Coupling the ozonesonde and biomass burning measurements with modeling can create a more complete data set to better understand the conditions under which biomass burning plume can impact surface measurements and potential links to ozone. In 2020 and 2021, UH (PIs Flynn and Wang) and Baylor (PIs Sheesley and Usenko) were funded to investigate biomass burning plumes in El Paso and Houston. Going forward, we suggest that additional ozonesonde launches in Houston could target periods which are identified in near-real time to have potential biomass burning impacts. These launches would provide a more complete picture by supplementing the surface measurements, remote sensing satellite products, and transport modeling efforts. Similarly, establishing a biomass burning measurement site in the San Antonio area would provide a continuous record of potential smoke impacts on San Antonio. This site would allow for a more complete characterization of the conditions during ozonesonde launches as well as identifying periods that could be targeted for additional launches. This site could also aid in the identification of periods of smoke from agricultural burning in Mexico and Central America. Together, these two programs can provide a more comprehensive understanding of the impact of biomass burning plumes on Texas ozone and air quality.
- *Ozonesonde data can be used to identify days affected by stratospheric air.* Stratospheric ozone is a major component of tropospheric ozone globally. Previous studies combining observations and modeling have demonstrated stratospheric intrusion events can cause local and regional surface ozone exceedances under certain conditions. However, such studies have not been conducted in a systematic manner for Texas where a rich dataset that by the end of the 2020 field campaigns will include 120+ ozonesondes from each of San Antonio and El Paso, 50+ from Austin, and 600+ from the Houston area. Sonde profile analysis is one way to identify potential ozone-rich intrusions from stratospheric-tropospheric exchange (STE). There are a couple of other ways to leverage this data set to determine the contributions of STE. One is to use high resolution potential vorticity analysis. Some studies have used O<sub>3</sub>/CO ratios to track stratospheric influence at the surface. If El Paso, San Antonio, Houston, and other cities had trace-level CO monitors

with ppb resolution, stratospheric influence could be directly verified with measurements. Another way may be through 3-dimensional transport modeling. Yuxuan Wang (University of Houston) recently demonstrated the high-resolution regional version of the GEOS-Chem global chemical transport model has a good ability in recreating measured ozone vertical profiles. Thus, the GEOS-Chem model can be used to do a reanalysis of past ozonesonde launches in Texas to better identify and quantify stratospheric influence on near-surface ozone. Specifically, transport tracers can be implemented in GEOS-Chem to separate air masses of stratospheric origin from those of tropospheric and surface origins. The relative contribution of the stratospheric tracer compared to the tropospheric/surface tracers will be a quantitative metric to decompose ozonesonde profiles into stratospheric vs. non-stratospheric components at different levels. The modeling approach and potential vorticity analysis can be corroborated for cross validation. The outputs would not only document and quantify past observed events of stratospheric intrusion but also generalize typical conditions when such events are most likely to happen. The latter part would provide valuable information to guide future ozonesonde launches to better capture stratospheric intrusion events on ozone in Texas.

- *Ozonesonde data analyses can be combined with other analyses (diurnal cycle analysis, synoptic weather pattern analysis, back trajectory analysis, clustering analysis) to more fully describe the characteristics of high ozone days, and to understand how meteorology, emissions, and chemistry combine to make high ozone in Texas.* For the Houston-Galveston-Bazoria (HGB) area, Bernier et al. (2019) broke surface ozone diurnal cycles into four clusters based on how specific features of the diurnal cycle varied (e.g., slope of ozone change in the morning) that were found to associate with synoptic meteorological processes such as the Bermuda High and the low-level jet. Using this method of clustering to characterize ozone variability, Bernier et al. found that the clustering was greatly influenced by early morning ozone values and had a strong correlation with the afternoon peak. The same approach used in Bernier et al. (2019) can be applied to similar studies of the San Antonio and El Paso areas. Further, this analysis could be paired with analysis from the twice-daily paired ozonesonde launches from the recent and upcoming field campaigns from San Antonio and El Paso. The pair-launched ozonesonde data can also be applied to clustering analysis by some well-designed features to distinguish the ozone contributions from background, long-range transport, and local productions.
- *Ozonesonde data can assist in demonstrations of international influences upon the non-attainment status of El Paso.* Air quality in the El Paso-Juarez airshed is complicated by the contribution of emissions from both El Paso in Texas and Ciudad Juarez in Mexico and local circulation patterns around the mountains. To gain a better understanding of the chemistry in El Paso, we must also understand the links with Juarez. Having access

to CAMS-like data from Juarez could help better understand the area's overall air quality and improve analysis under the ozonesonde programs. It is possible that statistical analyses, such as studying CO/NO<sub>x</sub> ratios in relation to back trajectories, may provide insight to determine if there are unique chemical characteristics by area. Modeling efforts may be able to provide some insight as well, particularly when paired with other measurements and analysis.

- *Ozonesonde data can be used to understand how seasonal weather patterns such as the southwestern US monsoon affect the number of high ozone days that occur in a given year.* The average morning and afternoon profiles of ozone and relative humidity on days with twice daily (dawn/afternoon) ozonesonde launches from the UTEP campus, which primarily during the 2019 and 2020 monsoon seasons, showed the mean ozone concentration from 3 to 7 km AMSL is nearly uniform ranging from 58 to 60 ppbv and coincides with relatively moist air. The moist air suggests there would not be stratospheric influence on days where profiles are similar to this pattern. The nearly uniform ozone in this range may be related to the monsoon season since nearly all of the twice-daily paired flights occurred during the monsoon season. Also, it may be the launch location's (UTEP campus) to the Franklin Mountains is a factor. The mountains may push a layer of air upwards and lead to mixing above them.
- *Ozonesonde data can also be used to determine the stability of the atmosphere, which can be closely related to whether or not the weather is conducive to high ozone.* Atmospheric stability is one of the key factors affecting ozone, along with local emissions, long-range transport, recirculation and stagnation, and stratospheric influences. By studying all of these phenomena with ozone sonde data and other related data sets, the causes of specific ozone episodes can be identified.
- *Ozonesonde data from 2020 can be used to study the effects of the COVID-19 lockdown upon air quality.* The lockdown resulted in drastically reduced emissions in some areas, and these reductions had substantial effects upon air quality. The year 2020 provides an interesting case study in which to examine air quality, especially in the Spring season, under conditions with a substantial reduction in NO<sub>x</sub>, particularly from mobile sources that are associated with commuting traffic. Analysis of surface monitor data, balloon profiles, and model results would help us better quantify sources of ozone production, especially as anthropogenic contributions are substantially reduced compared to a typical year.

## 6. REFERENCES

- Allwine, K Jerry, and C David Whiteman. 1994. “Single-Station Integral Measures of Atmospheric Stagnation, Recirculation and Ventilation.” *Atmospheric Environment* 28 (4): 713–21.
- Appenzeller, Ch, and H C Davies. 1992. “Structure of Stratospheric Intrusions into the Troposphere.” *Nature* 358 (6387): 570–72.
- Bernier, Claudia, Yuxuan Wang, Mark Estes, Ruixue Lei, Beixi Jia, Sing-Chun Wang, and Jiajia Sun. 2019. “Clustering Surface Ozone Diurnal Cycles to Understand the Impact of Circulation Patterns in Houston, TX.” *Journal of Geophysical Research: Atmospheres* 124 (23): 13457–74.
- Draxler, R R, and G D Rolph. 2011. “HYSPLIT (HYbrid Single-Particle Lagrangian Integrated Trajectory) Model; National Oceanic and Atmospheric Administration, Air Resources Laboratory READY Web Site.” *Air Resources Laboratory READY Web Site*.
- Haman, Christine L, Barry Lefer, and Gary A Morris. 2012. “Seasonal Variability in the Diurnal Evolution of the Boundary Layer in a Near-Coastal Urban Environment.” *Journal of Atmospheric and Oceanic Technology* 29 (5): 697–710.
- Kerr, J B, H Fast, C T McElroy, S J Oltmans, J A Lathrop, E Kyro, A Paukkunen, H Claude, U Köhler, and C R Sreedharan. 1994. “The 1991 WMO International Ozonesonde Intercomparison at Vanscoy, Canada.” *Atmosphere-Ocean* 32 (4): 685–716.
- Kleinman, Lawrence, Yin-Nan Lee, Stephen R Springston, Linda Nunnermacker, Xianliang Zhou, Robert Brown, Kristen Hallock, Paul Klotz, Daniel Leahy, and Jai H Lee. 1994. “Ozone Formation at a Rural Site in the Southeastern United States.” *Journal of Geophysical Research: Atmospheres* 99 (D2): 3469–82.
- Komhyr, W D. 1986. “Operations Handbook-Ozone Measurements to 40-Km Altitude with Model 4A Electrochemical Concentration Cell (ECC) Ozonesondes (Used with 1680-MHz Radiosondes).” National Oceanic and Atmospheric Administration, Silver Spring, MD (USA ....
- Komhyr, W D, R A Barnes, G B Brothers, J A Lathrop, and D P Opperman. 1995. “Electrochemical Concentration Cell Ozonesonde Performance Evaluation during STOIC 1989.” *Journal of Geophysical Research: Atmospheres* 100 (D5): 9231–44.
- Komhyr, Walter D. 1972. “Electrochemical Concentration Cell for Gas Analysis.” Google Patents.
- Langford, A O, K C Aikin, C S Eubank, and E J Williams. 2009. “Stratospheric Contribution to High Surface Ozone in Colorado during Springtime.” *Geophysical Research Letters* 36 (12).
- Langford, A O, R J Alvarez II, Jérôme Brioude, Stéphanie Evan, L T Iraci, G Kirgis, S Kuang, T Leblanc, M J Newchurch, and R B Pierce. 2018. “Coordinated Profiling of Stratospheric Intrusions and Transported Pollution by the Tropospheric Ozone Lidar Network (TOLNet) and NASA Alpha Jet Experiment (AJAX): Observations and Comparison to HYSPLIT, RAQMS, and FLEXPART.” *Atmospheric Environment* 174: 1–14.
- Levy, Ilan, Uri Dayan, and Yitzhak Mahrer. 2008. “Studying Coastal Recirculation with a Simplified Analytical Land-sea Breeze Model.” *Journal of Geophysical Research: Atmospheres* 113 (D3).
- Li, Wei, Yuxuan Wang, Claudia Bernier, and Mark Estes. 2020. “Identification of Sea Breeze Recirculation and Its Effects on Ozone in Houston, TX, During DISCOVER-AQ 2013.”

- Journal of Geophysical Research: Atmospheres* 125 (22): e2020JD033165.
- McPeters, Richard D, and Gordon J Labow. 2012. “Climatology 2011: An MLS and Sonde Derived Ozone Climatology for Satellite Retrieval Algorithms.” *Journal of Geophysical Research: Atmospheres* 117 (D10).
- Miloshevich, Larry M, Holger Vömel, Ari Paakkunen, Andrew J Heymsfield, and Samuel J Oltmans. 2001. “Characterization and Correction of Relative Humidity Measurements from Vaisala RS80-A Radiosondes at Cold Temperatures.” *Journal of Atmospheric and Oceanic Technology* 18 (2): 135–56.
- Morris, Gary A, Bonne Ford, Bernhard Rappenglück, Anne M Thompson, Ashley Mefferd, Fong Ngan, and Barry Lefer. 2010. “An Evaluation of the Interaction of Morning Residual Layer and Afternoon Mixed Layer Ozone in Houston Using Ozonesonde Data.” *Atmospheric Environment* 44 (33): 4024–34.
- Morris, Gary A, Mark R Schoeberl, Lynn C Sparling, Paul A Newman, Leslie R Lait, Lee Elson, Joe Waters, Robert A Suttie, Aidan Roche, and Jack Kumer. 1995. “Trajectory Mapping and Applications to Data from the Upper Atmosphere Research Satellite.” *Journal of Geophysical Research: Atmospheres* 100 (D8): 16491–505.
- Neu, Urs, Thomas Künzle, and Heinz Wanner. 1994. “On the Relation between Ozone Storage in the Residual Layer and Daily Variation in Near-Surface Ozone Concentration—a Case Study.” *Boundary-Layer Meteorology* 69 (3): 221–47.
- Ngan, Fong, Daewon Byun, Hyuncheol Kim, Daegyun Lee, Bernhard Rappenglück, and Arastoo Pour-Biazar. 2012. “Performance Assessment of Retrospective Meteorological Inputs for Use in Air Quality Modeling during TexAQS 2006.” *Atmospheric Environment* 54: 86–96.
- Reid, S J, G Vaughan, A R W Marsh, and H G J Smit. 1996. “Accuracy of Ozonesonde Measurements in the Troposphere.” *Journal of Atmospheric Chemistry* 25 (2): 215–26.
- Reiter, Elmar R. 1975. “Stratospheric-tropospheric Exchange Processes.” *Reviews of Geophysics* 13 (4): 459–74.
- Rolph, Glenn, Ariel Stein, and Barbara Stunder. 2017. “Real-Time Environmental Applications and Display System: READY.” *Environmental Modelling & Software* 95: 210–28.
- Shapiro, M A. 1980. “Turbulent Mixing within Tropopause Folds as a Mechanism for the Exchange of Chemical Constituents between the Stratosphere and Troposphere.” *Journal of Atmospheric Sciences* 37 (5): 994–1004.
- Smit, Herman G J, Wolfgang Straeter, Bryan J Johnson, Samuel J Oltmans, Jonathan Davies, David W Tarasick, Bruno Hoegger, Rene Stubi, Francis J Schmidlin, and T Northam. 2007. “Assessment of the Performance of ECC-ozonesondes under Quasi-flight Conditions in the Environmental Simulation Chamber: Insights from the Juelich Ozone Sonde Intercomparison Experiment (JOSIE).” *Journal of Geophysical Research: Atmospheres* 112 (D19).
- Stauffer, R M, G A Morris, Anne Mee Thompson, E Joseph, G J R Coetzee, and N R Nalli. 2014. “Propagation of Radiosonde Pressure Sensor Errors to Ozonesonde Measurements.”
- Stein, A F, R R Draxler, G D Rolph, B J B Stunder, M D Cohen, and F Ngan. 2015. “NOAA’s HYSPLIT Atmospheric Transport and Dispersion Modeling System, B. Am. Meteorol. Soc., 96, 2059e2077.”
- Thompson, Anne M, Herman G J Smit, Jacquelyn C Witte, Ryan M Stauffer, Bryan J Johnson, Gary Morris, Peter von der Gathen, Roeland Van Malderen, Jonathan Davies, and Ankie PETERS. 2019. “Ozonesonde Quality Assurance: The JOSIE–SHADOZ (2017) Experience.” *Bulletin of the American Meteorological Society* 100 (1): 155–71.

- Thompson, Anne M, Jacquelyn C Witte, Richard D McPeters, Samuel J Oltmans, Francis J Schmidlin, Jennifer A Logan, Masatomo Fujiwara, Volker W J H Kirchhoff, Françoise Posny, and Gert J R Coetzee. 2003. “Southern Hemisphere Additional Ozonesondes (SHADOZ) 1998–2000 Tropical Ozone Climatology 1. Comparison with Total Ozone Mapping Spectrometer (TOMS) and Ground-based Measurements.” *Journal of Geophysical Research: Atmospheres* 108 (D2).
- Wang, Junhong, Harold L Cole, David J Carlson, Erik R Miller, Kathryn Beierle, Ari Paukkunen, and Tapani K Laine. 2002. “Corrections of Humidity Measurement Errors from the Vaisala RS80 Radiosonde—Application to TOGA COARE Data.” *Journal of Atmospheric and Oceanic Technology* 19 (7): 981–1002.
- Wang, Sing-Chun, Yuxuan Wang, Mark Estes, Ruixue Lei, Robert Talbot, Liye Zhu, and Pei Hou. 2018. “Transport of Central American Fire Emissions to the U.S. Gulf Coast: Climatological Pathways and Impacts on Ozone and PM<sub>2.5</sub>.” *Journal of Geophysical Research: Atmospheres* 123 (15): 8344–61. <https://doi.org/10.1029/2018JD028684>.
- Waugh, Darryn W, and R Alan Plumb. 1994. “Contour Advection with Surgery: A Technique for Investigating Finescale Structure in Tracer Transport.” *Journal of the Atmospheric Sciences* 51 (4): 530–40.

## 7. APPENDIX: OVERVIEW OF OZONESONDES AND FLIGHT DATA

Ozone profiles in for this project were measured using the electrochemical concentration cell (ECC) type ozonesonde instrument (Komhyr 1972; Komhyr 1986). A detailed description of the standard ozonesonde chemistry is found in Morris et al. (2010). Validation studies have demonstrated the ECC sonde precision to be  $\pm 6\%$  near the ground and  $-7\%$  to  $+17\%$  in the upper troposphere (Kerr et al. 1994; W D Komhyr et al. 1995; Reid et al. 1996).

The 2019 campaigns from San Antonio and El Paso employed the InterMet iMet-4 radiosonde, which collects pressure, temperature, humidity, GPS location, and GPS-derived wind speed and direction. The 2017 campaigns from San Antonio and El Paso employed the InterMet iMet-1 radiosonde as have all flights from Austin and Houston since 2010. Prior to 2010, the flights from Houston used the Vaisala RS80-15N radiosondes (Thompson et al. 2003; Miloshevich et al. 2001; J. Wang et al. 2002). Most flights with the Vaisala radiosondes from 2006 – 2009 made use of a small global positioning system (GPS) unit fitted inside of the lid of the ozonesonde packaging to acquire, height, latitude, and longitude from which wind speed and wind direction are derived. The performance characteristics of the InterMet iMet-1 radiosondes have been found to be quite similar to those of the Vaisala RS80-15N radiosondes (Stauffer et al. 2014).

Our default balloon size is the 600-gram balloons that carry our payloads to 27 – 30 km before bursting. We use 350-gram balloons that carried our payloads to altitudes of 22 – 24 km before bursting in instances when a lower burst altitude had a more favorable expected landing site based on the balloon trajectory.

All ozonesondes use 0.5% KI solution recommended by the Jülich Ozone Sonde Intercomparison Experiment (JOSIE), which found biases  $<5\%$ , a precision of 3 – 5%, and an accuracy of 5 – 10% below 30 km (Smit et al. 2007; Thompson et al. 2019).

The full ozonesonde conditioning and calibration procedures can be found in a manual online at <http://ir.stedwards.edu/natural-sciences/ozone>.

### 7.1 FLIGHT DATA

The following data files are available for all ozonesonde flights.

“\*.txt” Ascii text files in one of two formats. Flights data since August 2013 use SHADOZ formatted files. In addition to what is listed above for the INTEX-B formatted files, the data in these files also includes a column for integrated column ozone (DU) from the ground to the altitude specified in each line of the data file (this column falls between the ozone mixing ratio column in ppmv and the wind direction column) and the intercell current in microamps (labeled, “uA” in the file since symbol font is not available in an ascii text). The headers for these files contains some additional information beyond that listed above for the INTEX-B files. The first 10 lines are identical. Lines 11 and 12 describe the ozonesonde type (and number) and

radiosonde type (and number) respectively. Line 13 contains the KI solution formulation. Line 14 describes the pump corrections that have been applied to the data. Lines 15 and 16 provide the pump flow rate (seconds per 100 mL) and background currents (in microamps, again written as “uA”) from the calibration procedure. With this information from the header and the data provided in the columns of the data file, it is possible for users to calculate the ozone concentrations for themselves (not the case for the older, INTEX-B formatted files). Given that advantage, it is desirable to reprocess all of the project data and put the data in SHADOZ formatted files, replacing the INTEX-B formatted files. Line 17 contains the burst pressure, while lines 18 and 19 contain estimates of the tropopause height (km) and mixed layer height (km) as determined by the processing software. To identify the tropopause height, we use the NOAA definition (vertical gradient of less than 2 °C/km). To identify the mixed layer height, we examine the gradients in ozone, temperature, and relative humidity, identifying the first altitude that shows a change in the first derivative of these quantities with respect to altitude. Line 20 contains the pressure offset (hPa) that has been applied to the data based on the difference between the burst altitudes recorded by the GPS and derived from the pressure altitude. Line 21 contains the column ozone integrated to the burst altitude (DU), while line 22 contains the SBUV residual above burst altitude column ozone, as determined by Richard D McPeters and Labow (2012) and line 23 contains the constant mixing ratio residual above the burst altitude (again in DU). Lines 24 and 25 contain the ozone column integrated from the ground to the tropopause and to the top of the mixed layer respectively (both in DU), using the heights appearing on lines 18 and 19 respectively. Line 26 contains the missing or bad data value (if you see this value in the data table, it indicates the data is missing or has been flagged as bad). Finally, line 27 contains the contact information for the PI.

- “\*o3pp\*” Profiles of ozone partial pressure, temperature, and potential temperature from the surface to balloon burst (up to 40 km maximum altitude).
- “\*h2omr\*” Profiles of ozone mixing ratio in both ppmv and ppbv units, and of relative humidity, again from the surface to balloon burst (up to 40 km maximum altitude).
- “trop” Profiles of ozone mixing ratio in ppbv, relative humidity, and potential temperature from the surface to 15 km. Descending data are also plotted in lighter colors when available. Note that the scientific community does not tend to use the descending data, although some of the data is undoubtedly valuable.
- “SkewT” The standard Skew T plot used by meteorologists to easily diagnose atmospheric stability, these graphs show both temperature and dew point temperature profiles from the surface to 100 hPa (~16 km). Skew T plots became standard beginning in August 2011. When earlier data are reprocessed to produce the SHADOZ formatted files, these plots also will be generated.

“PrepSheet” Scans of the ozonesonde conditioning and calibration preparation sheets are available and posted for each flight.

For all GPS-enabled flights, the following plots are also available on the website:

“wind” Profiles of wind speed and wind direction from the surface to the balloon burst altitude (maximum altitude of 40 km).

“trop wind” Profiles of wind speed and wind direction from the surface to 15 km, with descending data plotted in lighter colors.

“\*.kml” Google Maps of balloon flight trajectories, with markers placed every 10 minutes of the flight, with the launch site marked by the green “balloon” marker, ascending data marked by the green flight path, descending data marked by the red flight path, and projected landing site marked by the yellow “balloon” marker.

## 7.2 STANDARD HYSPLIT BACK TRAJECTORIES FOR EACH FLIGHT

The TOPP website includes links to back trajectories calculated with the HYSPLIT model (Draxler and Rolph 2011) and Stein et al. (2015) for all flights. HYSPLIT trajectory images on our website use software described in Rolph, Stein, and Stunder (2017).

The following HYSPLIT trajectory figures appear in conjunction with each and every flight on the project website.

“500” HYSPLIT ensemble trajectory runs initialized in a  $5 \times 5$  ( $1^\circ \times 1^\circ$  or smaller) grid at 500 m above ground level (AGL). Runs extend back in time up to 96 hours from the time of the launch. The coherence of the ensemble is indicative of the reliability of the trajectory calculations. At the bottom of each graph, the altitude of the parcels is shown.

“1000” As above but initialized at 1000 m AGL.

“1500” As above but initialized at 1500 m AGL.

“2000” As above but initialized at 2000 m AGL.

“2500” As above but initialized at 2500 m AGL.

“3000” As above but initialized at 3000 m AGL.

“BL” Single parcel HYSPLIT trajectories run back in time up to 96 hours, initialized over the launch site at 500, 1000, and 1500 m (boundary layer).

“LFT” Single parcel HYSPLIT trajectories run back in time up to 96 hours, initialized over the launch site at 2000, 2500, and 3000 m (lower free troposphere).

The “BL” and “LFT” trajectory calculations should be used in combination with the altitude specific ensemble calculations in order to establish the uncertainty/reliability of the single-parcel

calculations. No single trajectory is reliable – an ensemble viewpoint must be maintained (Morris et al. 1995; 2010).

Modeled air parcel back trajectories provide an approach that aids interpretation of ozone profiles and enhances our understanding of ozone exceedance events. A number of models exist (e.g., Flexpart, HYSPLIT, the NASA GSFC Trajectory Model, the CMAQ Trajectory Model), and different meteorological analyses can be used to drive the trajectory calculations (e.g., NCEP, ECMWF, EDAS), many of which provide data at multiple horizontal and temporal resolution scales. Research back in the 1990's indicated that the temporal resolution of the meteorological data was a more important factor than its spatial resolution in producing reliable, realistic air parcel simulations (Waugh and Plumb 1994).

One of the challenges for trajectory simulations of tropospheric transport relates to convective events. Even very high-resolution meteorological analyses (e.g., the EDAS 40 km) will be unable to reproduce events that occur on smaller spatial scales. When creating trajectory simulations to understand features observed in balloon profiles, features associated with such events cannot be properly simulated. Even large-scale atmospheric features seen in profiles may not be precisely reproduced in trajectory simulations.

Another challenge for trajectory simulations in the troposphere is related to post-frontal subsidence. The appearance of strong descent at all, even if not strong enough to link definitively the simulated air parcel to the upper tropospheric/lower stratospheric (UT/LS) region, does indicate that the air parcel possibly originated in the UT/LS region.

A trajectory simulation is not wrong or invaluable because it cannot reproduce the precise timing and location of features appearing in atmospheric tracer fields (like ozone). We instead need to rely upon an ensemble of trajectories, initialized over reasonable spatial and/or temporal domains, to permit meaningful interpretations of likely air parcel histories. Single partial back trajectories, therefore, are not particularly helpful or meaningful. In particular, no hypothesis can be confirmed, nor should any policy be based on single parcel trajectory calculations. Trajectory models provide one tool to help us better understand the role of transport in interpreting ozone profiles. The larger the number of trajectories included in the simulations, the more useful the simulations. The ensemble approach to analysis is the most reliable, but even this approach needs to be combined with other forms of analysis and coupled with other data sets to prove most useful.